2019

SYNTHESIS, DESIGN, AND EVALUATION OF THE FLUORESCENT DETECTION OF POLYCHLORINATED BIPHENYLS(PCBs) IN AQUEOUS SYSTEM

Irfan Ahmad
University of Kentucky, irfan.ahmad@uky.edu
Digital Object Identifier: https://doi.org/10.13023/etd.2019.413

STUDENT AGREEMENT:

I represent that my thesis or dissertation and abstract are my original work. Proper attribution has been given to all outside sources. I understand that I am solely responsible for obtaining any needed copyright permissions. I have obtained needed written permission statement(s) from the owner(s) of each third-party copyrighted matter to be included in my work, allowing electronic distribution (if such use is not permitted by the fair use doctrine) which will be submitted to UKnowledge as Additional File.

I hereby grant to The University of Kentucky and its agents the irrevocable, non-exclusive, and royalty-free license to archive and make accessible my work in whole or in part in all forms of media, now or hereafter known. I agree that the document mentioned above may be made available immediately for worldwide access unless an embargo applies.

I retain all other ownership rights to the copyright of my work. I also retain the right to use in future works (such as articles or books) all or part of my work. I understand that I am free to register the copyright to my work.

REVIEW, APPROVAL AND ACCEPTANCE

The document mentioned above has been reviewed and accepted by the student's advisor, on behalf of the advisory committee, and by the Director of Graduate Studies (DGS), on behalf of the program; we verify that this is the final, approved version of the student's thesis including all changes required by the advisory committee. The undersigned agree to abide by the statements above.

Irfan Ahmad, Student

Dr. Thomas D. Dziubla, Major Professor

Dr. Stephen Rankin, Director of Graduate Studies

SYNTHESIS, DESIGN, AND EVALUATION OF THE FLUORESCENT DETECTION OF POLYCHLORINATED BIPHENYLS(PCBs) IN AQUEOUS SYSTEM

DISSERTATION

A dissertation submitted in partial fulfillment of the
requirements for the degree of Doctor of Philosophy in the
College of Engineering
at the University of Kentucky

By

Irfan Ahmad

Lexington, Kentucky

Director: Dr. Thomas D. Dziubla, Professor of Chemical and Materials Engineering

Co-director: Dr. J. Zach Hilt, Professor of Chemical and Materials Engineering

Lexington, Kentucky

2019

ABSTRACT OF DISSERTATION

SYNTHESIS, DESIGN, AND EVALUATION OF THE FLUORESCENT DETECTION OF POLYCHLORINATED BIPHENYLS(PCBs) IN AQUEOUS SYSTEM

The exposure to halogenated persistent organic pollutants (POPs), such as polychlorinated biphenyls (PCBs), has been linked to numerous inflammatory diseases, including diabetes, cancer and lowered immune response. PCBs have low solubility in water, and they interact with other contaminants, making their detection quite challenging. While, there have been several attempts at improving the ease of detection and sensing of PCBs, gas chromatography-mass spectrometry (GC-MS) remains the gold standard. However, despite its ubiquitous use, GC-MS is a challenging technique that requires high skill and careful sample preparation, which are time-consuming and costly. As such, there is still a need to develop a sensing system that can detect PCBs in a more efficient manner.

In this work, we hypothesize that the dilute concentration of PCBs in water can be detected using a fluorescent displacement assay. To test this hypothesis, we screened a series of fluorescent molecules that were used as a fluorescence quenching pair. The displacement pair(BaP/curcumin) was evaluated in polymer microparticles (MPs) for higher sensitivity. Curcumin was immobilized to the MPs and BaP was kept free for easy displacement in the solution. MPs indicate good binding of BaP that does not come off in the solution. However, BaP displaces from the MPs in the presence of PCB. The enhanced signal of BaP indicates the presence of a novel hydrophobic interaction between BaP and PCB in water. This hydrophobic interaction leads to the successful detection of PCB. BaP fluorescence increases with trace concentrations of PCBs in water. To determine the selectivity and robustness of this response, the impact of pH, ionic strength and humic acid to mimic freshwater conditions are explored. BaP was able to detect PCBs in the micromolar range. The fluorescent dye was then immobilized on the polymer network for enhanced sensitivity and recovery. For this purpose, BaP analog pyrene is used, which behaves similar to BaP in water with PCB. This molecule was functionalized into the monomer and is polymerized into the hydrophilic polymer network for pH-based swelling, to allow PCBs within its network for the interaction with pyrene. These MPs are characterized using different techniques and their interaction with PCBs was studied.

KEYWORDS: Polychlorinated biphenyl, fluorescence, quenching, Benzo[a]pyrene, pyrene, esterification, functionalized polymer microparticles, hydrophobic interaction

Irfan Ahmad

(Name of Student)

October 11th, 2019

Date

SYNTHESIS, DESIGN, AND
EVALUATION OF THE FLUORESCENT DETECTION
OF POLYCHLORINATED BIPHENYLS(PCBs) IN AQUEOUS SYSTEM

By
Irfan Ahmad

Dr. Thomas Dziubla
Co-Director of Dissertation

Dr. J. Zach Hilt
Co-Director of Dissertation

Dr. Stephen Rankin
Director of Graduate Studies

October 11th, 2019
Date

DEDICATION

To My Mother

ACKNOWLEDGEMENTS

First of all, I am sincerely grateful to my advisor Dr. Thomas Dziubla, for giving me an opportunity to pursue my doctoral in his research group. He constantly kept my doctoral journey interesting and challenging. I also would like to thank my co-advisor Dr. J. Zach Hilt, who has taken care of my research track with great effort and spirit.

I greatly appreciate their patience and constant guidance throughout my research career. I would like to thank my lab mates (Dziubla lab group) Dustin Salvage, Kelley Wiegman, Dr. Carolyn Jordan, Dr. Vinod Patil, Dr. Prachi Gupta, Dr. Sundar Prasanth Authimoolam, Dr. Andrew Lakes and also members from Hilt Lab, Dr. Shuo Tang, Dr. Trang Mai, Dr. Angela Gutiérrez, Molly Frazar and Rishabh Shah for their insightful discussions and great work and research environment. I also acknowledge my friends Dr. Abdul Rehman and Dr. Nandita Raha for making my stay in Lexington memorable. A thank you to my committee members (Dr. Kelly Pennell and Dr. Yinan Wei) and examiner Dr. Luke Bradley for their valuable suggestions for my thesis. This work is dedicated to my mother (Musarat Bano), my sisters (Samina Shaheen, Rubina Shaheen, and Dr. Raheela Shaheen), two kids(Shaylynn and Nafees) and my wife(Tonya Ahmad). A thank you to my family for our continuous challenges to keep the work and family life balance.

TABLE OF CONTENTS

LIST OF TABLES

LIST OF FIGURES

CHAPTER 1. INTRODUCTION

Polychlorinated biphenyls (PCBs) are man-made chemicals that were introduced in the environment as early as 1929 by Monsanto Chemicals in the United States.[1,2] They remain detectable in the environment, despite the ban on their production in 1970s. The Stockholm Convention categorized PCBs as persistent organic pollutants (POPs). According to the United Nations Environmental program[3], "POPs are chemical substances that persist in the environment, bioaccumulate through the food web, and pose a risk of causing adverse effects to human health and the environment". The Stockholm Convention has defined twelve different chemicals as POPs and divided them into three categories (pesticides, industrial chemicals, and by-products). PCBs are one of them that fall under the "industrial chemicals" category. PCBs have very stable chemical and physical properties under high temperature and pressure; it is non-flammable and non-conductive. These unique properties made PCBs ideal for hundreds of commercial and industrial applications including capacitors, heat transfer fluids, insulating and cooling fluids in transformers, in caulking material for sealant, plasticizers in paint and lubricating material, etc. The distribution of commercial applications of PCBs is shown in figure 1.1. Before July 2, 1979, nearly all the capacitors were 100% filled with PCBs.[4] PCBs allowed the capacitor's size to be smaller that lowered the cost and even some cities and insurance companies required to use only PCB containing electrical parts where fire-resistance was serious.[5] On the other hand, PCBs have saved many lives over the decades that could have been lost by using less fire-resistant electrical parts.[6] PCBs were present

in almost all of the buildings and still present in old schools and hospital buildings that still have old paints and caulking material.

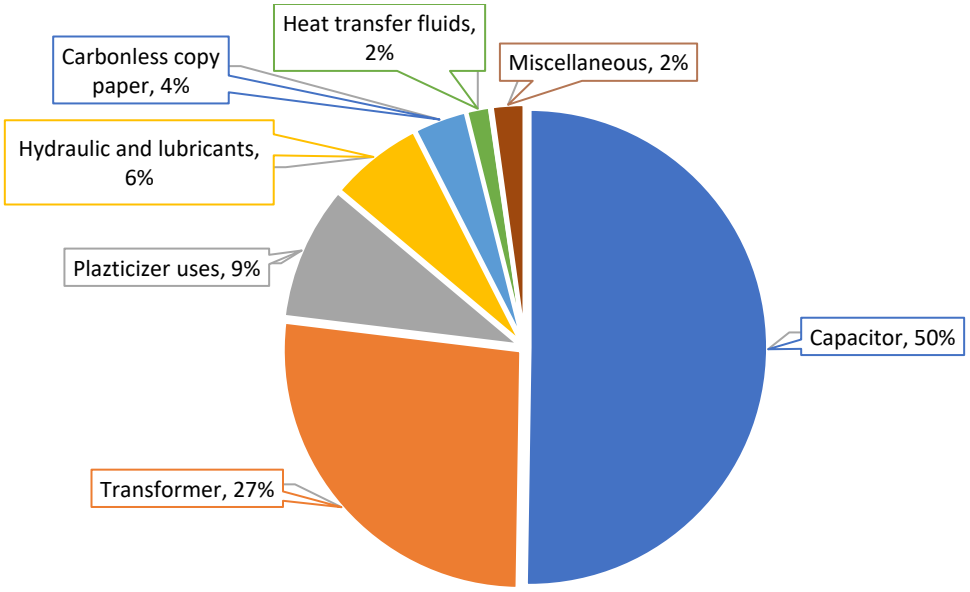

Figure 1.1: Industrial uses of PCBs (1929~1975).[7]

Although it was first commercially manufactured in 1929, the toxic effects started getting attention in the 1930s and it took a couple of more decades and few incidents to consider PCBs harmful enough to ban commercial production. PCBs have adverse effects on human health; they are carcinogenic, cause neurotoxicity and decrease the normal brain functions that lead to the disruption of many other normal body functions. It is very important to keep the PCB level close to none in our intake. EPA has an enforceable level of 0.0005 ppm (0.0015 µM, based on the average molecular mass of 329.0186 g/mol) of PCBs in water.[8] The history of PCBs is illustrated below in figure 1.2.

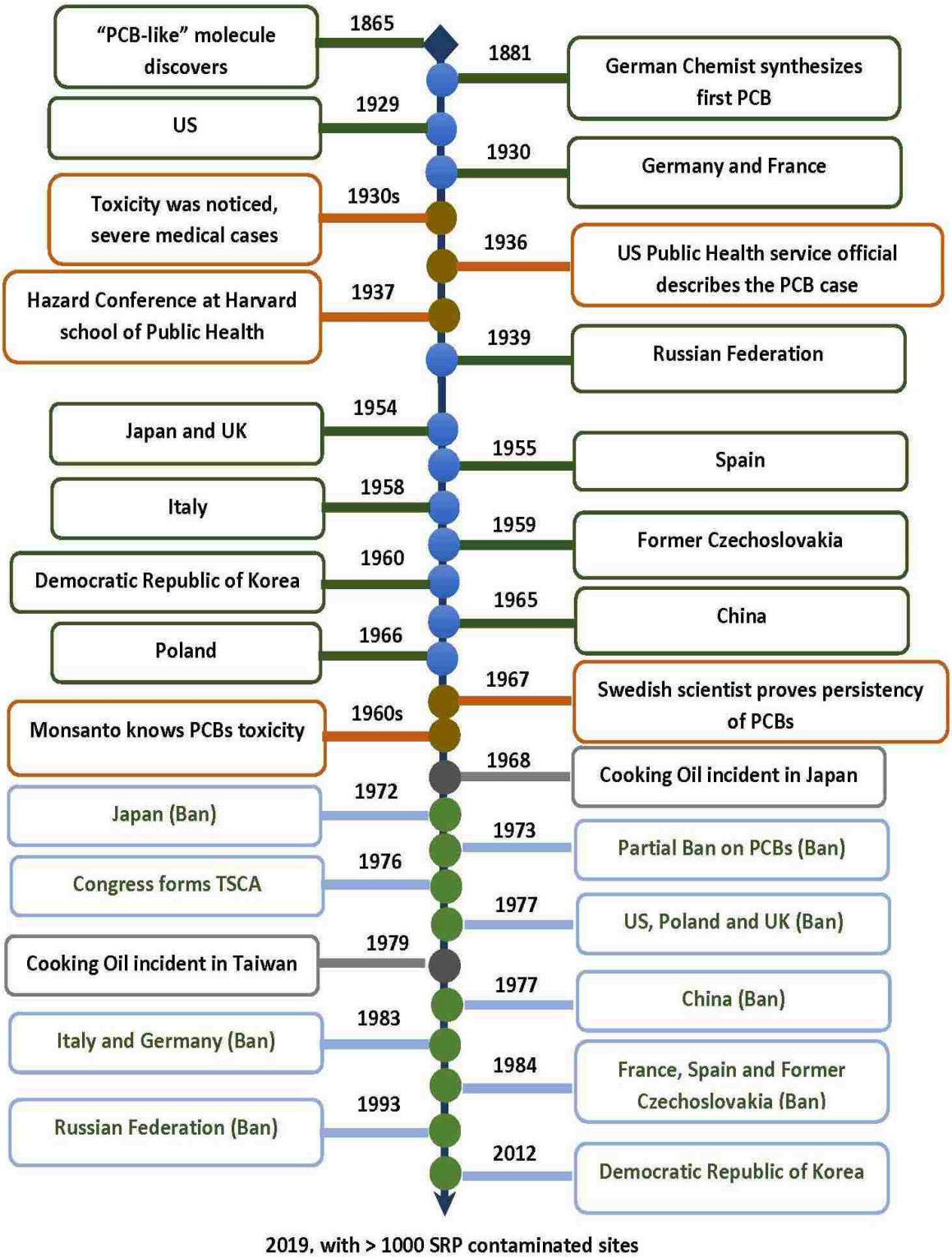

Figure 1.2: Timeline with known history related to PCBs.[9–23]

It is very important to have methods that are capable of detecting PCBs in water. PCBs accumulate in body fat over time. The continuous exposure to a very low concentration can cause long term health effects. Based on the adverse effects on human and animal health and the resilient nature of PCBs. There are various sensing methods mentioned in the literature for PCBs. These techniques can either detect PCBs in the solvent or indirectly sense PCBs by pairing it with another molecule. Each method has some limitations. For example, Gas chromatography Mass spectroscopy (GC-MS) is used as a standard technique for detecting PCBs in a sample. This instrument can detect PCBs directly in the organic solvent. It needs high sample purity, which leads to time-consuming extraction and sample processing. It also needs organic solvent extraction[24], to concentrate PCBs for analysis. However, GC-MS is a highly sophisticated technique that requires well-trained personnel for better results reproducibility. These solvents have environmental risk and hence improved methods are needed to avoid these deficiencies. There are other techniques being developed for sensing PCBs. These methods detect the changes in properties of analytes resulting from the interaction with PCBs. Most sensors are classified as biosensors that have biological derived aspects; such as an antibody, enzyme, lipid, nucleic acid, tissue structures, receptor, antigen, organelle, or biomimetic component. These components interact or bind with PCBs to change their properties in density, thickness or elasticity. Biosensors have several drawbacks, for example, high enzyme processing cost, longer response and recovery time, reusability challenges and nonspecific interactions.[25,26] There is still a need for an inexpensive, easy and stable system to sense PCBs. In order to develop a new method for PCB detection, affinity and

displacement-based technique will be used to attract PCBs. This will reduce the need of sample purification as compared to existing methods. The affinity-based capture and sensing method is well documented in the literature with antibodies, where it uses “plug and play” approaches. Antibodies can bind almost any molecule and can replace any substances (polyaromatic hydrocarbons) with environmental side effects.[27] However, antibodies have cost and long-term stability issues [28–30], which can limit usage for capturing and sensing of PCBs in the water.

Other techniques are being studied to detect PCBs including surface-enhanced Raman scattering (SERS), surface plasmon resonance (SPR), electrochemical impedance sensors, whole-cell sensors, and micro-flow immunosensor chips. While these systems are exciting possibilities for quantifying and detecting PCBs in environmental standards, none has become a standard of detection owing to the limited flexibility and is too costly to be a survey approach.[24,27–30]

The research work presented here proposed new techniques for the detection of PCBs in water. This method uses a fluorescence technique that is relatively low cost, easy, sensitive, fast and can be used with the minimum technical background. The complete work has divided into four parts. Firstly, we hypothesized that PCBs can be indirectly detected using a fluorescent displacement assay. We started with the fluorescent interaction of polyphenolic molecules with other fluorophores to screen a quenching pair that will be used for PCBs sensing.

Secondly, we selected the polyphenolic molecule for immobilization due to the presence of multiple functionalized sites. It will provide biomimetic pockets for the fluorophore

binding, which will be displaced by PCB. It involves chemical modification of the polyphenolic molecule by acryloyl chloride for crosslinking into the polymer chain. In this way, one of the molecules from the first part was polymerized into the polymer network. It acted as a pocket for the capturing and displacement of the fluorescent probe with PCBs in the water.

Thirdly, we hypothesized that PCB can form a complex with a hydrophobic dye in water that will change the fluorescent properties of the fluorophore. This work utilized the hydrophobic effect in which water makes clathrate cage around the molecules and pushes them to stay close to each other. This phenomenon changes the fluorescence properties of the fluorophore that results from the hydrophobic interaction of the molecules. We also demonstrated that this kind of interaction is affected by the presence of physical properties and impurities in the water.

Lastly, polymer particles are prepared to immobilize the fluorophore to enhance their sensitivity and stability and possible recovery. Functionalized pyrene was first linked with the linker molecule through the esterification reaction that was confirmed using different characterization techniques and then this pyrene monomer was polymerized with the polymer. These particles are studied using fluorescence techniques and their interaction with PCBs was evaluated.

CHAPTER 2. BACKGROUND

2.1 PCBs as a worldwide problem (World history of PCBs)

The first “PCB-like” molecule was first discovered in 1865 in the byproduct of coal tar. A few years later, a German chemist synthesized PCBs in 1881. In the US and Europe, its commercial production started in 1929, while Japan’s production of PCBs started in 1954 with China following in 1965. As a result of this production, PCBs are present in every part of the world. In the mid-1930s, its toxicity was recognized due to several medical cases and research published linking PCBs to adverse health effects.[11] In 1967, Swedish scientists proved that PCBs were present in the food chain; in birds, fish, pine needles, even their children's hair.[12] Owning to the harmful effects of PCBs, production was banned in 1972 in Japan. The US stopped in 1979 and Europe in the mid of 1980s. The Democratic People’s Republic of Korea was the final country to continue to produce PCBs until they planned to reconsider its production in 2012.[13] An estimated total cumulative production states that 1 to 1.5 million tons of PCBs products were manufactured worldwide.[13] The US produced nearly 600,000 tons of PCBs between 1930 and 1977. Whereas, Europe produced around 450,000 tons up through 1984. Industrial products containing PCBs were exported all over the world. The US alone is responsible for around 46% of global PCBs contribution. Figure 2.1 shows the spatial distribution of PCBs industrial consumption based on the population density. Europe, US, Japan, and Korea are more prominent among the countries that used PCBs.[31] Whereas, figure 2.2 shows the worldwide production of PCBs. Until 1970s, capacitors were consuming around 50% of the PCBs and transformers were the second largest industrial product containing PCBs.

Due to the presence of these old electrical parts and their poor disposal and handlings, PCBs are found all over the world. PCBs are still present in transformers in Havana, Cuba, in cooking oil in some African countries, in welding cooling oil in Sri Lanka.[32] PCBs effects were also found in arctic polar bears and in 90 % of German sheep livers.[32]

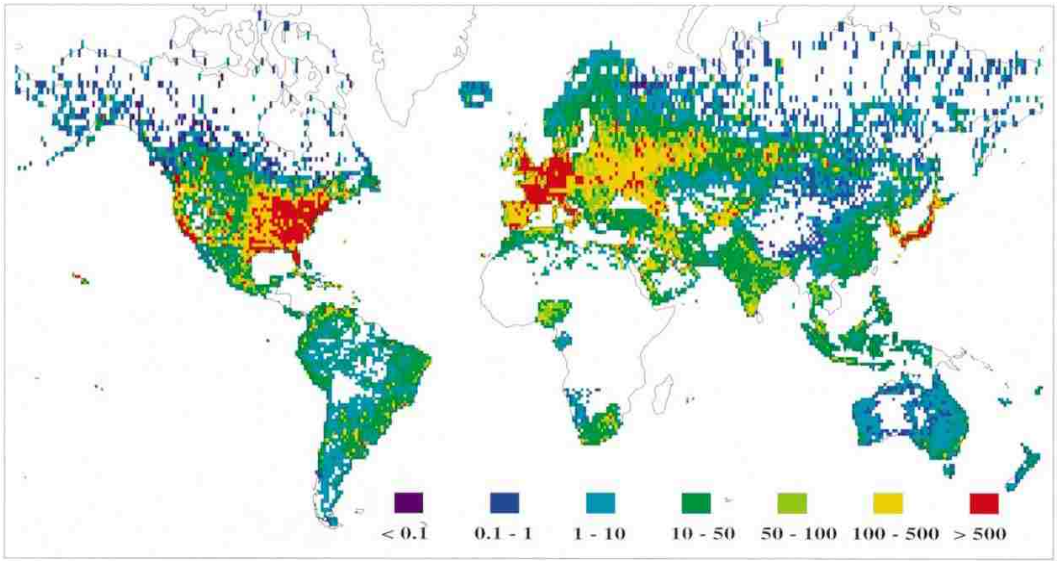

Figure 2.1: Estimated cumulative global usage of PCBs (legends in ton) with 1° X 1° longitude and latitude resolution.
(Reprinted from The Science of the Total Environment, 290, Knut Breivika, Andy Sweetman, Jozef M. Pacyna, Kevin C. Jones, "Towards a global historical emission inventory for selected PCB congeners — a mass balance approach 1. Global production and consumption", 195, Copyright (2002), with permission from Elsevier).[33]

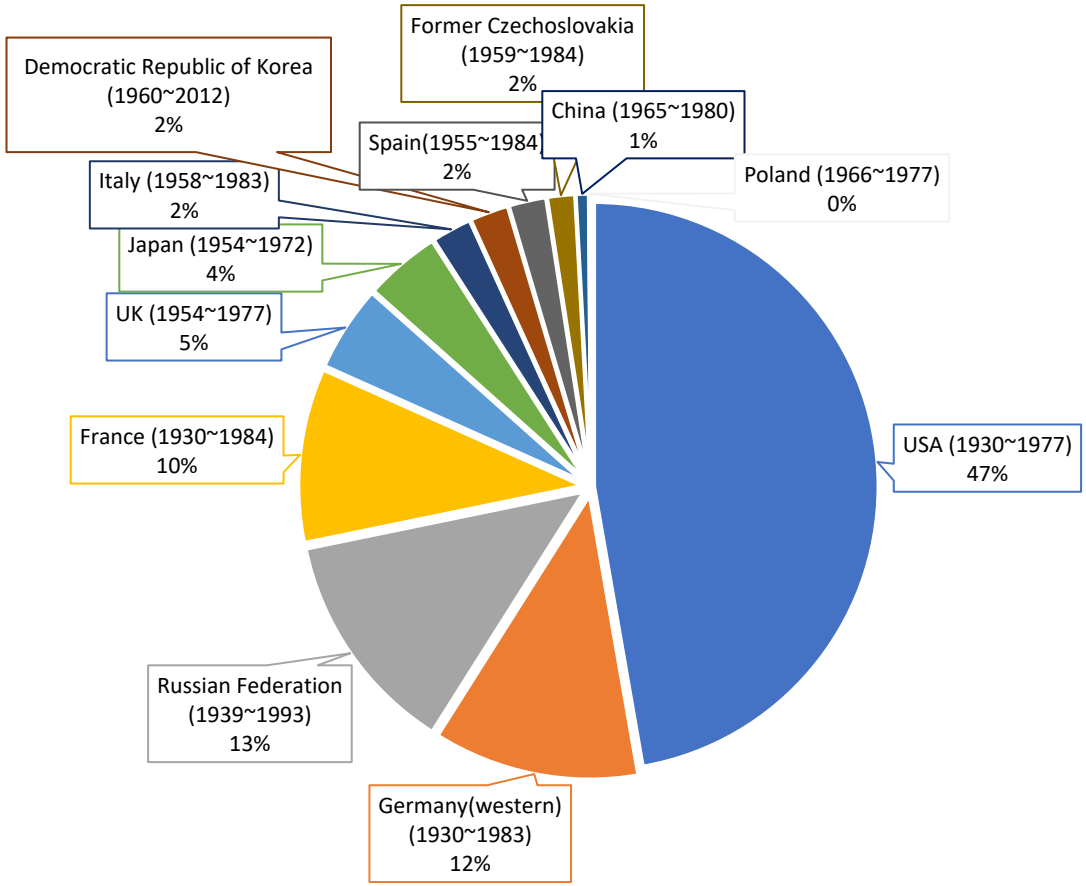

Figure 2.2: Worldwide contribution of PCBs from countries with known production.[9,10,16–22,33]

2.2 PCB chemistry

PCBs can have anywhere from 1 to 10 chlorine atoms attached, resulting in 209 possible combinations, or congeners, based on the number of chlorine atoms and the orientation. All of these congeners vary in their degree of hydrophobicity and toxicity. PCB congeners are based on the "BZ number" [34], a number that is associated with the structural arrangement of PCB congener and the increasing number of chlorine atoms in the family sequence. It ranges from PCB-1 (2-Monochlorobiphenyl) to PCB-209 (1,1'-Biphenyl, 2,2',3,3',4,4',5,5',6,6'-decachloro) as shown in figure 2.3.

Figure 2.3: PCB-1 and PCB-209 structure based on the BZ number.

There are three groups of PCBs congeners, non-ortho substituted coplanar PCBs (e.g. PCB 169, PCB 126 and PCB 77), ortho-substituted non-coplanar PCBs (e.g. PCB 153 and PCB 104) and mix planar PCBs (e.g. PCB 118) with one or two chlorines in the ortho position.[35,36] Legacy PCBs were produced commercially such as PCB-77 and PCB-126. Nonlegacy PCBs are the unintentional byproducts of the paint manufacturing process (e.g. PCB-11), which are not found in commercial PCBs mixture.[37,38]

PCBs are tasteless and odorless chemicals that have various physical appearances from an oily liquid to solid. While their color ranges from colorless to light yellow. The danger of PCBs is they can coexist in sediments and in vapors or aerosols. PCBs have extraordinary stability under high pressure and high temperature. In addition, PCBs also have very good chemical resistance, this made them a perfect candidate for electrical parts, heat transfer fluids, dielectric fluids, plasticizers, flame-retardants, solvent extenders, and organic diluents.[39–42]

2.3 PCBs in the environment and in the food chain

PCBs waste is an enduring problem for humanity. Exposure to high levels of PCBs can cause major health issues. PCBs containing products such as capacitors, oil, and transformers were discarded at numerous waste sites. Over time these chemicals seep directly into the groundwater from the landfills. PCBs have moved to the fifth position among 275 hazardous substances.[43] As of April 2019, 1337 locations were listed on EPA's "National Priorities List (NPL)" for cleanup with 53 proposed sites.[44] These sites are contaminated with different substances that pose a threat to human health. EPA has listed more than 500 sites contaminated with PCBs that are being considered for Superfund National Priorities list.[43] PCBs can travel over a wide region through water and air many miles away from the dumping site. PCBs have been detected in old school buildings, construction material including caulking, oil-based paints, and old fluorescent lights.[45–47] From the dumping sites, PCBs waste makes its way into the soil, water, and air. Animals, birds, marine life and plants absorb this waste. Humans intake PCBs either

directly from water, air or through other food containing PCBs. The possible known routes of PCBs distribution in the environment are shown in figure 2.4.

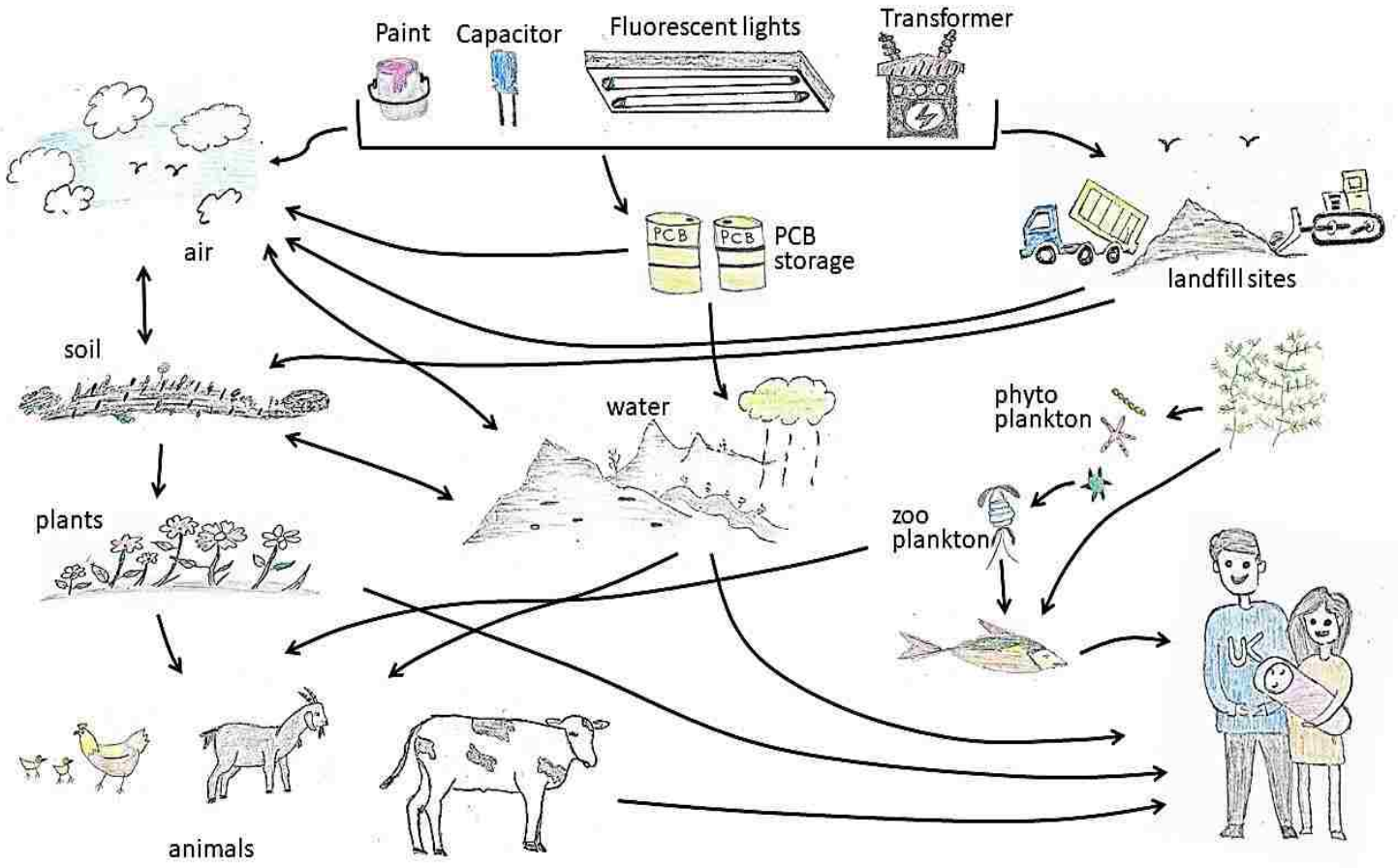

Figure 2.4: The food chain of PCBs

2.3.1 PCBs regulations and recommendations

In 1976, Congress formed the Toxic Substances Control Act (TSCA) to control the use, distribution, and disposal of dangerous chemicals including PCBs. It provided EPA with authority for keeping records, reporting, testing requirements and restrictions related to chemical substances.[14] Six chemicals including PCBs receive special attention under TSCA, PCBs violation can cause plenty of one year and/or up-to $25,000 per day.[48] According to the Clean Water Act (CWA), Industrial disposal of PCBs is illegal, and any spill of PCBs is required to be reported to the EPA. The main goal is to keep PCBs level zero in drinking water, however, the maximum level is strictly monitored at 0.0005 ppm(0.0015 μM)[49], FDA has a range of 0.2 to 3.0 ppm(0.6 μM to 9.12 μM) of PCBs in all foods, and for paper food-packaging its limit is 10 ppm(30.4 μM).[50] Whereas, World Health Organization (WHO) allows PCB intake of 6 μg/kg(0.018 μM) per day.[50] As a result, each agency has allowable exposure limits of PCBs for food, air, and water that are summarized in table 2.1.

Table 2.1: Standards, regulations, and recommendations for PCBs (adopted from ATSDR)[56]

Agency	Area of Interest	Range	Comments	Reference
FDA[1]	Food: environment	0.6 µM to 9.12 µM – (All foods) 6µM – (Fish) 30.4 µM – (Paper food-packaging materials)	Enforceable; Acceptance level	51
WHO[2] FAO[3]	Food: environment	0.018 µM per day	Allowable daily intake	52
OSHA[4]	Air: workplace	1.0 mg/m^3 for PCBs with 42% chlorine (average molecular formula of $C_{12}H_7Cl_3$) 0.5 mg/m^3 for PCBs with 54% chlorine (average molecular formula of $C_{12}H_5Cl_5$)	Enforceable; TWA[a], PEL[b] Both standards include all physical forms of vapor, aerosols, sprays, fog, and PCB-loaded dust particles.	53
NIOSH[5]	Air: workplace	1.0 µg/m^3	Advisory*; TWA (10-hour)	54
EPA[6]	Drinking water: environment	0.0015 µM	Enforceable MCL[c]	55

[1]FDA: Food and Drug Administration
[2]WHO: World Health Organization
[3]FAO: Food and Agriculture Organization
[4]OSHA: Occupational Safety and Health Administration
[5]NIOSH: National Institute for Occupational Safety and Health
[6]EPA: Environmental Protection Agency
[a]TWA: Time-Weighted Average: WA concentration for a regular workday and a 40-hour workweek to which almost all workers may be repetitively exposed.
[b]PEL: Permissible Exposure Limit: the highest level of PCBs in the air to which a worker may be exposed, averaged over an 8-hour workday
[c]MCL: Maximum Contaminant Level: enforceable level for public water system
* It is based on the minimum reliable detachable concentration of PCBs and its carcinogenicity. NIOSH also recommends keeping the workplace exposure level to the minimum
Molar concentrations of PCBs are calculated based on the average molecular weight of 329.0186 g/mol

2.3.2 PCBs in air and water

PCBs are released into the air from water when water is warm and also when PCB concentration in water is high. However, PCB's water solubility and vapor pressure are very low.[21] This causes them to partition between water and air. PCBs adsorb into the particles in the water which causes the actual concentration of PCBs higher than the theoretical solubility.[57,58] PCBs tend to stick with organic matters in the environment. Humic substances are amphiphilic in nature and are abundantly available in the soil. This allows PCBs to remain buried in the earth for a very long time. PCBs are present in water in three ways, one, freely dissolved in water at very low concentration, second attached to the amphiphilic molecule or third, adsorbed into the particles in the water.

2.3.3 PCBs route to the human body

Although there is no more production of PCBs. Most importantly, PCBs concentration in the environment and in the human body has already built up from over 70 years of exposure in the populace living in tainted areas.[59] The main source of PCBs to the human body is through the food and it accounts for approximately 90% of total exposure, and most of it comes from animal origin and fish exposure.[60] This section will break down these exposure routes in detail.

2.3.3.1 PCBs in dairy, meat, and eggs

There is a wide consumption of milk, meat, eggs, and their derived products. After European Union (151 million metric tons), the US is the second-biggest producer of cow milk with 96.34 million metric tons.[61] The United States is the world's largest beef and

buffalo producer, 11-12 million tons as of 2014. As shown in figure 2.4, beef, goat, pig and chicken fall in-between the food cycle. They either consume the plants that contain PCBs or drink contaminated water. Humans consume these animals either for meat or use their products in the form of milk, eggs or other dairy items. PCBs have been found in dairy, meat, eggs, vegan products and also in some bakery items [62,63], it is summarized in table 2.2 and 2.3. All products have a very low concentration of PCBs and are safe to consume under FDA's PCB limits. However, continuous consumption of PCBs in contaminated food items with an allowable limit can increase the accumulation of PCBs within the human body. PCBs excretion process from the human body depends on the number and position of chlorine atoms. PCBs can transform into persistent metabolites and store in specific tissues and/or body fluids and do not easily eliminate. PCBs can also combine with glutathione and glucuronic acid in the body and make water-soluble substances that excrete in urine and feces.[64]

Table 2.2: Meat and dairy products in the US and the presence of PCBs in it.

Food Source	US	PCBs(pg/g)[62]	Limit
Milk (million lb.)[65]	202,455		1.5 mg/Kg[66]
Dairy products[65]			1.5 mg/Kg[66]
Butter (Million lb.)	1,852.1	0.455	
Cheese (Million lb.)	12,477.9	0.129	
Frozen products (Million gal.) (Regular hard ice cream, total low-fat ice cream, and hard sherbet.)	1,244.1		
Nonfat dry milk (Million lb.)	1,825.8		
Meat (Million lb.)[67]			3 ppm[68]
Beef	26,699	0.125	
Pork	25,806	0.158	
Lamb and mutton	147		
Broilers	41,488	0.130	
Turkeys	5,983		
Table eggs, mil. doz.	7,658	0.036	0.2 ppm[68]
Vegan Food [62]		0.008	

Table 2.3: PCBs in different foods [63] (PCBs average molecular weight 329.0186 g/mol)

Food	Level in µM Mean	Level in µM Min	Level in µM Max
Salmon, steaks/fillets, baked	0.07410	0.02735	0.16716
Catfish, pan-cooked w/ oil	0.01292	0.05167	0.05167
Butter, regular	0.00967	0.06079	0.36472
Popcorn, popped in oil	0.00517	0.02735	0.09118
Chicken breast, oven-roasted	0.00413	0.09118	0.03039
Eggs, fried	0.00374	0.03039	0.11853
Tuna, canned in oil	0.00304	0.12157	0.12157
Brown gravy, homemade	0.00228	0.09118	0.09118
BF, vegetables and chicken	0.00207	0.09118	0.09118
Pancakes made with egg, milk, and oil	0.00152	0.06079	0.06079
Beef (loin/sirloin) steak,	0.00152	0.06079	0.06079
Pork chop	0.00137	0.06079	0.06079
Meatloaf, beef	0.00137	0.06079	0.06079
Crackers, butter-type	0.00076	0.03343	0.03343
Veal cutlet	0.00076	0.03039	0.03039
Pork roast	0.00070	0.03039	0.03039
Lamb chop	0.00070	0.03039	0.03039
Chicken, drumsticks and breasts	0.00070	0.02735	0.02735
Corn/hominy grits	0.00070	0.03039	0.03039
Cornbread	0.00070	0.03039	0.03039
Biscuits, baked	0.00070	0.03039	0.03039
Raisins	0.00070	0.03039	0.03039
Chicken potpie	0.00027	0.01216	0.01216
English muffin, plain, toasted	0.00070	0.03039	0.03039
Beef roast	0.00070	0.03039	0.03039
Candy, caramels	0.00046	0.01824	0.01824

2.3.3.2 PCBs in fish

PCBs from water bodies can go to the marine plants, planktons or directly to the fish. Small fish prey on these plants and microorganisms. Bigger fish that eat small fish, accumulating more PCBs. PCBs level in a fish can reach a thousand times higher than the PCBs concentration in the water. A bottlenose dolphin was found with a PCB concentration of 6080 μM, which is 40 times higher than the waste disposal requirements.[69] Inuit native (Canadian arctic people) diet includes fish and fats from seals; contains an alarming level of PCBs (48 μM) in their fats. It is far higher than the safe fish concentration set by the EPA (0.28 μM). [69]

Agencies including federal, state, local or tribal issues an advisory for the water body for the affected type of fishes and contaminants. According to the National Listing of Fish Advisories (NLFA), in 2011 states issued 223 new fish advisories making 4,821 total advisories [70] for various contaminants. For PCBs, between 2010 and 2011 the advisories increased from 1084 to 1102 (Table 2.4). It includes four states that have statewide advisory, and nine states have coast water advisory. In 2004, EPA and FDA issued advice for young children, women who are pregnant or might become pregnant and nursing mothers.[70]

Table 2.4: Number of water-bodies and size of waters under advisory, for 2010 and 2011.[70]

contaminant	Number of Waterbodies Under Advisory		Lake Acres		River Miles	
	2010	2011	2010	2011	2010	2011
PCBs	1,084	1,102	6,071,877	6,080,041	131,224	131,657

2.3.3.3 PCBs in mother's milk

In infant age, breast milk and formula milk are the main sources of food. FDA requires a limit of 0.6 µM(0.2 ppm) of PCBs for infant and junior foods.[68] Breast milk is complete diet food for infants and provides all necessary nutrients for the baby, and delivers protection against a number of diseases.[71] PCBs enter the body mainly through the environment, dietary intake, and in utero to unborn children.[72–76] PCBs are stored in blood, tissues, fats and breast milk inside the human body. It is a common perception that the majority of the newborn who is exposed to PCBs is through the contaminated mother's milk.[77] The level of PCBs in European and North American women's breast milk is higher than the women from non-industrialized countries.[78] According to the study in 2001-2004, women of ages, 16-49 had a median level of 30 ng/g PCBs in blood serum. The 95th percentile concentration among these women was found to be 106 ng/g.[70]

2.3.3.4 Volatile airborne PCBs

Higher chlorinated PCBs are foodborne PCBs (PCB-153, PCB-138, etc.) that accumulate in animal fats and transport through food consumption. Whereas, lower chlorinated PCBs

(e.g., PCB-52, PCB-28, etc.) are more volatile and hence classified as airborne PCBs.[79] The contaminated indoor air in some schools and industrial buildings has measured up to 13000 ng/m^3 of PCBs; some of them were PCB-28, PCB-52, PCB-118, PCB-105, and PCB-77.[80,81] For air at the workplace, OSHA recommends maximum limit of 1 mg/m^3 for 42% chlorinated PCBs and 0.5 mg/m^3 for 54% chlorinated PCBs.[53] Whereas, NIOSH has a limit of 1 µg/m^3.[54] Presence of low chlorine causes low lipophilicity and high volatility, these PCBs could evaporate from water surface, soil, and building material along with water vapors and dust. PCBs were widely used in paints and caulking materials, these materials were used in hospitals, auditoriums, and schools. Moreover, anaerobic environment and photodegradation can convert highly chlorinated PCBs to low chlorinated PCBs [57,82], which can enter into the air. Airborne PCBs have very low concentration, but continuous inhaling of contaminated air can increase the level of PCBs in the body. PCBs from larger water bodies in the urban areas evaporate into the atmosphere [83–85], population around these water bodies are in continuous exposure of airborne PCBs.

2.3.3.5 Miscellaneous routes

Other than the above-mentioned routes, there are some other possible ways through which PCBs can enter the human body. People who are living close to the contaminated sites or working in cleaning and sampling in the contaminated area can be exposed to PCBs through the skin. Similarly, people who swim or sail in water bodies also absorb PCBs through the skin.

2.4 Effect of PCBs on human health

Studies show that PCBs can cause neurotoxicity in both adults and children. Even the PCBs exposure in the uterus and through lactation can lead to the lower IQ level, decrease in neuromuscular functions, weakened memory and learning, slow development of reading and other behavioral deficiencies.[86–88] Immunotoxicity might be one of the highly sensitive indications of PCBs contamination.[89] Structurally, PCBs match the thyroid hormone's structure.[90] PCBs affect the growth in humans and animals; it hinders the functions of the thyroid hormone and can reduce its circulation level, which can affect brain development.[91,92] PCBs are also endocrine-disrupting chemical, it can show estrogenic behavior by binding to the estrogen receptor and affect the reproductive system.[93] PCBs are also responsible for hypertension, obesity, and diabetes, all of these conditions lead to cardiovascular diseases.[94] The latest research shows that PCBs also decrease sperm quality in human and domestic dogs.[95] The toxic effects of PCB congeners depend on the number and position of chlorine atoms. Higher chlorinated PCBs has high lipophilicity, chemical stability, and low hydroxylation, it makes them persist longer in body, and they can have half-lives of 10-15 years.[96] Whereas, low chlorinated PCBs easily metabolite in the body with half-lives of within days. Low chlorinated PCBs and their metabolites have demonstrated of causing mutagenicity, carcinogenicity, and interference with hormone homeostasis.[97–100] Both planar and nonplanar PCBs are toxic as they cause the loss of cell viability.[101] PCBs with biphenyl rings in a single plane are also called dioxin-like PCB congeners. Whereas, noncoplanar PCBs are called non-dioxin like PCB congeners. Dioxin-like PCBs exhibits dioxin toxicity.[102]

For example, there have been two mass poisoning incidents in Yusho (Japan) in 1968 and Yu-Cheng (Taiwan) in 1979 due to contaminated cooking oil.[15] It left 1800 patients in Japan with 300 dead.[103] While in Taiwan, 1991 people were directly exposed including 70 children in utero.[104] It caused symptoms of hypersecretion, acne, pigmentation of skin and nails and also meibomian glands, eye discharge, a decrease of sperm mobility, headache and numbness and a decrease of IQ score in children.[105,106] PCBs were used in cooking oil plants as heat transfer medium during the last manufacturing process and leakage caused the cooking oil contamination with PCBs. The research focused on the long term health effects of the victims from the two incidents demonstrated adverse health effects even after several years of exposure.[97,107] In the year 1968, 400,000 birds in Japan died after eating food contaminated with PCBs.[108] Since the liver is the main detoxifying organ in the human body, it is more affected by the contaminants. PCBs causes the liver damage.[109–111] Studies show that PCBs also targeted the immune system of victims from Japan and Taiwan. They have adverse health effects, including immune system suppression, cancer induction, nervous systems effect, as well as increased inflammatory and cardiovascular diseases.[36,94,112]

2.5 Water quality and need for PCBs sensing

According to the Clean Water Act (CWA), Industrial disposal of PCBs is illegal, and any spill of PCBs is required to be reported to the EPA. The main goal is to keep PCBs level zero in drinking water, however, the maximum level is strictly monitored at 0.0015 µM(0.0005 ppm). According to EPA data from figure 2.5, PCBs fall in 5th place among the water quality impairment in the US. PCBs have more than 6000 impairments out of total 71,795

impairments that are around 8% on the CWA section 303(d) list. There is a need for successful detection of PCBs presence in water and other sources to keep this carcinogenic pollutant away from the human intake.

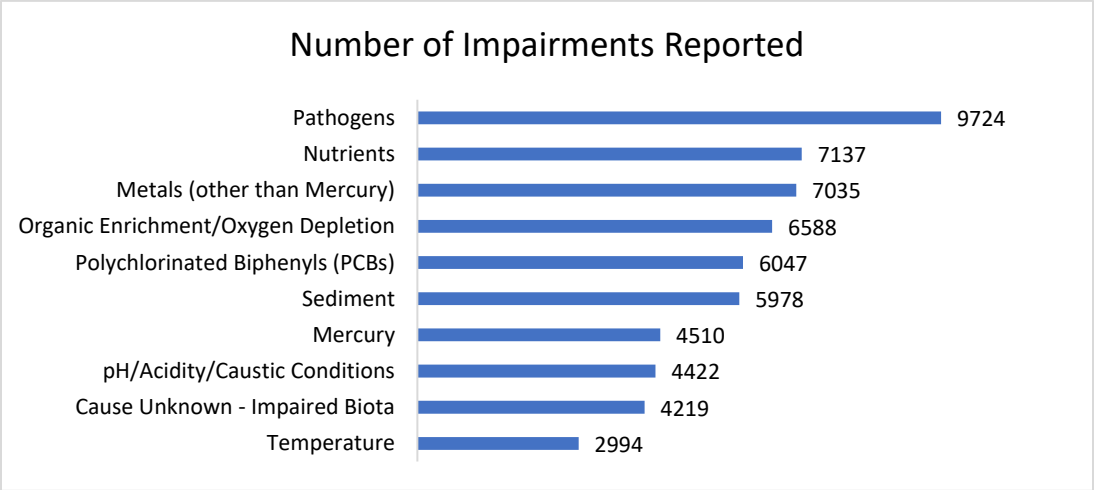

Figure 2.5: Top 10 impairments(adopted from EPA, 2017) [113]

2.6 PCBs detection techniques

With the increasingly harmful effects of PCBs on human and biological life, a lot of efforts have been put into developing techniques that can detect chlorinated and hydroxylated PCBs. There are two main sensing systems, direct sensing of PCBs from the solution and indirect sensing system. In an indirect sensing system, PCB is detected using a second analyte; this analyte is biological or non-biological, it interacts with PCB and the changes in the properties of the analyte give the indirect measurement of PCBs presence. These sensors are further divided into subcategories that are shown in figure 2.6.

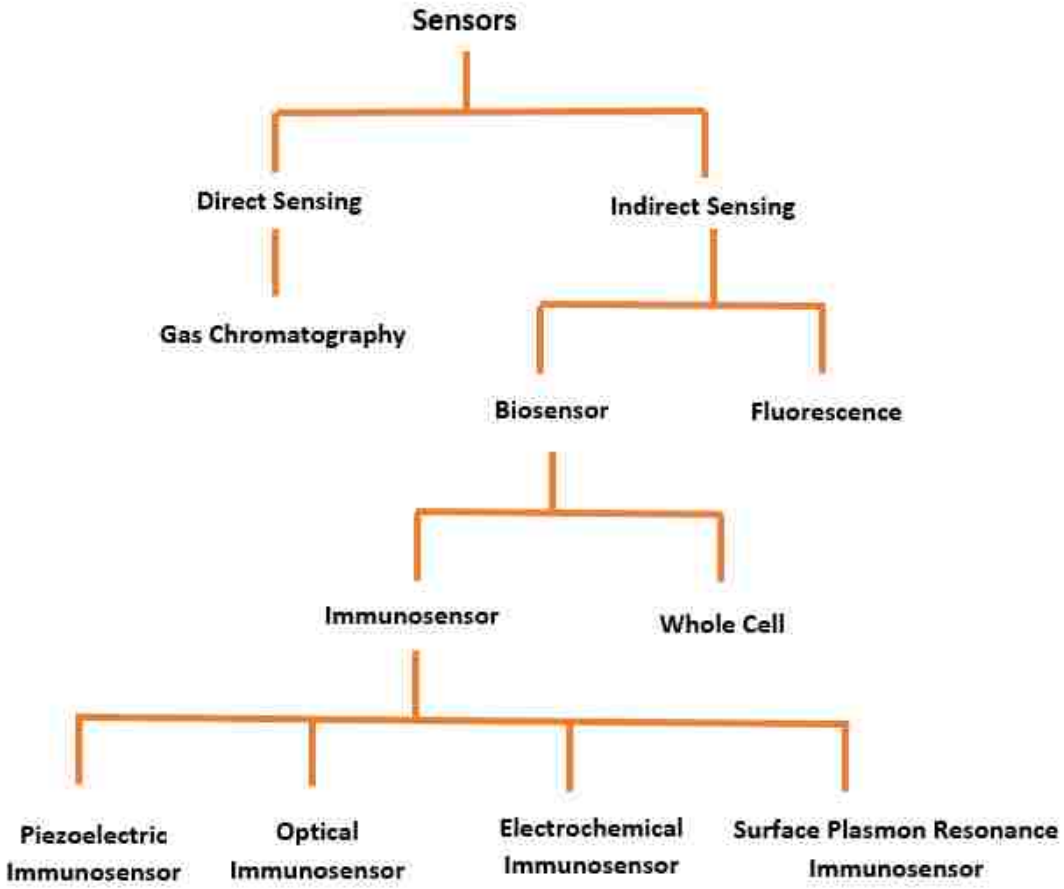

Figure 2.6: Classification of Sensor Technologies for PCB detection and quantification.

2.6.1 Direct sensing of PCBs

2.6.1.1 Gas Chromatography (GC)

GC is a chromatography technique that can vaporize the liquid samples, these vapors are then carried by the mobile phase (inert gas) to the GC column. Depending on the chemistry of the sample, they travel at numerous speeds in the column and separated. Each compound leaves the column one after another and enters the detector. GC is equipped with types of detectors based on the application as shown in figure 2.7. For example, a gas chromatography-electron capture detector (GC-ECD) uses the electron

capturing technique for the detection of molecules. The electron emitter emits electron that causes the ionization of the analyte molecules and it changes the current between collector anode and cathode. The analyte concentration is proportional to the degree of electron capture. GC-ECD is widely used for the sensing of halogenated compounds in the environment. Another type is gas chromatography-mass spectroscopy (GC-MS) that ionizes the chemical species and then separate ions based on the mass-to-charge ratio. It is the most common instrument for the detection of PCBs.[114]

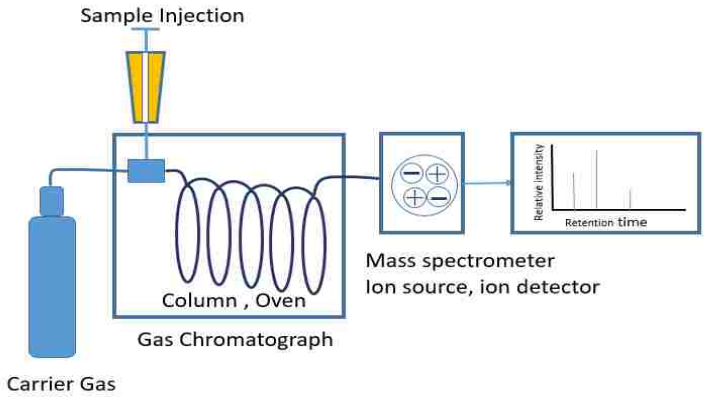

Figure 2.7: Gas chromatogram instrument equipped with the detector and readout.

Since PCB is highly hydrophobic, it attaches to other organic matters (e.g. humic acid) in water or fats in animals or in the human body. PCB must be separated and extracted in hexane and the sample is then fed to the instrument. GC-MS development history goes back to 1950s.[115–117] Today, it is widely used in the detection of compounds. The gas chromatogram is mentioned in literature as early as the 1970s for the detection of PCBs.[118–120] EPA has issued the proper methods of using gas chromatography (METHOD 8082A) for the detection of PCBs. EPA used gas chromatography technique to detect 26 types of Aroclor and PCB congeners using a single or dual column. However, GC is a highly

expensive, time-consuming technique. The reliability and the reproducibility in GC results depend on the highly skilled level of the person operating it.

2.6.2 Indirect sensing of PCBs

Due to the limitations of the GC instrument, indirect sensing techniques are achieving more and more popularity, because of sample preparation ease and relatively low cost. In the indirect sensing technique, a second organic molecule, inorganic metal or biological spices is used. This allows the GC to register the change in response based on the PCBs presence in the sample. GC can also be used as part of the indirect sensing techniques. Indirect sensing includes antibodies, aptamers, biomimetic sensors and surface photovoltage, etc.

2.6.2.1 Fluorescence-based detection

Fluorescence is a technique where a molecule is illuminated at a wavelength; it almost immediately reradiates the light that is detected. The wavelengths of incident emitted light are the characteristics of each fluorescent molecule. Some molecules excited directly, and the emitted wavelength is recorded which corresponds to the concentration of the molecule in the solvent. Some molecules combined in a pair with other molecules for their indirect detection. There are various fluorescence-based techniques listed in the literature to sense molecules e.g. intensity-based sensing, lifetime-based fluorescence response, Förster resonance energy transfer, wavelength shift, wavelength ratiometric response, and anisotropy-based sensing and polarization assays.[121] PCBs and other pollutants cannot be excited directly; however, they are detectable with the help of a

suitable fluorescent molecule. These pairs can cause one or more combinations of changes in fluorescence energy, spectra shift or change in spectral shape.

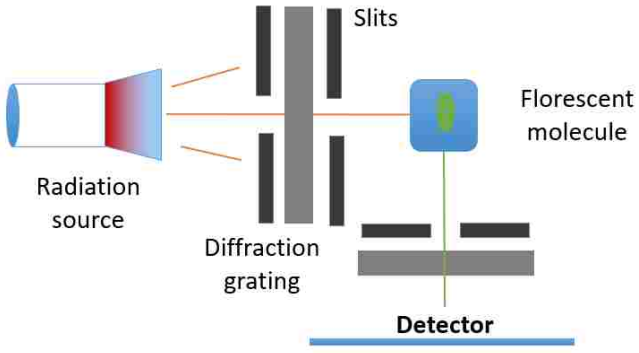

Figure 2.8: Detection using fluorescence spectroscopy.

The operation of the fluorescence instrument is shown above in figure 2.8. The lamp excites the sample at a wavelength, it causes the radiation from the sample and this light is detected by the sensor that gives the indirect measurement of PCBs in the solution. In our published work [122] and in this thesis we have demonstrated successful detection of PCBs using the fluorescence technique.

2.6.2.2 Biosensors

Biosensors are the detectors consist of biological element coupled with the transducer, that makes it a physicochemical detector.[123–125] The biological part can consist of an enzyme, antibody, lipid, receptor, nucleic acid, antigen, organelle, tissue structures or biomimetic component. These biological elements are specific for an analyte with high selectivity; it works like lock and key. When an analyte binds or interacts with the biological component, it changes its properties (density, thickness, elasticity, etc.). These

changes are sensed by the transducer, which in result produces an output signal(optical, electroluminescent, electrochemical, electrical, thermal, acoustical or piezoelectric, etc.) proportional to the analyte concentration. A typical biosensor is shown in figure 2.9. The solution can contain a mixture of unalike analyte molecules. However; bio-receptor have an affinity for a specific analyte. Once the analyte interacts with the receptor, the signal is triggered, and the transducer converts this signal to the readable form. Several types of biosensors have been developed so far for the detection of PCB and its family. These biosensors are categorized based on the biological components used in them.

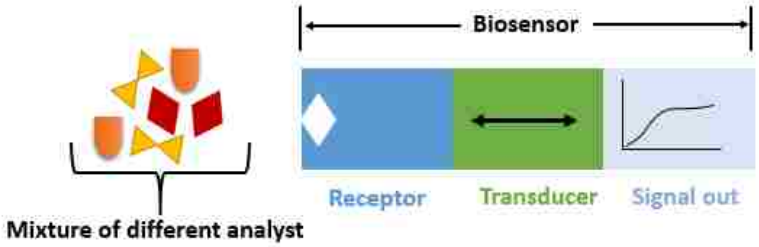

Figure 2.9: In a biosensor, a "receptor" interacts with the analyte, where a transducer converts the signal to an electronic form that is readily measured.

2.6.2.2.1 Whole-cell biosensor

Whole-cell biosensor (WCB) uses microorganisms consisting of bacteria, yeast or other single-cell systems. A typical whole-cell sensor is displayed in figure 2.10. WCB has advantages over other sensors, especially analytical sensors, which detect the total concentration of the analyte regardless of the actual bioavailability. Whereas, living cells reflect the actual bioavailability of the pollutant.[126] This bioavailability is more important for human and animal life. The performance of the WCB is the characteristics of the

selection of reporter genes as well as the sensitivity and selectivity of molecular detection (e.g. PCB) that results from the binding of the analyte to the regulatory protein.[127] Cells are generally experimentally modified and incorporated with both bioreceptor and transducer, to boost the sensitivity.[128]

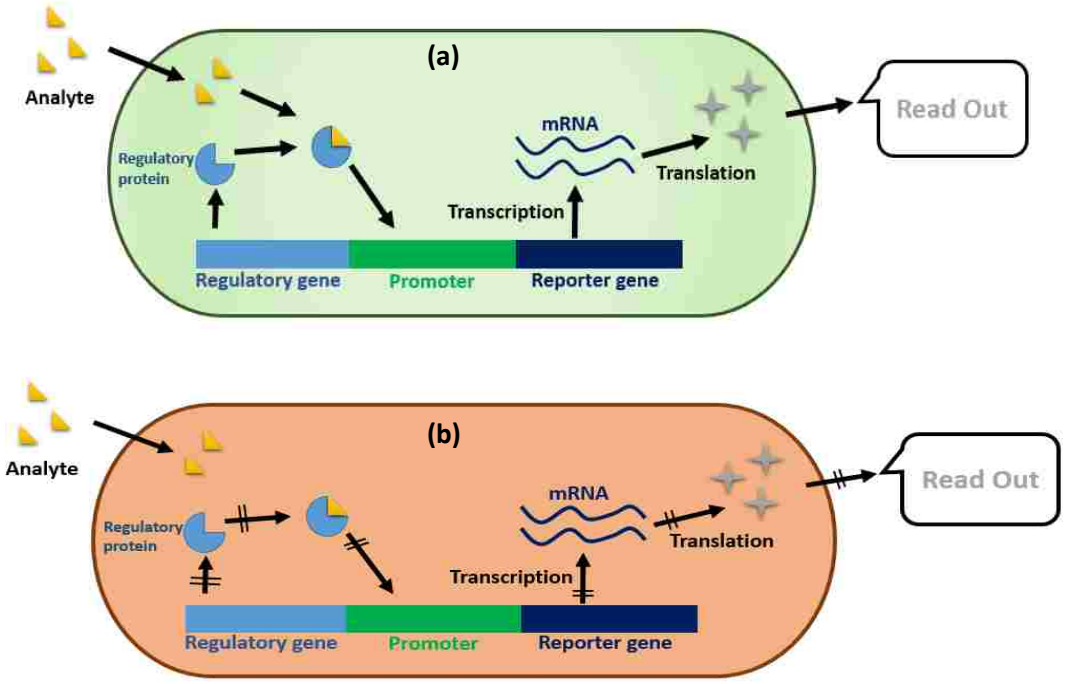

Figure 2.10: (a)- Switched on whole-cell biosensor. (b)- Switched off whole-cell biosensor.

For WCB, bioassays are divided into two types *switched off* and *switched on* assays.[129] In switched off assay based whole-cell biosensors, degree of inhibition is recorded in the cellular normal activity that corresponds to the toxicity of the analyte, this activity can take place at any stage along the reaction pathway as shown in figure 2.10(b). Whereas, in switch on assays, the target chemical promotes the fusion of regulatory protein to the promoter that further triggers the reporter gene for the quantification [129], figure 2.10(a). Gavlasova *et al.*, used the WCB for the sensing of PCBs. The author used the optical

properties for the detection of pollutants. In their work, encapsulated cells of Pseudomonas sp. strain P2 were used, as it can degrade PCBs.[130–133] These cells were recovered from the PCB-contaminated site in the Czech Republic. Cells were trapped in the silica and produced yellow *meta* ring fission metabolite for the indirect detection of PCBs. This WCB successfully detected 0.5 mg/l (Delor 103) and 0.2 mg/l (2.2', 4, 4' CB) with 4 times reusability and 2 weeks storage capacity.

In another work, Turner *et al*., exploited the bioluminescent properties for the detection of hydroxylated polychlorinated biphenyls (OH-PCBs) using WCB. In their work, they used Pseudomonas azelaica strain HBP1. It contains *hbpCAD* genes that are responsible for the degradation of OH-PCB.[134,135] The authors used plasmid (pHYBP109) containing a fusion of "regulatory gene *hbpR*- Promoter *hbpCAD* gene- *luxAB* reporter gene" and it was converted to *Escherichia coli*. OH-PCB interacts with the regulatory gene *hbpR* that triggers the transcription through *hbp* promoter, and it results in expression from *luxAB* reporter gene. The addition of decanal causes the luciferase and this bioluminescence is directly proportional to the OH-PCB.

Xu et al., used the hybrid analytical technique for the detection of PCBs. Their proposed WCB was able to detect biphenyls successfully. PCBs were first converted to biphenyl using Mg/K_2PdCl_6 catalyst. They used *bph* operon to obtain BphR1 regulatory protein. Cells formed 2-hydroxy-6-oxo-6-phenylhexa-2,4-dienoic acid [HOPD] when exposed to the biphenyls and form a complex of HOPD-BphR1. Which activated the *pE* promoter that caused the production of reporter protein of β-galactosidase from *lacZ* gene[136]

proportional to the biphenyl concentration. β-galactosidase was detected using the chemiluminescent technique.

2.6.2.2.2 Immunosensor

Immunosensors are the biological binding sensors that are based on the immunoassay technique. Whereas, the immunoassay is the interaction between antibody and antigen. These sensors are used for the quantification of the analyte based on the reaction between the analyte(antigen) and antibody.[137] Immunoassay is a competitive or non-competitive binding test that is widely used in the detection of diseases, drug monitoring, detection of pollutants and other molecules. In case of competitive binding, an analyte that is unlabeled competes against the labeled antigen and decreases the detectable signal.

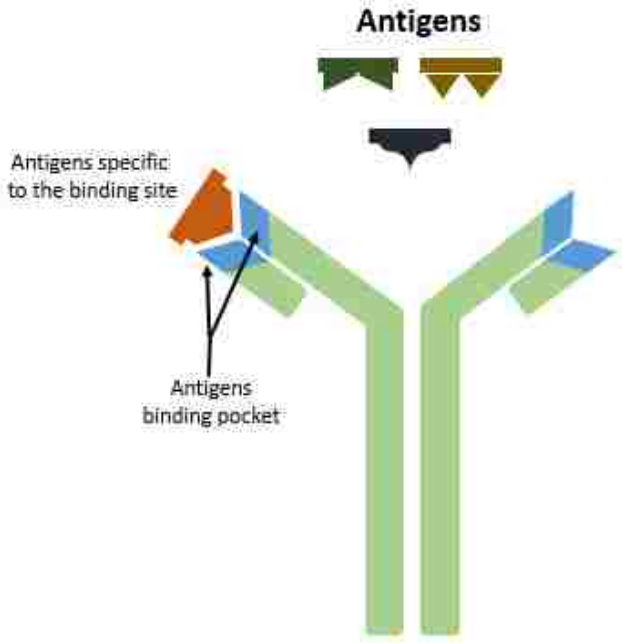

Figure 2.11: Each antibody has an affinity towards the specific antigen.

Whereas, noncompetitive binding uses labeled analyte that generates the signal proportional to the antigen concentration in the system. The resultant signal increases with increasing the concentration of the analyte. Typically, antibody uses for the immunoassay is shown above in figure 2.11. The antibody is also termed as an immunoglobulin (Ig), these are Y-shaped proteins that are produced by plasma cells and are classified by isotype. These proteins differ in their structure, which dictates their functions and specific antigen binding. These proteins are used by the immune system and are categorized into five types of antibodies; IgA, IgE, IgG, IgM, and IgD.[138] These classifications are based on the difference in amino acid sequence in the base area.[139]

Immunosensor is the type of biosensor that consists of mainly two parts, one sensing element known as immunoassay and second, the transducer, that converts the binding event to the readable signals [140], as shown below in the figure 2.12.

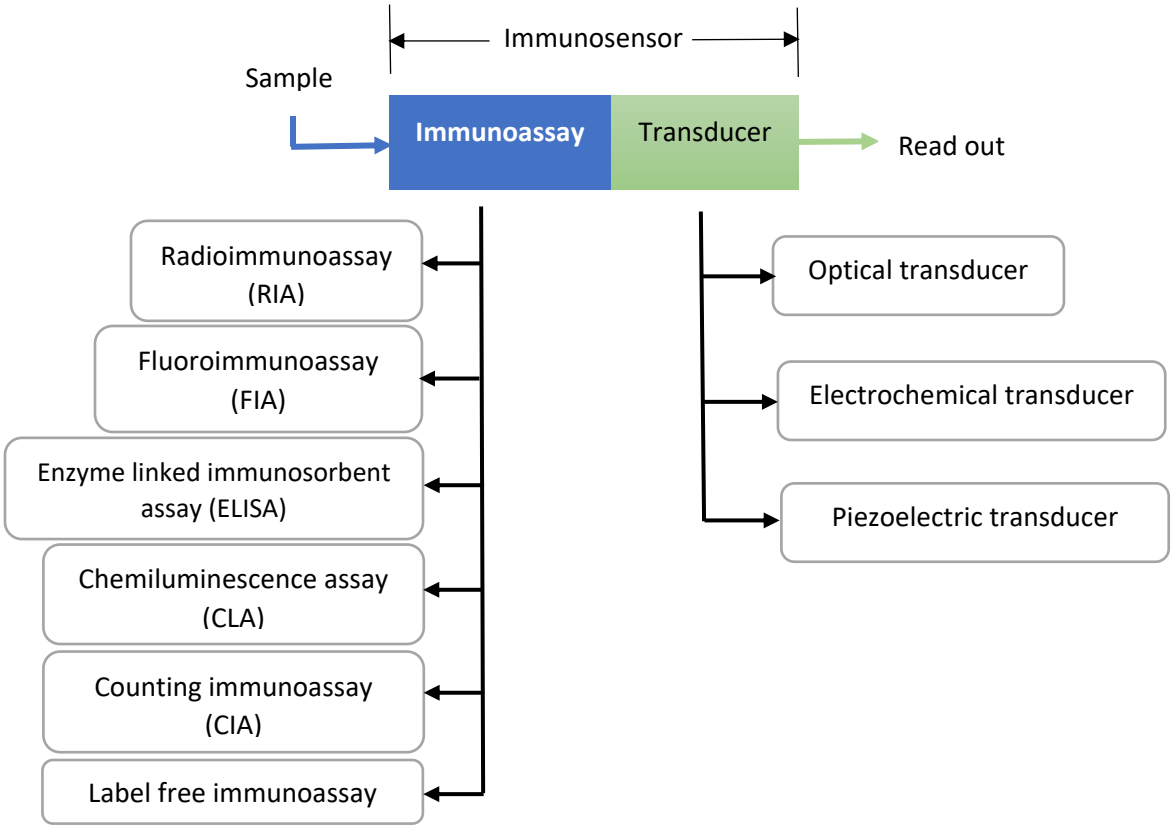

Figure 2.12: Immunosensor consists of two parts, immunoassay, and transducer. Both immunoassay and transducer have different types. Only three types of transducer are mentioned here.

Radioimmunoassay (RIA): These are the earliest assays developed. It uses a radioisotope linked to the antigen that binds to the related antibody. The antigen to be measured is added that competes with the radiolabeled antigen and occupy its binding site. The unbound radiolabeled antigen is washed away, and radioactivity of the antigen-antibody complex is measured. The signal is inversely proportional to the antigen concentration. This technique is outdated because of the potential dangers associated with radioactive labeling.

Fluoroimmunoassay (FIA): In this assay, antigen or antibody is labeled with a fluorescent molecule. After incubation, the antigen-antibody complex is separated, and the signal is measured with the help of fluorescence spectroscopy.

Enzyme-linked immunosorbent assay (ELISA): In this assay, the antibody is linked to the enzyme. This complex is incubated with antigen immobilized to a solid surface. The antibody-enzyme attached to the antigen and unbound is washed away. The enzyme-substrate is introduced that changes the color of the assay.

***Chemiluminescence assay (CLA*)**: This is the variation of ELISA. In CLA enzyme changes the substrate to the chemical product that emits photon instead of the visible light.

Counting immunoassay (CIA): It uses antibody coupled polystyrene beads. Antigen causes the agglomeration of these particles. Free particles are counted using an optical particle counter.

Label-free immunoassay: This immunoassay does not need labeling of antibody or antigen. However, needs special methods of detection that include surface Plasmon resonance, measuring the change in the resistance of the electrode or change in optical properties.

Optical transducer*:* It converts the optical signals (frequency, phase, and amplitude) of the antigen-antibody complex to the readable electrical output.

Electrochemical transducer: It converts the chemical changes of the antigen-antibody complex to the readable electrical output.

Piezoelectric transducer: This transducer converts the change in mass of antigen-antibody complex to electrical signals using quartz crystal.

2.6.2.2.2.1 Piezoelectric immunosensor

Piezoelectric immunosensor is one of the simple very sensitive sensors with high selectivity. It can detect the antigen in gas and in the liquid phase at the picogram level. A typical piezoelectric immunosensor is shown in figure 2.13. Antigen or antibody can be immobilized on the surface. The crystal oscillates under the voltage. When the antigen-antibody complex is formed, it changes the mass of the surface. This change in mass changes the oscillating frequency of the crystal which is a signal for the attached analyte.[141,142] Přibyl *et al*., measured the PCBs in the pure organic solvent and also in

phosphate buffer with 5% DMSO using the piezoelectric quartz crystal. In their work, they used anti-PCB polyclonal antibody immobilized on gold electrodes in an orientation way using protein A.[143]

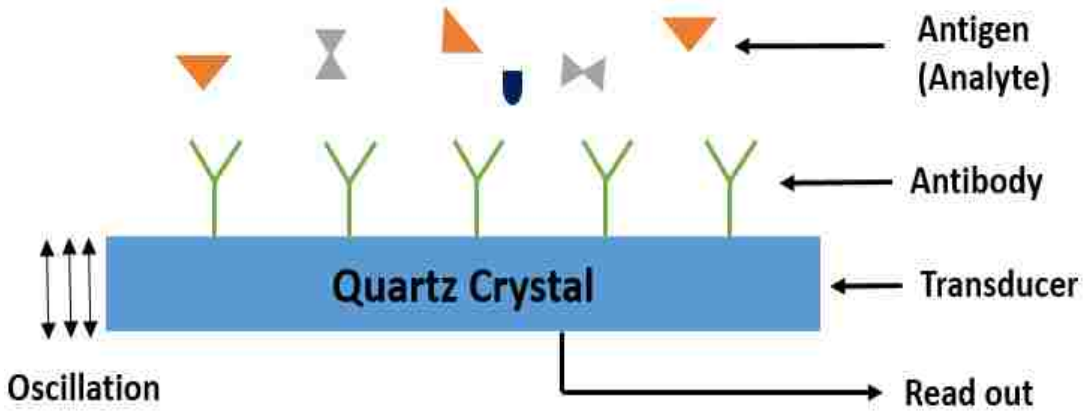

Figure 2.13: Typical piezoelectric immunosensor for the detection of antigen. The specific antigen is attached to the antibody; it changes the oscillating frequency of the crystal.

2.6.2.2.2.2 Optical immunosensor

Optical immunosensor is one of the most popular methods in biosensors, it is mainly because of using visible light with the nondestructive operation, it also has an advantage of rapid signal generation and reading.[144] In this sensor, antigen or antibody is immobilized on the surface of the transducer. The interaction of analyte changes the optical properties, such as emission, absorption, reflectance, refractive index or scattering. Change in the signal is detected with the help of photodiodes or photomultiplier. The optical sensor is shown in figure 2.14, the incident light interacts

with the antibody-antigen complex assembly and measure the change in the signal that is related to the analyte concentration.

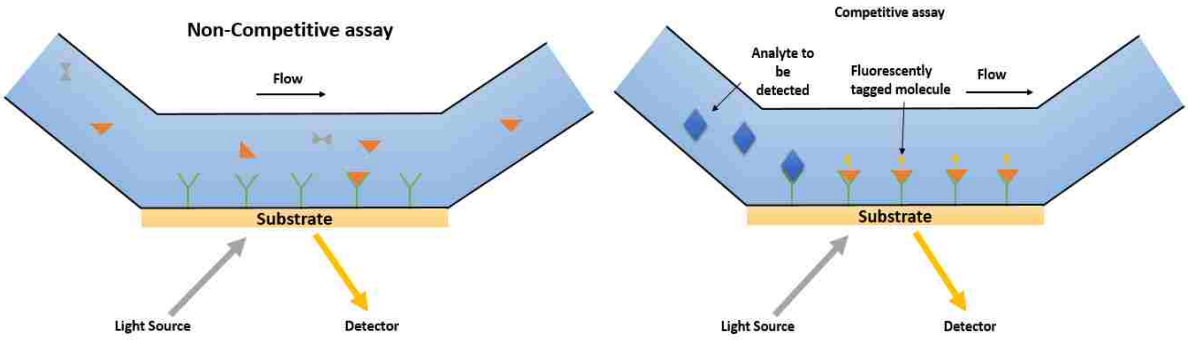

Figure 2.14: The analyte can be detected using fluorescence-based competitive assay or using a label-free method by sensing the change in other optical properties e.g. refractive index, scattering or absorption.

These sensors can use the antibody-antigen complex's optical properties as a non-competitive assay and detect the change in absorbance, scattering or refractive index of the radiations. On the other hand, the sensor can be based on the competitive assay, in which the system is saturated with a fluorescently tagged molecule that will be replaced by the analyte of interest and a decrease in the radiation intensity. Zhao *et al.*, applied fluorescence-based competitive assay to detect PCBs using fiber optic immunosensor.[145] In their work, they coated fiber optic with the polyclonal anti-PCB antibody. This antibody was saturated with fluorescein (FL) conjugate of 2, 4, 5- trichlorophenoxybutyrate (TCPB). The antibody-coated fiber was mounted in the flow cell. When PCBs saturated solution was passed, PCBs replaced the FL-TCPB bound to the antibodies and consequently

decreases the resultant fluorescence signal. Zhao *et al*. successfully detected four different Aroclors(1015, 1232, 1250 and 1262).

2.6.2.2.2.3 Electrochemical immunosensor

In the case of electrochemical sensors, the binding event of the antibody and antigen creates an electrical signal as shown in figure 2.15. This reaction takes place at the interface of the electrical conductor, which is a metal or semiconductor. There are many types of electrochemical sensors such as amperometric sensors (electric current as a signal), electrochemical impedance sensors (voltage difference as a signal), electrochemical luminescence sensors (emission as a signal) and photoelectrochemical sensors (reaction initiates with light and current is produced).[146] Electrochemical sensors have low sensitivity, high reliability, and low power consumption.[147] It is very important to get an amplified signal with minimum noise.[147,148] These sensors are generally equipped with highly affinity-based antibodies and the selection of suitable labeling amplifies the signal.

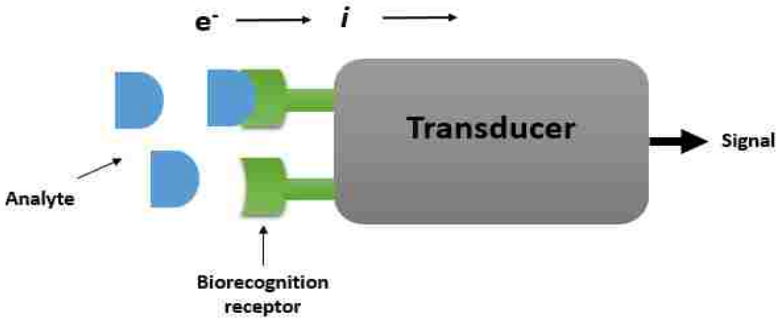

Figure 2.15: The binding event of antigen and antibody causes a chemical reaction that produces a signal.

Most common labels mentioned in literature are carbon nanotubes, bioactive enzymes, magnetic beads, nanoparticles, bi-enzyme system, metal ions, and quantum dot.[140,149–157] Enzyme-linked immunosorbent assay (ELISA) has attained a lot of attraction for quantification purposes of hydrocarbons and PCB like chemicals.[158–160] The redox enzyme produces redox species that is converted to the output signal.[161]

Centi *et al.*, used the IgG PCB28 antibody for the sensing of PCBs (Aroclor 1242, 1248, 1254 and 1016) using disposable magnetic beads coated. Where carbon-based screen-printed electrodes were used as a transducer, enzyme PCB28-AP (4, 4 -dichlorobiphenyl–alkaline phosphatase conjugate) as the tracer and α–Naphthyl phosphate as enzyme-substrate deposited on the screen-printed strip.[162] They measured the electrochemical reaction using differential pulse voltammetry (current against applied potential). Del Carlo *et al*., also used ELISA based enzyme-linked immunofiltration assay (ELIFA^{TM}). They used the nylon membrane to immobilize bovine serum albumin conjugate of PCB. After the competition with Aroclor 1260, 1248 and 1016 (10 ng/ml to 10 μg/ml) in the presence of antibodies, the PCB antigen that reacted with the immobilized PCB was estimated using alkaline phosphate-based antibody. In this work, naphthyl phosphate was used as a substrate for the detection using screen-printed electrodes with differential pulse voltammetry.[163] End*o et al.,* used a micro-flow immunosensor chip for PCBs sensing. They exploited the fluorescence properties of the fluorogenic substrate to indirectly measure the coplanar PCBs. Coplanar PCB antibodies (IgG) were first immobilized on the polystyrene beads and exposed to the mixture of coplanar PCB derivatives (6-[(3, 3’, 4’ -trichlorobiphenyl-4-yl) hexanoic acid, 4-methoxy-3, 3’, 4’-trichlorobiphenyl]) and their

horseradish peroxidase (HRP) conjugate. The introduction of Amplex™ Red dye reacted with the HRP conjugated coplanar PCB derivative and produced fluorescence signal.[164] Bender *et al.,* used the direct electrochemical immunosensor technique. They used pyrrole and polyclonal anti-PCB to synthesize conductive antibody membrane and measured the current as an output signal.[165]

Another type is the photoelectrochemical (PEC) sensors, a simple demonstration is shown in figure 2.16. In PEC instrument light radiation causes a charge transferring reaction between photoactive material, analyte, and electrode.[166] The absorbed photon causes the charge transfer and charge separation that leads to the conversion of the photon to electricity.[167] PEC is equipped with aptamers or antibody to increase the selectivity.[168–170] However, PEC oxidation process can affect the bioactivity of biorecognition molecules.[171] Molecular imprinting technique is the most common technique to overcome this problem.

Shi *et al.*, fabricated a photoelectrochemical sensor for the detection of PCB-101. They used molecular imprinting (MI) technique for high selectivity of PCB-101 in titanium dioxide(TiO_2) nanorods. TiO_2 also gives selective PEC oxidation. MI is used to build PCBs shaped cavities in the matrices for the "lock and key" model. They used fluorine-doped tin oxide (FTO) as a substrate and titanium dioxide as photocatalyst imprinted with PCB-101 pockets.[171] The sensor was first incubated in PCB solution and then a LED lamp of 365 nm was used to irradiate the sensor.

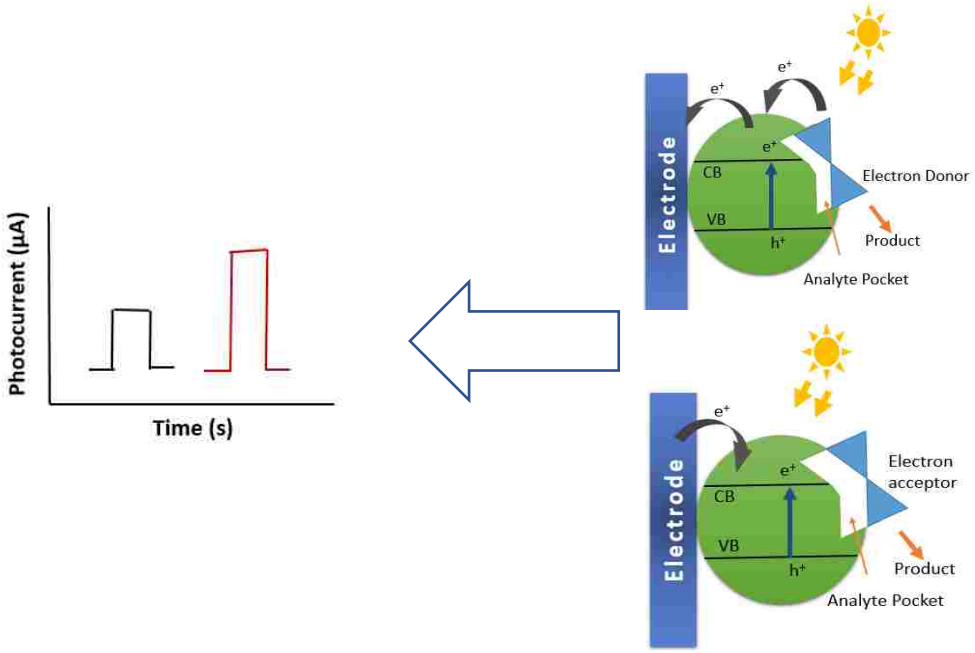

Figure 2.16: Photochemical sensors can have biological binding sites (enzyme or aptamers), or semiconductor material are used with molecular imprinting technique for high sensitivity, selectivity, and stability. CB: conductive band, VB: valence band.

2.6.2.2.2.4 Surface-Enhanced Raman spectroscopy

Raman scattering uses monochromatic light from the laser and molecules cause inelastic scattering of the light. Photons are absorbed and reemitted by the sample that changes their frequency. This shift can provide information about the rotational, vibrational and other low-frequency transition in the molecule. Raman spectroscopy is used in liquid, gaseous or solid samples. Raman spectroscopy has limitations of being very weak. Moreover, fluorescence interruption from impurities and laser can destroy the sample. The weakness of Raman spectroscopy can overcome by using surface-enhanced Raman spectroscopy (SERS). It uses the metal surface with nanoscale roughness for molecule absorbance that enhances the signals as shown in figure 2.17.

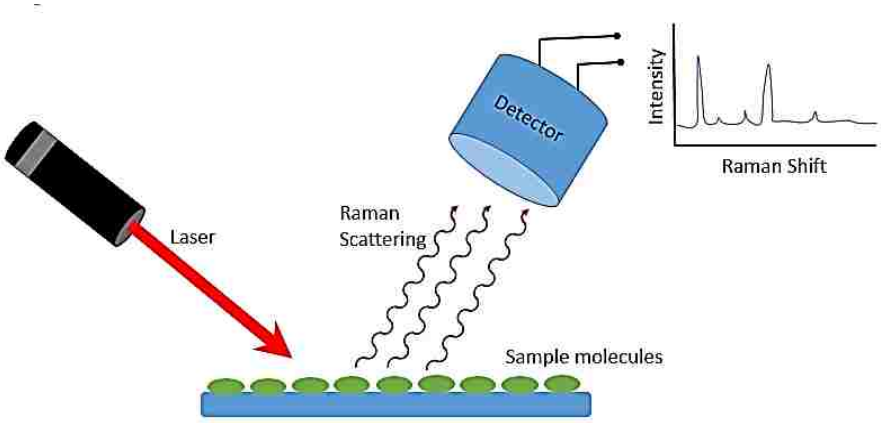

Figure 2.17: Molecules are adsorbed on the rough metal surface for enhanced spectroscopy.

The enhancement factor SERS are from 10^{10} to 10^{11}.[172,173] Which enables it to detect the presence of a single molecule.[174–177] Zhou *et al*. used the silver nanorods as a substrate for SERS. First, the rod was incubated in PCB solution in acetone for 30 min then spectroscopy was performed for PCBs detection.[178] Steenland *et al.*, utilized thiol (decanethiol) based partition layers on silver film over nanosphere substrate. The layer was incubated in PCBs (PCB-47 and PCB-77) solution for 4 hours and then spectroscopy was performed.[86] Fu *et al.*, used aptamers modified SERS microfluidic sensor for PCB 77 detection. They covalently attached mercapto aptamers to the Ag nanocrown array using thiol linker. These aptamers have high selectivity for PCB 77 that increased the selective detection of PCB 77 by SERS.[179]

2.6.3 Sensors limitations

Although biological and non-biological sensors provide exciting opportunities for the detection of PCBs. However, these sensors have some limitations, for example for biosensors, enzyme extraction, isolation and purification cost are high. The enzyme might lose the activity after immobilization on the transducer. Furthermore, sensors consisting of a single cell have longer response time and substrate needs to be transported into the cytoplasm. Whole-Cells biosensors need to be reenergized after use to overcome the longer recovery. In case of antigen/antibody, the binding reaction is usually very stable and stronger conditions are needed to reverse the reaction to reuse the biosensor. For magnetic biosensors, nonspecific interaction can take place between magnetic nanoparticles that can lead to false-positive or artifacts in the measurements.[25,26] Whereas, gas chromatography(GC) is a complex and very expensive technique.[180,181] GC needs tedious time-consuming sample preparation and extraction steps that increase the chances of error in the analytical method, it can also affect the analysis through decomposition or loss of analyte.[182] In extraction steps GC uses organic solvents such as hexane and chloroform in relatively higher volumes that are not nature-friendly.[183]

In our current work, we used the fluorescent spectroscopy technique, which is a relatively low-cost method. Fluorescent technique can detect the interaction between two molecules based on their fluorescence properties in the form of energy transfer or quenching. Combinations of different fluorophore pairs are screened for the displacement assay to detect PCBs in water. Furthermore, PCBs also show the presence of hydrophobic interaction with another dye in water. The presence of hydrophobic dye

and PCBs form a complex, which possesses new fluorescent properties. This interaction is also sensitive to different water properties. Additionally, the hydrophobic interaction of PCBs and fluorophore is also studied using hydrophilic polymer microparticles functionalized with the dye.

2.7 Conclusions

PCBs are very toxic carcinogenic chemicals and their toxicities are known worldwide. There are fast-growing sensing techniques summarized in figure 2.6 as an alternative to the gas chromatography. These sensing systems vary from direct sensing of PCBs in pure organic solvents to the indirect sensing systems using various kinds of biological or biomimetic systems with different transducer systems. The sensitivity of these sensors is very important. Fluorescence or optical-based sensors with biomimetic nature can soon attain a lot of attention because of their sensitivity, selectivity, life span and easy to use. This chapter summarized the PCB's toxicity and the sensing methods used in literature so far. These sensors have exciting wide range of applications to detect analytes in the environment. However, PCBs have 209 distinctive congeners and most of the methods used in literature are limited for specific PCBs. There is still a need to develop a system that is not specific to only one type of PCB, relatively low cost and fast to use. In the upcoming chapters, we have evaluated unique new methods for PCBs sensing in water.

CHAPTER 3: SYNTHESIS, DESIGN, AND EVALUATION OF POLY(CURCUMIN) MPS FOR THE FLUORESCENT DETECTION OF PCBS USING A DISPLACEMENT ASSAY

3.1 Introduction

PCBs are comprised of two benzene rings connected with a single carbon-carbon bond and can contain anywhere from 1 to 10 chlorine atoms. There are many techniques that can detect PCBs as mentioned in chapter 2. However, all these techniques have limitations that reduce their portability and ease of use. In this work, we have evaluated a new technique of sensing PCBs in water using fluorescence spectroscopy. This technique is relatively low cost, highly sensitive and fast that can be miniaturized for the field applications. Fluorescence spectroscopy uses light to excite a molecule at a particular wavelength, which absorbs the light, resulting in the excitation of the molecule to a higher energy state. The excited molecule releases the absorbed energy in the form of radiative or non-radiative emission. In non-radiative relaxation, energy is transferred as vibrations or heat to the solvent without any photon emission and in case of radiative relaxation, energy is released in the form of the photon as shown in figure 3.1. Since energy loss takes place during vibrational relaxation, the emitted photon has lower energy as compared to the excitation photon that results in a red-shift of the emission spectra.[184] PCBs have very weak UV absorbance at 257 nm. The shape of the fluorescence spectra for various PCBs is almost identical, which makes them hard to distinguish. However, other fluorescence techniques that include indirect sensing approaches can be utilized to detect the presence of the molecule that is otherwise not able to be directly detected. For example, researchers have successfully used Förster resonance energy transfer(FRET) or

quenching, the formation of new excimers, shifting of fluorophore wavelength and ratiometric measurement of wavelengths, as a way of identifying the presence of non-fluorescence or low fluorescence molecules.[185]

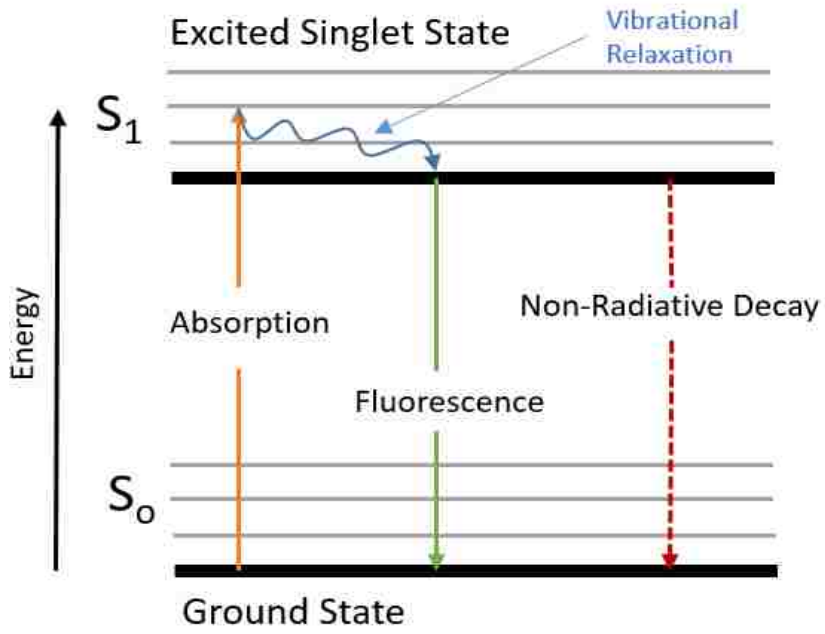

Figure 3.1: Jablonski diagram illustrating the radiative and nonradioactive decay. The absorption of a photon moves an electron to a higher energy state. Some of the energy is lost in the form of vibrational relaxation. The electron moves to the ground state after emitting a photon of a different wavelength.

Fluorescent displacement methods (using FRET/quenching) are also mentioned in literature as an alternative way to detect analytes in solution. This technique can also be developed for PCBs sensing. Kattke et al. designed the FRET-based immunoassay for the detection of *aspergillus amstelodami* using the quantum dot (QD) and black hole quencher (BHQ) with the antibody, in which BHQ is displaced by the *A. amstelodami* due to its higher affinity.[186]

In this chapter, special emphasis is given to the plant-derived polyphenols (e.g. quercetin, curcumin, flavonoids, etc.) for the detection of PCBs. Polyphenols have good fluorescence properties and some of them are used in dyes.[187] The presence of an aromatic ring indicates the structural properties of polyphenols are exploitable for the molecular imprinting and π-π stacking. Curcumin, which is a natural yellow-orange dye has been used as a fluorescent sensor for ions.[188,189] Curcumin can interact with other molecules to make a quenching pair. The curcumin-based system in our research group has demonstrated the successful binding of PCBs in the water. To enhance the efficiency of displacement pair a stable backbone system is proposed comprising of the polymeric network.

Polymers have a wide range of applications for environmental remediations such as removal of lead, zinc and mercury ions.[190,191] Melvin et al. studied the sorption of PCBs to three food packaging films including polyethylene, polyvinyl chloride (PVC), and polystyrene.[192] Polyethylene showed higher uptake of PCBs as compare to the other two polymers, which indicated the particles fabricated with polyethylene have enhanced affinity for PCBs. Molecular imprinting is the new technology where template-shaped cavities are created in polymer matrices to form a stable polymer with selectively high molecular recognition properties.[193] Meng et al. fabricated the molecular imprinted polymer for the sorption of estrogenic pollutants from the water using alpha-estradiol as a template.[194] Schematic of molecular imprinting is shown in figure 3.2 (a). More recently, growing attention has been bestowed to polymers equipped with biomimetic pockets due to their high affinity and selectivity.[195,196] Researchers have successfully mimicked the

interactions present in the biological system to develop synthetic materials with remarkable new properties for the detection and capturing in various fields of engineering, medicines, nanotechnology, biotechnology, and many others.[197–200] Biological elements (e.g. proteins, peptides, ssDNA, etc.) were incorporated into the synthetic architectures to design biohybrid materials. Researchers have developed porphyrin-containing compounds, which possess enhanced binding properties for the detection of environmental contaminants such as pentachlorophenol and paraoxon.[201,202] PCBs have been extensively studied to understand its interaction and binding with the biological taxonomy.[203–205] For example, antibody S2B1 possesses high selectivity and binding affinity for non-ortho, coplanar chlorinated PCB congeners. Pellequer et al. performed the computational analysis to study the PCB binding pockets of antibody S2B1[203] as shown in figure 3.2(b,c). PCB-specific antibodies form sterically constrained pockets with highly aromatic residues of tyrosine and tryptophan.[203,206,207] This permits the π-π stacking interactions between PCB and antibody. Similar binding associations are seen in environmental interactions between PCBs and humin matter in soil and sediments. [208–210] These biomimetic binding pockets can be synthesized into the polymer system using aromatics moieties for adsorption and dislodgment of fluorescent molecules with PCBs. The simple concept of this combination is shown in figure 3.2(d).

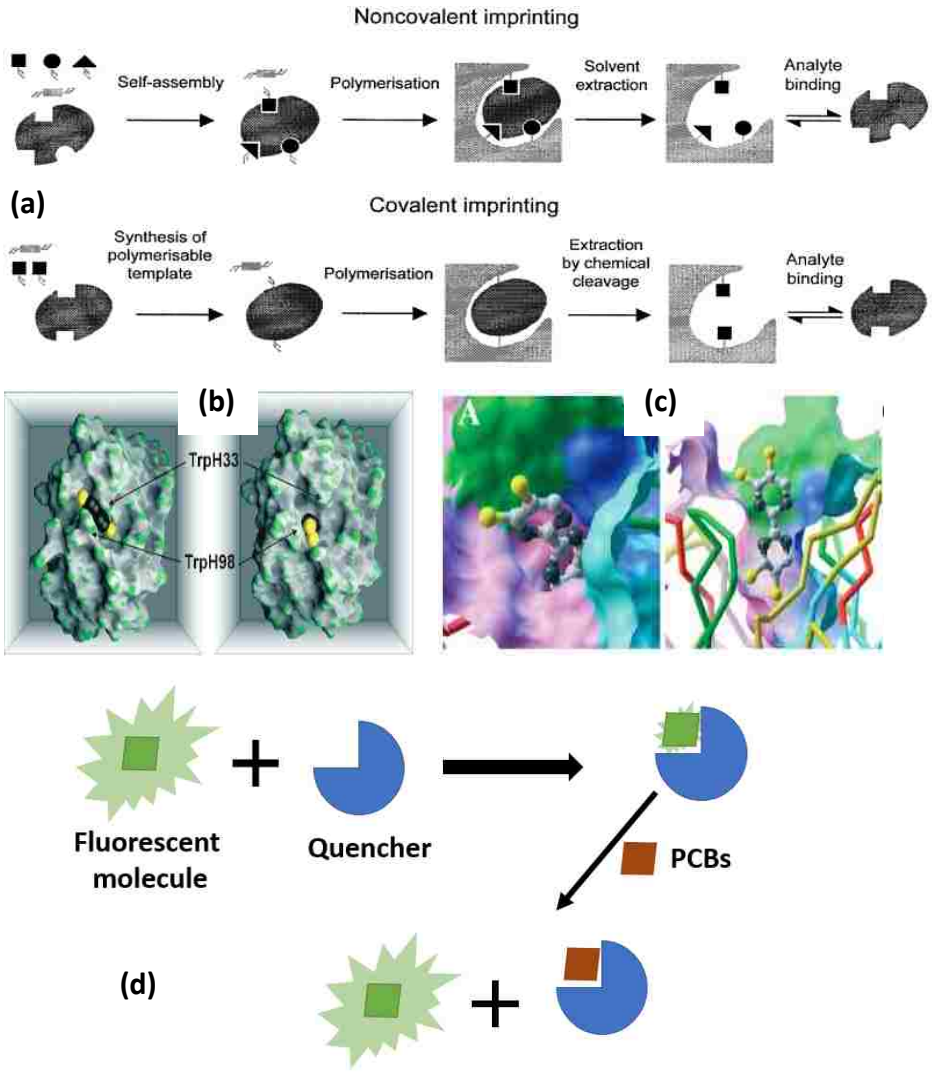

Figure 3.2: (a)- Schematic representation of noncovalent and covalent molecular imprinting procedure to create molecular recognition pockets in the polymer network.[197] (Reprinted with permission from Haupt, K. & Mosbach, K. "Molecularly imprinted polymers and their use in biomimetic sensors". Chem. Rev. 100, 2495–2504 (2000). Copyright (2000) American Chemical Society). (b)- Molecular surface representation of the S2B1 model, rendered using GRASP. The antibody has pockets for PCB77, (Molecular surface view of deep pocket). (c)- View with surface cut away to show binding of the rings in deep and shallow pockets.[203](Reprinted with permission from Pellequer, J. et al. "Structural basis for preferential binding of non-ortho-substituted polychlorinated biphenyls by the monoclonal antibody S2B1". J. Mol. Recognit. An Interdiscip. J. 18, 282–294 (2005). Copyright (2005) John Wiley and Sons). (d)- Fluorescent molecule being quenched when it encounters the quencher and restores its fluorescence upon displacement with PCB molecule.

Where a fluorescent molecule will be quenched with the help of a quencher and it will be replaced by PCBs and after the replacement, the fluorescent molecule will restore its fluorescence properties. In this chapter, we hypothesized that PCBs can be indirectly detected by using the displacement assay in the combination of the polymer system. One of the molecules is trapped with the polymer structure and other molecules will be free for displacement. The trapped molecule will provide a binding cavity for the dye. The whole concept of this work is summarized in figure 3.3.

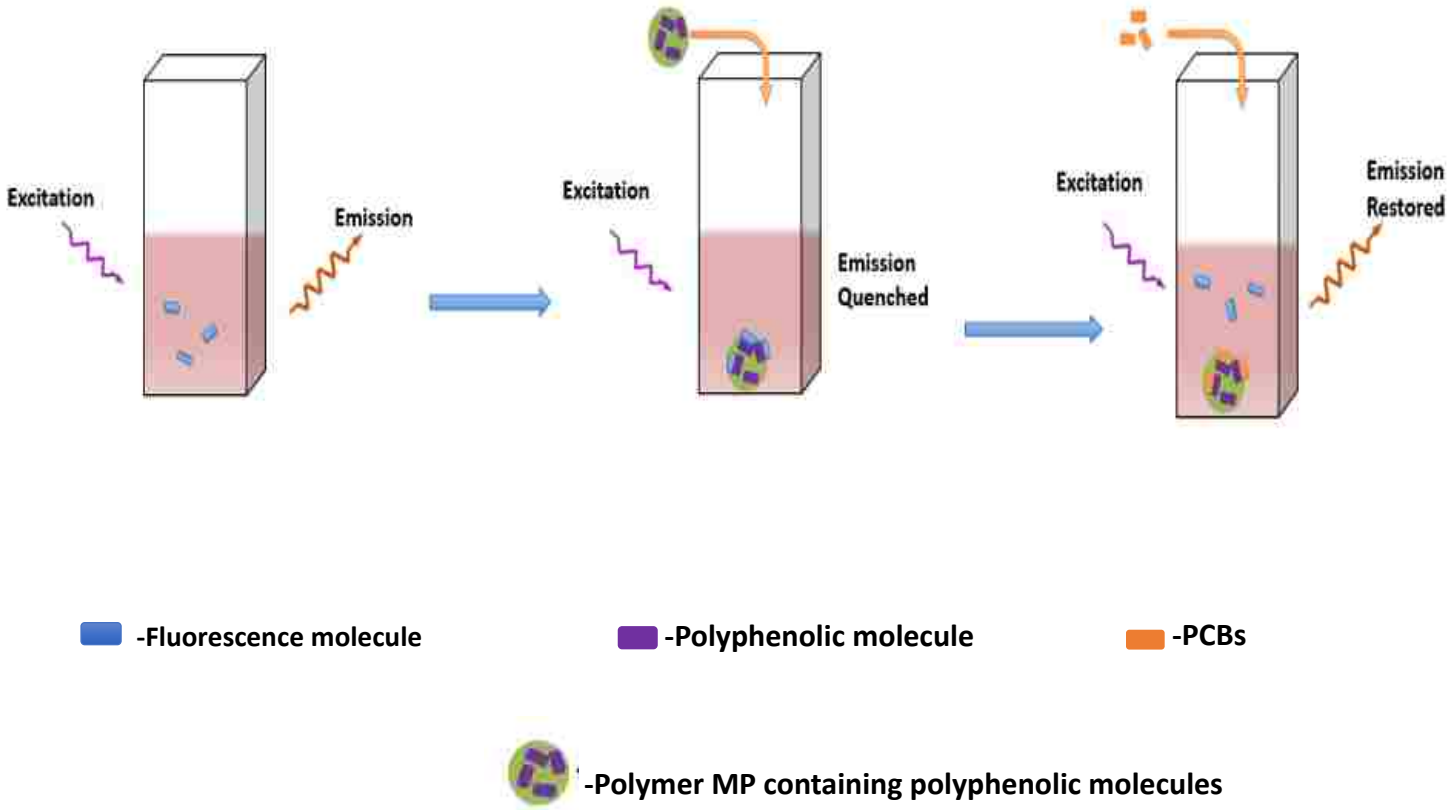

Figure 3.3: Displacement assay for the detection of PCBs. Polyphenolic molecules provide the biomimetic pockets and quenching interaction for the dye. Whereas, PCB replaces the dye and restores its signal back into the solvent away from curcumin

3.2 Experimental section

3.2.1 Material

Curcumin was purchased from Chem-impex International, Inc, (Wood Dale, IL). Acryloyl chloride, triethylamine (TEA), magnesium sulfate ($MgSO_4$), ammonium persulfate (APS), *N*,*N*,*N*',*N*'-tetramethylethylenediamine (TEMED), chlorogenic acid, potassium carbonate (K_2CO_3) were bought from Sigma-Aldrich (St. Louis, MO). Hydrogen chloride (HCl) and calcein red-orange were purchased from Fisher Scientific (Hampton, NH). Dimethyl sulfoxide (DMSO), ethanol (EtOH), dichloromethane (DCM), isooctane, acetone, acetonitrile (ACN) and anhydrous tetrahydrofuran (aTHF) were purchased from Pharmaco, (Brookfield, CT). Deionized (DI) water was obtained from a Milli-Q water purification system. Biphenyl, 3,3',4,4',5-Pentachlorobiphenyl (PCB-126), 2,2',4,4',5,5'-hexachlorobiphenyl (PCB-153) and 2,3',4,4',5-pentachlorobiphenyl (PCB-118) were purchased from AccuStandard Inc., (New Haven, CT). Poly(ethylene glycol) diacrylate (400 MW) (PEGDA) was purchased from Polysciences, Inc. (Warrington, PA). Benzo[a]pyrene (BaP) was purchased from Alfa Aesar, (Haverhill, MO). Molecular sieves of 3 angstroms were added to the solvents to keep them dry.

3.2.2 Methods

3.2.2.1 Screening of polyphenolic and non-polyphenolic molecules

For screening purposes, a variety of diverse molecules were selected, and their emission and excitation spectra were studied in DCM. Several polyphenolic molecules were studied. During the quenching process, they were paired with polyphenolic and non-

polyphenolic molecules. Based on the spectra overlap benzo[a]pyrene (BaP) was selected as a dye and curcumin as a quenching molecule.

3.2.2.2 Synthesis of curcumin multiacrylate

Curcumin multiacrylate was prepared using the developed protocol in the literature.[211] First, the solvents were dried with 3 angstroms molecular sieves for 24 hours. Curcumin was dissolved in aTHF in a three-neck round bottle. While TEA was introduced into the solution at curcumin: TEA concentration of 1:3 and the solution was purged with nitrogen gas. After that, acryloyl chloride was added dropwise under continuous stirring in an ice bath. The mixture was kept under dark conditions overnight. The precipitates of triethylammonium chloride were separated using vacuum filtration. THF solvent from the reaction was evaporated using rotary evaporation to obtain a solid product. This product was dissolved in DCM and an equal volume of 0.1M HCl was added to remove unreacted TEA. The solution was mixed and centrifuged to get an organic layer of product and DCM. Whereas, the excess acryloyl chloride was removed by mixing with an equal volume of 0.1 M potassium carbonate(K_2CO_3) followed by mixing and centrifuging. The organic phase of the product was separated. Lastly, the moisture was removed from the solution by adding magnesium sulfate($MgSO_4$) until no more bubbles were escaping from the solution. The resulting solution was filtered to remove magnesium sulfate and the solution was evaporated to get a yellow powder product. This product was stored in -20 ^oC conditions in a sealed bottle with desiccator packs until future use.

3.2.2.3 CMA loaded polyethylene glycol diacrylate microparticles

In order to prepare curcumin loaded PEGDA microparticles (MPs), APS was used as a free radical initiator and TEMED as a radical accelerator. APS and CMA stock solutions of 0.2 g/ml were prepared in DMSO. PEGDA was weighed in a glass vial and then the required volume of CMA stock solution was added to make CMA 6 mol% in the polymer. The mixture was vortex mixed to ensure uniform mixing. A glass template was prepared using two glass plates separated by the Teflon spacer. Sides and bottom of the template were covered with parafilm to avoid any leakage. In addition, binder clips were used to hold the plates together. APS (2wt %) and TEMED (APS/3) were introduced to the PEGDA/CMA solution. Total free DMSO was kept constant in a volume ratio of monomer to DMSO (3:1). The mixture was vortex mixed for a couple of seconds and transferred to the glass template using a pipette. Glass template was covered with aluminum foil and let it polymerize overnight. The film was then separated from the template and washed first with DMSO, followed by ACN:DCM (1:1) then Ethanol:DI water (1:1) and finally with DI water alone. The film was separated and dried in the freeze dryer.

The dry film was then cryomilled to obtain microparticles using a SPEX Sample Prep 6875D Freezer/Mill using liquid nitrogen. The film was cut to fit within the stainless-steel milling tubes. The film was subjected to two milling cycles of 10 minutes each at 15 cycles per second CPS (max), with 3 minutes pre-cool and 5 min cooling in between two cycles. Microparticles were then collected and dried overnight in the freeze dryer and stored in a dark cold place.

3.2.2.4 BaP concentration study in DMSO/water solvent

To check how much BaP was loaded in 25% DMSO solvent without being crashed, different BaP concentrations were introduced into the solvent system and their spectra were recorded. The concentration of BaP and peak intensity were plotted to analyze the allowable limit of BaP.

3.2.2.5 Equilibrium time for BaP incubation with MPs

In order to, find the incubation time for BaP binding to the MPs, Poly(curcumin) MPs were loaded in a 2ml solvent containing 25% DMSO. Two types of samples were prepared here, in one sonicated MPs were used and in the second MPs were used without sonication to see the difference in the uptaking of BaP. After that, 2 µM of BaP was introduced to the samples. For each time point, three samples were prepared in a 7ml glass vial. The vials were covered with aluminum foil to minimize light exposure. Samples were placed on the plate shaker under continuous shaking. At a specific time, samples were centrifuged, and the supernatant was separated and analyzed in the fluorescence spectroscopy for both sonicated and un-sonicated MPs. After that, optimum conditions were determined for the next steps.

3.2.2.6 Maximum loading of BaP to the MPs

Poly(curcumin) MPs (1mg/ml) were dispersed in 25% DMSO solvent and then 9.1 µM of BaP was introduced in the solvent; vials were kept on the plate shaker. After that, BaP concentration was increased in stepwise fashion at 0.8 µM increments every 30 mins to a maximum concentration of 9.4 µM in the solvent. For each addition, separate samples

were prepared, and supernatant fluorescence spectra was recorded for free BaP in the solvent. Poly(curcumin) MPs loaded with 5.5 µM of BaP were selected for further studies. MPs were separated using centrifuging, dried overnight and then dispersed in isooctane for 12.5 hours to remove all the bounded BaP from the Poly(curcumin) MPs to the solvent. Fluorescence intensity of BaP was recorded in isooctane and from the calibration curve, the mass of BaP adsorbed to the MPs was calculated.

3.2.2.7 PCB detection through displacement

For the PCBs detection system, PCBs stock solution was prepared in DMSO. BaP (5.5 µM) loaded dried poly(curcumin) MPs (1mg/ml) were used. In order to facilitate the displacement of BaP from the MPs, organic solvent was introduced along with water. For this purpose, DMSO was kept at 5% and 10% in water. BaP loaded poly (curcumin) MPs were introduced into the solvent without any sonication and then PCB was introduced into the glass vials. Samples were placed on the plate shaker for 24 hours for maximum displacement. Glass vials were also covered with aluminum foil to minimize the light exposure. After 24 hours, the supernatant was separated using centrifuging and analyzed for the displaced BaP in the solution.

3.2.3 Characterization

3.2.3.1 High-Performance Liquid Chromatography (HPLC)

CMA was analyzed using reverse-phase HPLC (Water Phenomenex C18 column, 5 µm, 250 mm (length) x 4.6 mm (ID) on a Shimadzu Prominence LC-20 AB HPLC system. 1 ml solution of CMA was prepared in acetonitrile with a concentration of 100 µg/ml. A

gradient from 50/50 acetonitrile/water to 100/0 acetonitrile/water over 30 min at 1 ml/min was used with the column chamber set at 40 °C. The injection volume was 50µl for the sample. The chromatogram was recorded with elution time at 420 nm.

3.2.3.2 Particle size analysis

The particle size distribution was analyzed using Shimadzu SALD-7101 UV particle size analyzer operated using WingSALD software (ver. 1.02, Shimadzu). The refractive index was set to 1.4. First, the instrument was filled with water for blank calibration. After that, around 2 mg of MPs were dispersed into the water and sonicated for 2 minutes. The sample was introduced into the instrument and measured under stirring. Each sample was measured into triplicate.

3.2.3.3 Microscopy analysis

Poly(curcumin) MPs were dispersed into the water. Then few drops were introduced onto the glass slide. The water was evaporated, and particles were analyzed under an inverted optical microscope with epifluorescence attachment (Nikon) for Poly(curcumin) MPs shape and curcumin presence.

3.2.3.4 Fluorescence spectroscopy

Fluorescence spectroscopy was performed using a Cary Eclipse spectrophotometer. Samples were introduced into the spectrophotometer using a quartz cuvette from Starna Cells, Inc., (Atascadero, CA). All the samples were excited at 306 nm excitation wavelength and emission peak was recorded at 407 nm.

3.2.3.5 Fluorescence lifetime measurement

Fluorescence lifetime was measured using Horiba Scientific DeltaHub™ high throughput TCSPC (Time-Correlated Single Photon Counting) controller,(Kyoto, Japan). The solution of BaP and curcumin were prepared in DCM and excited at 393 nm.

3.3 Results and Discussion

3.3.1 Screening of fluorescent displacement assay

In order to identify a suitable displacement pair for PCBs sensing, various combinations of donor and acceptor molecules were screened. There are two types of quenching that can take place between two molecules, one is dynamic quenching (also known as FRET quenching) and the second one is static quenching. In dynamic quenching, quencher excitation spectra should overlap the emission spectra of the dye as shown in figure 3.4(a). Dynamic quenching occurs when an excited fluorophore exchanges its energy with a molecule or an atom in a non-radiative transition to the ground state. Energy transfer in dynamic quenching is a strong function of the distance between the two molecules. Whereas, in static quenching, the fluorophore forms a stable complex with quencher molecule in the ground state i.e. before the excitation occurs. When this complex is excited it instantly returns to the ground state without emitting a photon (figure 3.4(c)).[212] Both quenching can also take place at the same time. Based on the spectra overlap in figure 3.4(d), it was found that benzo[a]pyrene(BaP) possesses very good donor properties with curcumin as an acceptor/quencher molecule. BaP has an octanol-water partition coefficient of 6.07[213] and PCB-153 has an octanol-water partition coefficient of

7.79.[214] Given these molecules are both very hydrophobic, it was hypothesized that PCB's greater hydrophobicity would competitively displace BaP from the polymer binding sites. BaP and curcumin pair was first evaluated in DCM. BaP concentration of 2 µM was dissolved in DCM and then the solution was spiked with curcumin.

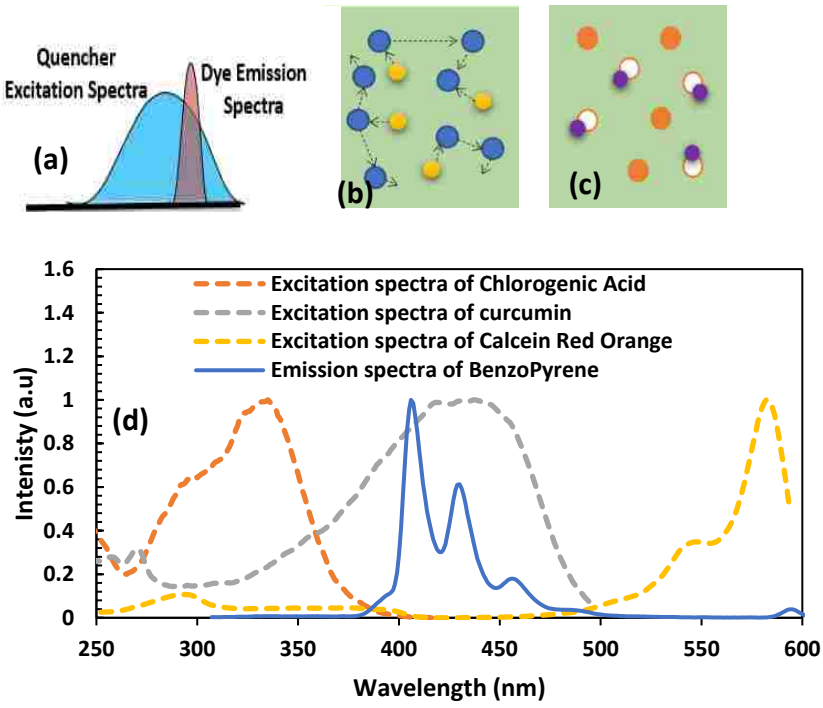

Figure 3.4: (a)- Spectra overlap for dynamic quenching. (b)- The collision of molecules that can cause dynamic quenching. (c)- Molecules are sticking together to make a non-fluorescent pair for static quenching. (d)- Curcumin excitation spectra overlap with the emission spectra of BaP; curcumin is a good quencher for BaP dye.

The effect of curcumin on BaP fluorescence spectra is shown in figure 3.5(a) and the peak ratios of BaP and curcumin are shown in figure 3.5(b). Quenching can either be dynamic quenching (equation 1) or static quenching (equation 2). Both quenching results in a straight line for the intensity ratio of the dye and are represented with the following equations.

$$\frac{I_o}{I} = (1 + K_d[Q]) \qquad \text{-(1)}$$

$$\frac{I_o}{I} = (1 + K_s[Q]) \qquad \text{- (2)}$$

Where,

I_0 = BaP peak intensity without curcumin

I = BaP peak intensity in the presence of curcumin

Q = The concentration of the quencher

K_d = Stern–Volmer constants for dynamic quenching

K_s = Association constant of the static complex

Both dynamic and static quenching cause a straight line for intensity ratio of the dye as shown in figure 3.5 (b) and in equations 1 and 2. It needs an additional experiment to differentiate the mechanism of quenching involved here. It was verified using one of the two ways. One, using temperature-based studies. Both static and dynamic quenching are temperature sensitive. In static quenching, pair forms a complex and only those dye molecules are excited which are not in the complex as described in figure 3.4(c). Increasing the temperature disfavors the complex formation and it lefts more dye

molecules without the quencher. Thus, in static quenching, increasing the temperature decreases the quenching ratio.

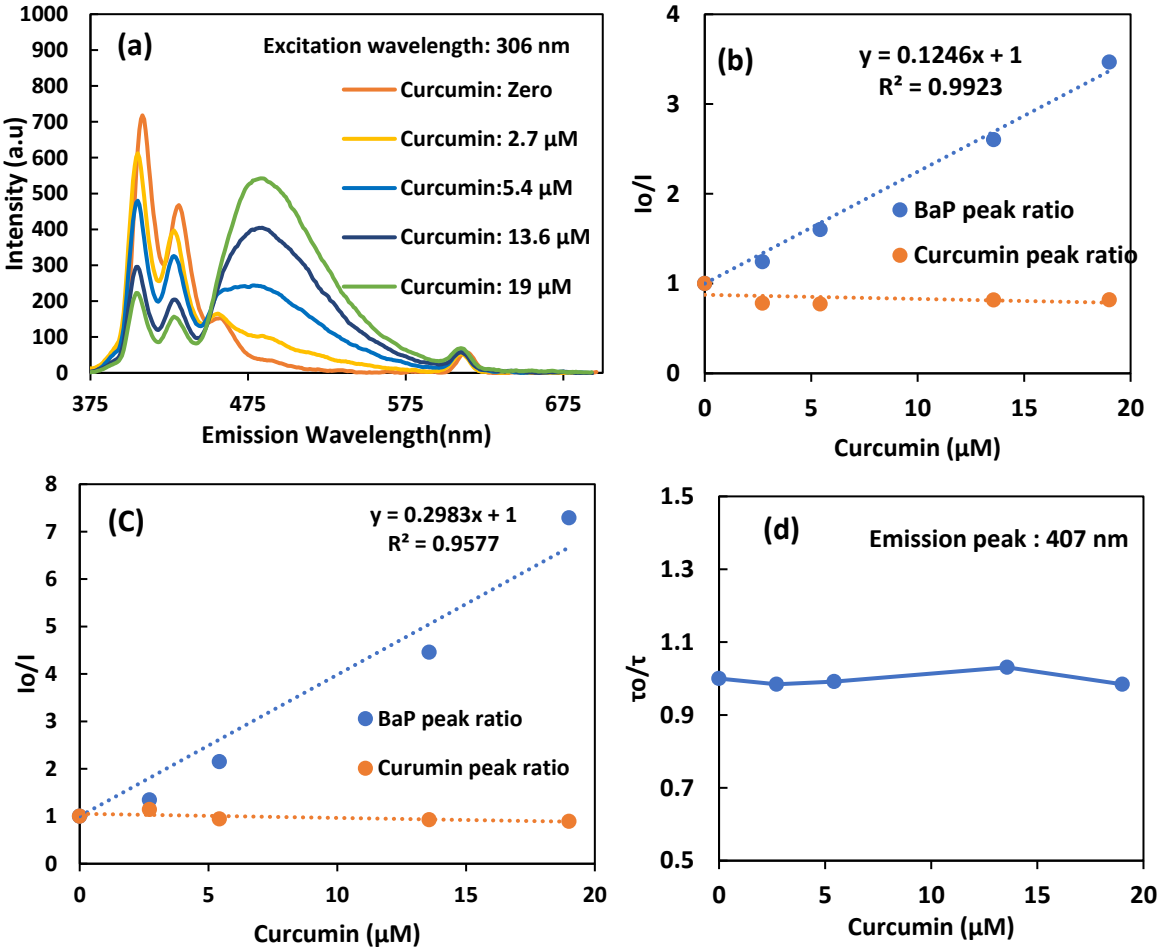

Figure 3.5: (a)- BaP, 2 µM, quenching with curcumin, the pair is excited at 306 nm. (b)- Intensity ratio for BaP(407nm) and curcumin(485nm) excited at 306 nm. (c)- Intensity ratio for BaP(407nm) and curcumin(485nm) excited at 393 nm. (d)- Fluorescence lifetime ratio for BaP in the presence of curcumin at an excitation wavelength of 393 nm.

Whereas, in dynamic quenching, raising the temperature increases the collisions (rate of interaction) between dye and quencher molecules that lead to higher quenching. Hence, dynamic quenching increases with increasing the temperature of the solution. Secondly, the mechanism of quenching can also be verified using fluorescence lifetime measurement of the dye in the presence of the quencher. Fluorescence lifetime is the time a fluorophore spends in the excited state before returning to the ground by emitting a photon.[215] In static quenching, only the dye that makes a complex with the quencher loses the fluorescence, whereas, the free dye molecules possess their original fluorescence properties and hence they exhibit the same lifetime with and without a quencher. In case of static quenching, fluorescence lifetime remains unaltered. However, in case of dynamic quenching, dye and quencher have collisions that change the fluorescence properties of the dye. For dynamic quenching, both fluorescent lifetime and intensity of dye decrease with increasing the quencher concentration. Dynamic quenching holds the following relationship between fluorescence lifetime and the intensity ratio.[216]

$$\frac{I_o}{I} = \frac{\tau_o}{\tau} \qquad \text{-(3)}$$

Where,

τ_o = Fluorescence lifetime of the dye in the absence of the quencher

$\tau =$ Fluorescence lifetime of the dye in the presence of the quencher

In this experiment, the fluorescence lifetime is measured at 393 nm, it is the lowest excitation wavelength available in the Time-Correlated Single Photon Counting (TCSPC)

instrument. BaP also excites and quenches at 393 nm as shown in figure 3.5(c). The fluorescence lifetime ratio of BaP in the presence of curcumin remains unaltered as shown in figure 3.5 (d). Although, based on the initial spectra overlap it was predicted that pair will exhibit dynamic quenching, but the fluorescence lifetime measurement indicates that BaP is experiencing static quenching in the presence of curcumin in DCM. The screened pair (BaP/Curcumin) shows the compatibility with the quenching model and it is suitable for PCBs detection system.

3.3.2 Characterization of curcumin multiacrylate

BaP does not have any functional groups that were modified for polymerization. However, it is easy to modify curcumin with functional group(s) to polymerize it in a polymer network. Curcumin in pure form has two or three hydroxyl groups. The presence of two benzene rings and the presence of linear carbon atoms make it hydrophobic that decreases its solubility and stability in the water. Furthermore, this molecule cannot be incorporated into the polymer chain without any modification. The conversion of curcumin to acrylate form is shown in figure 3.6. Synthesized CMA was analyzed with HPLC shown in figure 3.7. Samples were analyzed at 420 nm absorbance wavelength. Curcumin shows a characteristic peak around 6 min. Whereas CMA shows three distinguish peaks, the major peak around 10.5 min belongs to curcumin diacrylate. Peaks at 9 min and 9.8 min belong to mono and triacrylate. The ratio of curcumin, TEA and acryloyl chloride is 1:3:3 in the reaction. It gives 1% monoacrylate, 42.4% diacrylate and 56.6% triacrylate.[211] More detailed analysis and properties of CMA are discussed in literature.[211]

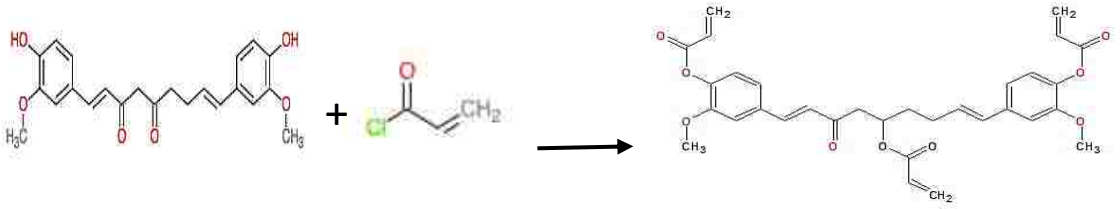

Curcumin Acryloyl chloride Curcumin multi acrylate

Figure 3.6: Curcumin converts to a mixture of mono-, di- and tri-acrylate. This mixture is called curcumin multiacrylate (CMA).

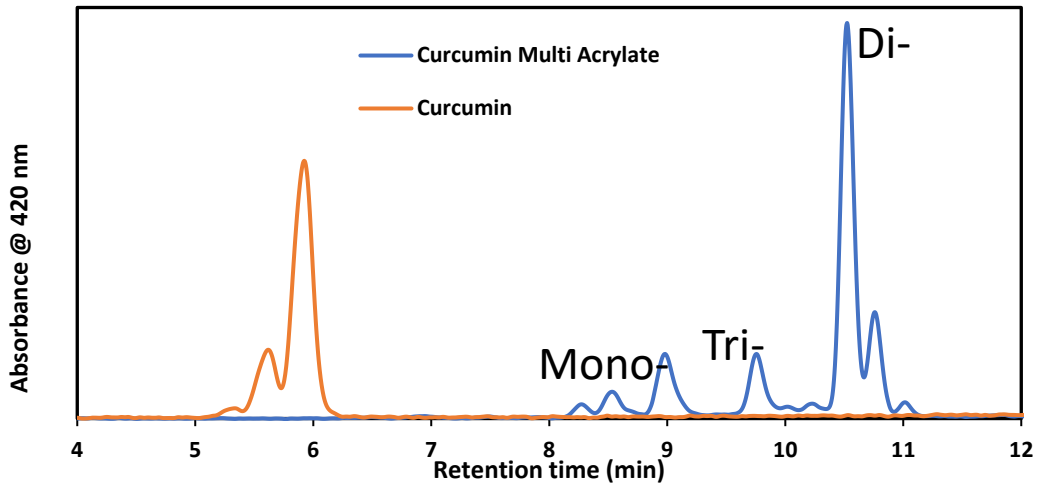

Figure 3.7: HPLC analysis of curcumin and curcumin multiacrylate. Peak around 9 min is mono-, around 9.8 min is tri- and around 10.5min is diacrylate. CMA was prepared using protocol given in literature.[211]

3.3.3 CMA loaded polyethylene glycol diacrylate

The synthesized CMA was polymerized with hydrophilic polymer (PEGDA). For synthesis, free radical polymerization was selected to form a non-degradable cross-linked polymer network. APS was used as a free radical source as it is inorganic and soluble in both water and DMSO. Polymerization was carried out in excess DMSO for the polymer chains to get

free space to readjust themselves within the network. The reaction was accelerated with TEMED; it is suitable for APS and is soluble in DMSO. The acrylates groups from the CMA react with the acrylate groups from PEGDA and result in a PEGDA network with curcumin inside the chains.

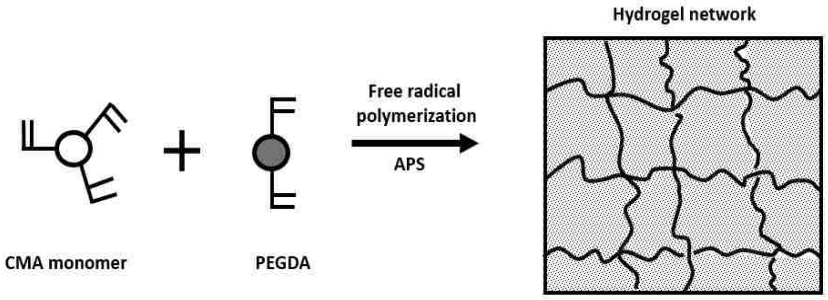

Figure 3.8: CMA has one to three acrylates groups and PEGDA has two acrylates groups. This helps in forming a crosslinked network.

3.3.4 Particle synthesis and size distribution analysis

Poly(curcumin) film formed in the previous step was cryo-ground to form microparticles used in this study, see figure 3.9. The yellow color confirms the presence of curcumin in the film. CMA was kept at 6-mole percent as a higher concentration of CMA does not fully polymerize within the polymer network. MPs have an advantage over the film with high surface area and are easy to use. For size distribution, poly(curcumin) MPs were suspended in DI water and analyzed using a Shimadzu SALD-7101 laser diffraction particle size analyzer with a 375 nm UV laser source. Figure 3.10 shows the particle size distribution; the average particle size diameter falls at 22.740 ± 0.654 µm. Figure 3.11

shows the images of Poly(curcumin) MPs taken from an optical microscope using white light. It shows these MPs are not spherical and do not have uniform size distribution.

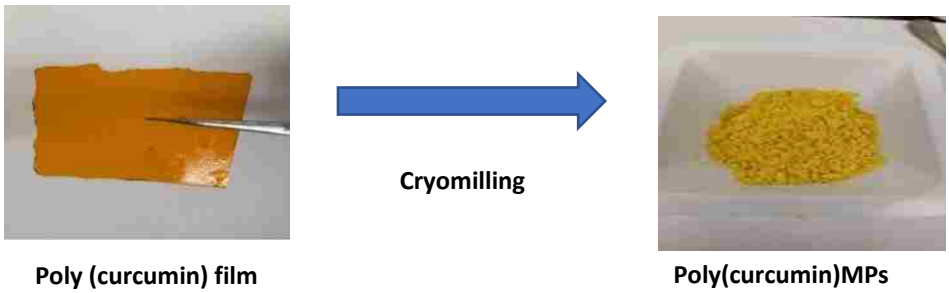

Figure 3.9: Poly(curcumin) film cryomilled to poly(curcumin) MPs using SPEX Sample Prep 6875D. The film was subjected to two 10 min milling cycles with a maximum milling rate of 15 cycles per second.

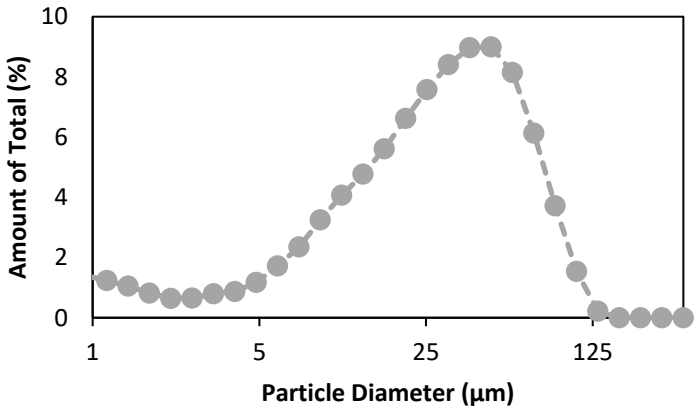

Figure 3.10: Particle size analysis of polymer(curcumin) MPs.

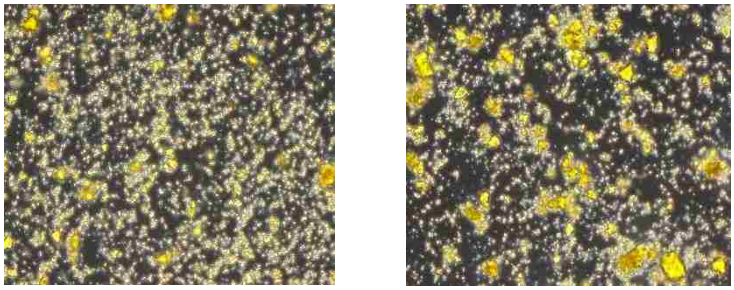

Figure 3.11: Spectroscopy images of the poly(curcumin) MPs under white light.

3.3.5 Allowable BaP concentration of BaP in DMSO based co-solvent

In order to assess the binding interaction effectively, a suitable partially organic solvent that has enough solubility for BaP but still allows particle interactions with BaP is needed. For this purpose, a partially organic solvent is selected. Three water-miscible organic solvents (ethanol, DMSO and acetone) were studied with volume concentrations of 10%, 20%, 25%, and 30%. BaP shows stability in 25% DMSO with no solvent background fluorescence spectra. BaP's maximum allowable concentration was determined in 25% DMSO. In figure 3.12, BaP intensity shows a linear increase with its concentration up to 2.4 µM and after that, the peak intensity is decreasing, no more BaP is solubilizing in the solvent. Beyond the solubility limit fluorophore molecules first start to stick together, this phenomenon decreases the peak intensity that is at 407 nm for BaP and this decrease is notable for 2.8 µM of BaP. This sticking of molecules introduces the excimer peak (new peak around 494 nm emission for BaP, discussed in section 3.3.8). Further increase in the concentration makes the visible precipitates of BaP. The solvent system with 25% DMSO is safe to use for BaP with a maximum concentration of 2.4 µM.

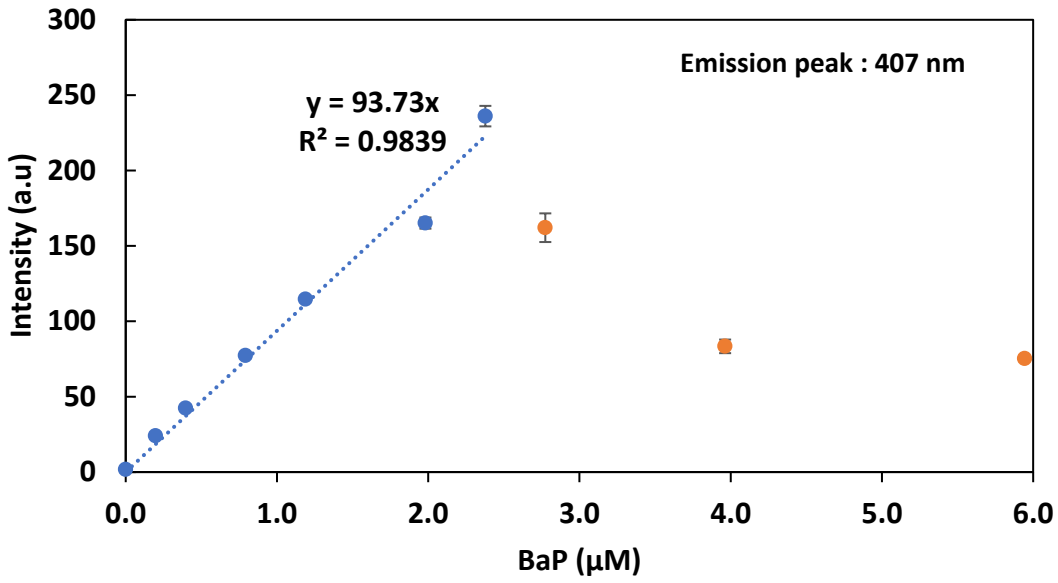

Figure 3.12: BaP shows solubility in 25% DMSO up to 2.4 µM. After that, it starts to make an excimer.

3.3.6 Equilibrium time for BaP incubation with poly(curcumin) MPs

To ensure binding equilibrium was obtained, a kinetic study was performed to identify the time needed for the poly(curcumin) MPs to adsorb maximum BaP from the solution. Poly(curcumin) MPs (1mg/ml) were introduced into two 25% DMSO solvent systems. One was sonicated for 15 min prior to the introduction of BaP and second were used as it is without sonication, to determine whether sonication was needed. Both suspended particles are shown in figure 3.14(d). After the introduction of BaP (2 µM) to the poly(curcumin) MPs containing the solution, glass vials were placed on the plate shaker. Only the supernatant is analyzed here to check the decrease in the concentration of the BaP with time. The decrease in the intensity of BaP in the supernatant shows how fast these molecules are migrating to the poly(curcumin) MPs. The biomimetic pockets on the

poly(curcumin) MPs in the form of curcumin provide π-π binding for BaP from the solvent (figure 3.13). A decrease in the supernatant intensity for sonicated and un-sonicated MPs are shown in figure 3.14(a,b). The signals from figure 3.14 (a,b) are converted to the mass of BaP in the solvent using the calibration curve from figure 3.12 and plotted in terms of a decrease in BaP mass in the supernatant with time in figure 3.14(c). Both, sonicated and un-sonicated systems have distinct kinetics. Sonicated poly(curcumin) MPs have very fast kinetics. It looks like equilibrium time for BaP adsorption is achieved within an hour.

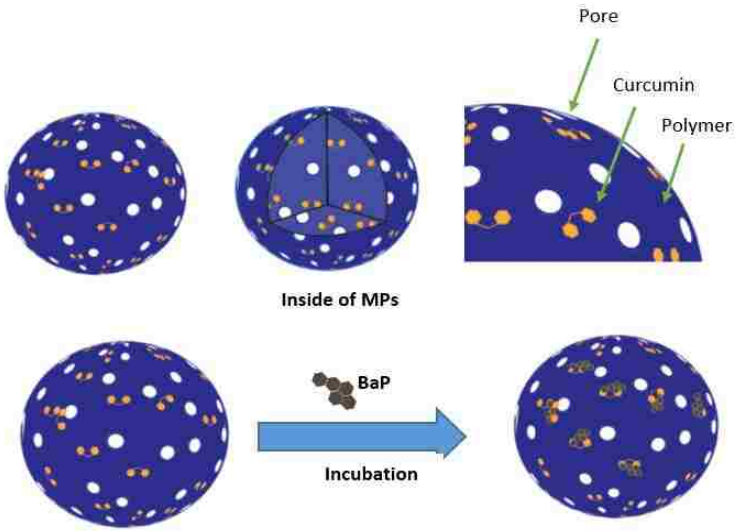

Figure 3.13: Interaction of BaP to the curcumin incorporated MPs. Curcumin acts as biomimetic pockets for π-π interaction for the capturing of BaP from the solvent.

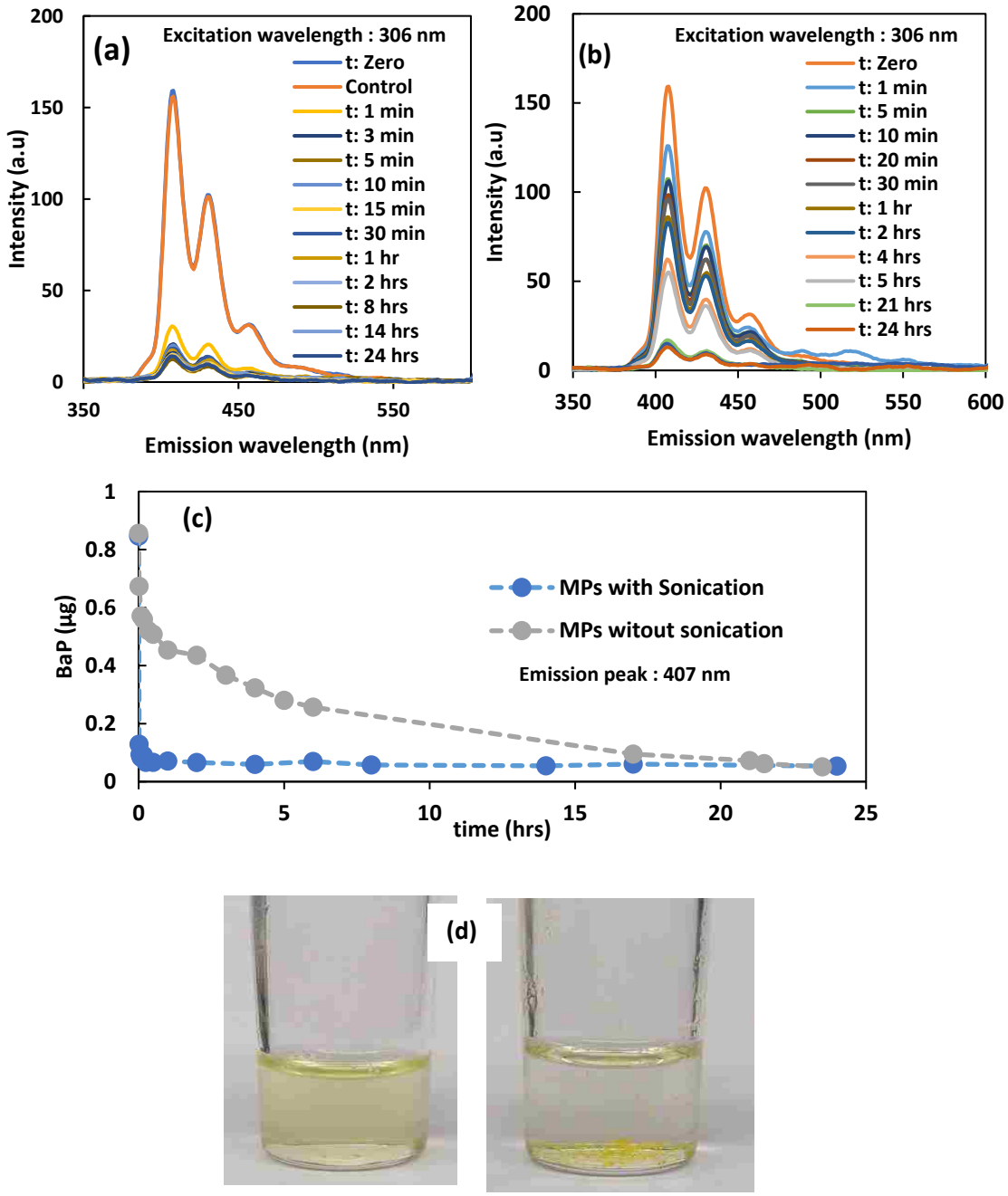

Figure 3.14: BaP uptake by sonicated and un sonicated MPs

(a)- Kinetics of BaP uptaking by the poly(curcumin) MPs. MPs were sonicated prior to the introduction of BaP. (b)-Kinetics of BaP uptaking by the poly(curcumin) MPs. MPs were used without any sonication. (c)-Decrease in the mass of BaP in the supernatant for both sonicated and un-sonicated poly(curcumin) MPs. (d)- Sonicated poly(curcumin) MPs (left) and un-sonicated poly(curcumin) MPs to the right.

3.3.7 BaP released from Poly(curcumin) MPs to the organic solvent

The decrease in the supernatant intensity suggests that BaP is possibly going to the poly(curcumin) MPs. It is very important to confirm that BaP is adsorbing to the poly(curcumin) MPs and to determine the mass of the BaP attached to the poly(curcumin) MPs. The best way is to desorb the BaP into a hydrophobic organic solvent. Dry poly(curcumin) MPs (1mg/ml) incubated with 2 µM of BaP re-dispersed in 2 ml of isooctane solvent. Isooctane has high BaP solubility as indicated in figure 3.16(b), the intensity is increasing with the concentration in a straight line. Moreover, isooctane has been also mentioned in the literature for contaminant extractions.[217,218] Each time point has its own three samples. The overall experimental scheme is shown in figure 3.15. The incubated MPs were separated, and the supernatant was analyzed for desorbed BaP. The intensity peak (407 nm) is plotted against the time in figure 3.16(a), to show the optimum time suitable for washing off the BaP from the MPs to the isooctane solvent. It has two parts, the first one is the BaP remaining in the supernatant after the incubation with poly(curcumin) MPs. This part is the same as figure 3.14(c). Whereas, the second part only deals with the BaP attached to the poly(curcumin) MPs. BaP release kinetics in figure 3.16(a) shows that its desorption into isooctane is very fast and most of it happens within 30 minutes.

Figure 3.16(b) shows the calibration curve for BaP in isooctane. Using this calibration curve for the BaP adsorbed to poly(curcumin) MPs and the calibration curve (figure 3.12) for unbounded BaP in the supernatant. A mass balance was applied on the 1 mg/ml of

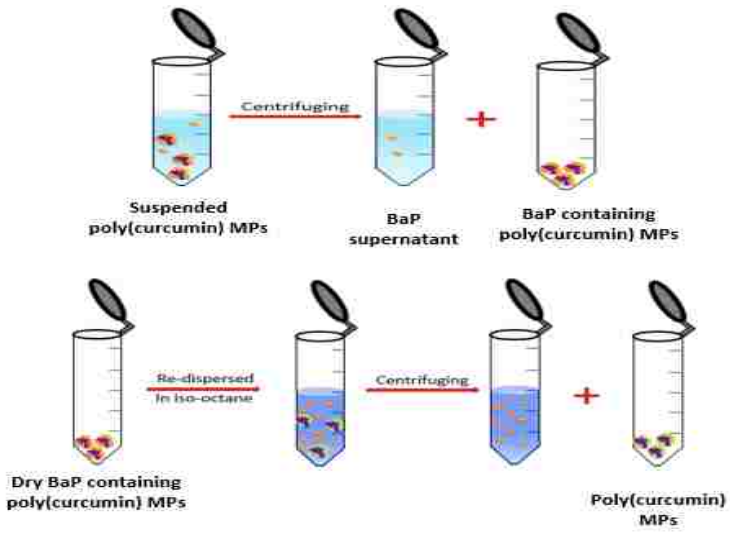

Figure 3.15: BaP in the supernatant and adsorbed to the poly(curcumin) MPs. BaP concentration in supernatant decreases while it increases in the MPs.

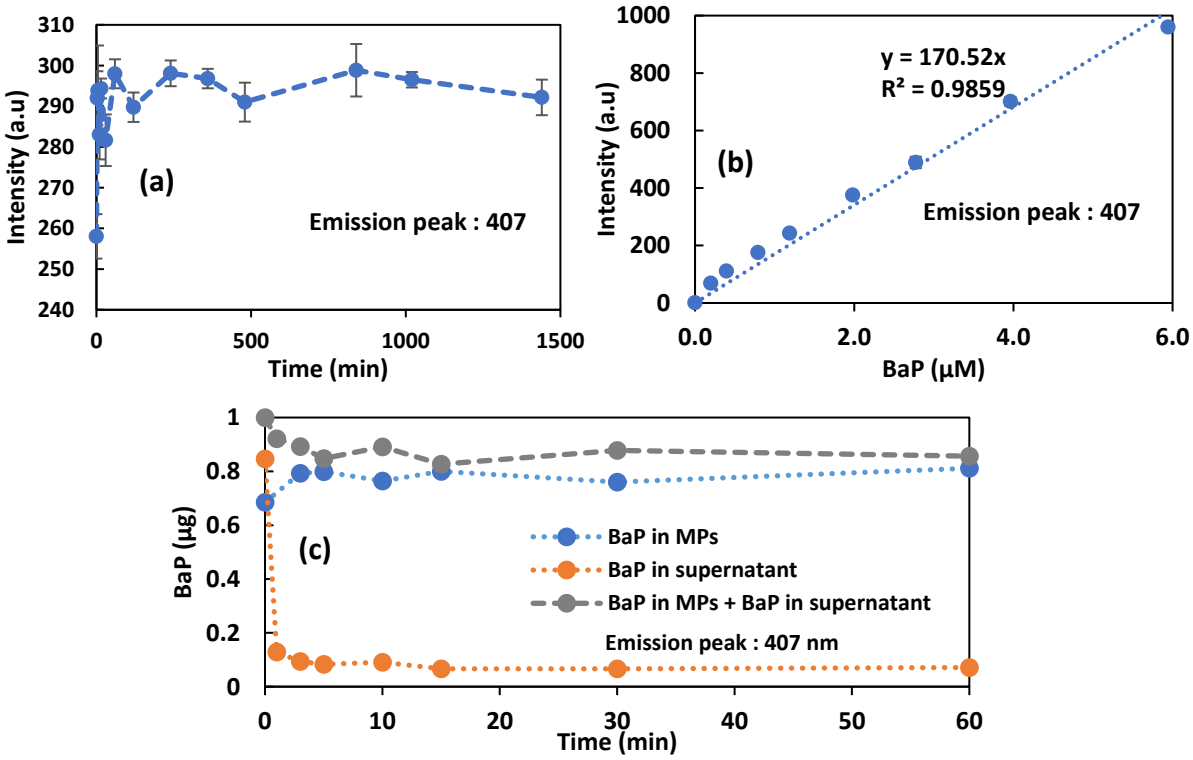

Figure 3.16: (a)- Leaching of BaP from the poly(curcumin) MPs, MPs were separated, and the supernatant was analyzed. (b)- BaP calibration in isooctane. (c)- Mass balance of BaP on the poly(curcumin) MPs.

poly(curcumin) MPs for 2 µM of BaP, it is shown in figure 3.16(c). Most of the BaP is being adsorbed to the poly(curcumin) MPs. More than 80% of BaP is going to the MPs and less than 10% is reaming in the solvent. There is still some loss around 10%, it is due to the handling, switching vials and attaching to the glass walls. Overall, this section shows a great affinity of curcumin moieties in the polymer backbone towards the fluorescent molecule (BaP) as a potential candidate for displacement assay.

3.3.8 Maximum loading of BaP to the Poly(curcumin) MPs

The adsorption kinetics of BaP from the DMSO based solvent and the release kinetics of BaP from the MPs into isooctane are utilized in this section to find the maximum loading of BaP to the poly(curcumin) MPs. For PCBs sensing it is very important to make sure that all the sites are covered with BaP so that PCB can replace it and generate the signal instead of binding to the empty sites and produce no signal. Poly(curcumin) MPs of concentration of 1mg/ml were dispersed in 25% DMSO solvent. First BaP (2.4 µM) was introduced and after 30 min, BaP was increased stepwise with each 0.8 µM addition. Supernatants for all the samples were separated and analyzed for BaP peak around 407 nm, and the excimer peak around 494 nm. Figure 3.17(a) shows the fluorescence spectra for BaP in the presence of 1mg/ml of poly(curcumin) MPs. Whereas, 3.17 (b) shows the peak intensities of BaP around 407nm and 494 nm in the presence of poly(curcumin) MPs and PEGDA MPs control. Both peaks of BaP in the presence of PEGDA MPs are higher than the BaP peaks in the presence of poly(curcumin) MPs. From the calibration curve for 2.4 µM of BaP in the solvent, it appears that PEGDA MPs are providing a non-specific binding to BaP. However, Poly(curcumin) MPs show higher binding due to the presence of curcumin in

the polymer network. Furthermore, the appearance of the excimer peak of BaP for PEGDA MPs also shows that BaP is sticking together instead of going to the MPs. Whereas, excimer peak for poly(curcumin) MPs is very low due to the availability of additional biomimetic moieties in the MPs. BaP sticks together at a higher concentration of 6.3 µM and above, showing that poly(curcumin)MPs are being saturated and no more BaP is going to the MPs. It suggests that 5.5 µM is safe maximum loading of BaP in 25% DMSO solvent containing 1mg/ml of poly(curcumin) MPs with 6 mole% CMA loading. Poly(curcumin) MPs incubated with 5.5 µM of BaP were separated and analyzed for the total loading of BaP using isooctane. The leached-out BaP is shown in figure 3.18(a). From the calibration curve of BaP in isooctane, it was found that BaP concentration of 5.2 µM as loaded onto the MPs out of 5.5 µM of total BaP introduced to the solvent. These BaP (5.5 µM) incubated poly(curcumin) MPs were re-dispersed in 25% DMSO solvent for 24hrs to find out the binding efficiency of BaP. The supernatant spectra of BaP are shown in figure 3.18(b). It was interpreted with the help of a calibration curve that only around 0.4 µM of BaP is losing from the Poly(curcumin) MPs. There is still plenty of BaP left on the MPs for displacement purposes to detect PCBs in water.

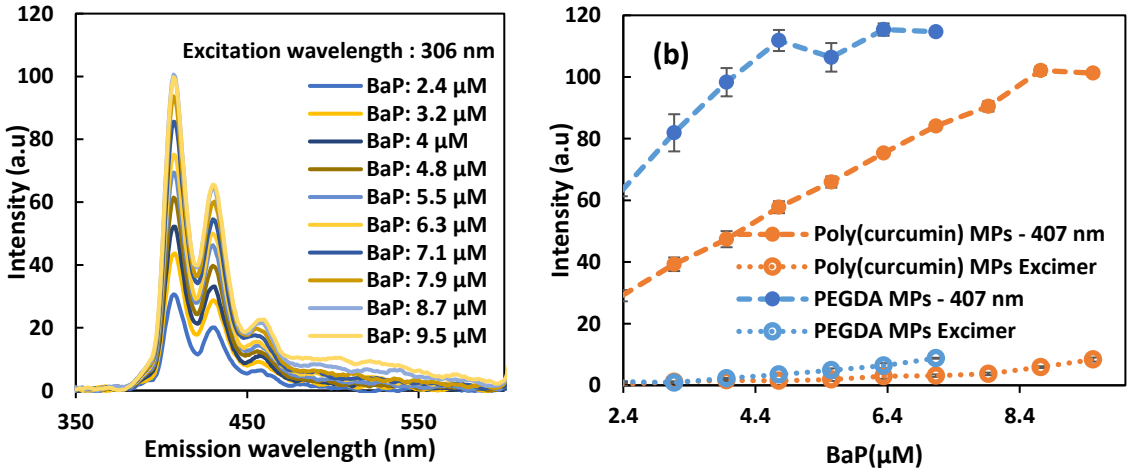

Figure 3.17: (a)-Different concentrations of BaP in 25% DMSO in the presence of poly(curcumin) MPs. (b)-BaP peak intensities in the supernatant in the presence of poly(curcumin) MPs and PEGDA MPs control.

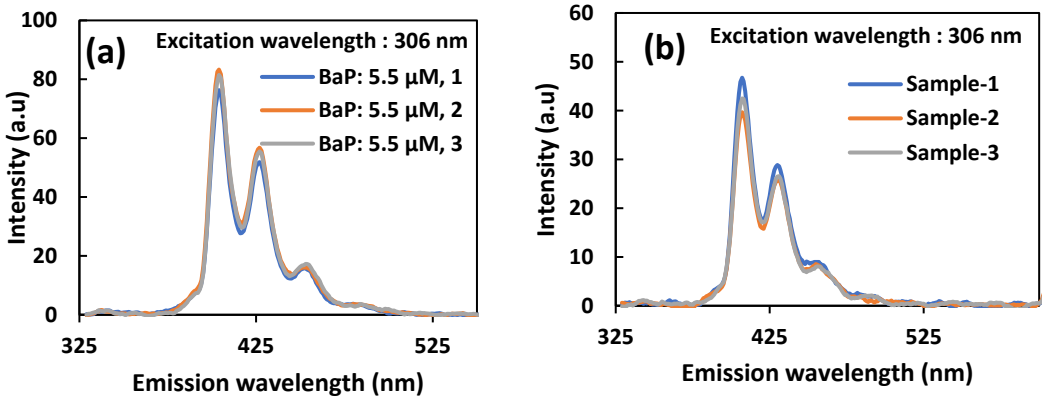

Figure 3.18: BaP adsorbed to MPs and BaP binding efficiency. (a)- BaP leaching to isooctane from 5.5 µM incubated poly(curcumin) MPs. It corresponds to **5.2 µM** of BaP into the solvent. Which proves that most of the BaP are going to the MPs. (b)- BaP (5.5 µM) incubated poly(curcumin) MPs re-dispersed in 25% DMSO for 24 hrs. It shows that only around **0.4 µM** is coming off the MPs.

3.3.9 PCBs detection using poly(curcumin) MPs

Detailed characterized BaP incubated poly(curcumin) MPs were finally evaluated for PCBs sensing in water. The scheme for this section is shown in figure 3.19. The aim of this section is to use the BaP incubated poly(curcumin) MPs and dispersed them in water containing PCBs and let PCBs displace BaP from the binding sites and restore their fluorescence intensity in the solvent. Since BaP has very low solubility in water, it is very important to use a solvent system that can facilitate the displacement phenomenon and solely driven by the PCBs. For this purpose, a small percentage of DMOS (5% and 10%) was introduced to the water. It will keep BaP in the solvent without crashing it out.

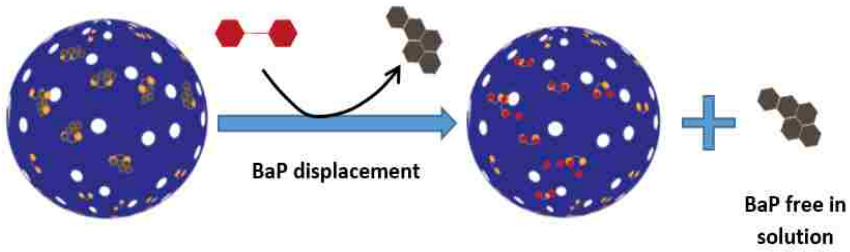

Figure 3.19: Displacement scheme of BaP with PCBs from the poly(curcumin) MPs dispersed in 5% and 10% DMSO solvents.

Poly(curcumin) MPs incubated with BaP were re-dispersed in 5% and 10% DMSO solvent with various concentrations of PCBs. The solvent system with 5% DMSO only has 30 µM of maximum concentration of the analytes, while 10% DMSO solvent has a maximum concentration of 60 µM. BaP intensity peak around 407 nm is plotted for 5% and 10% DMSO solvent in figure 3.20(a,b). Both PCB-126 and PCB-118 show little increase in the

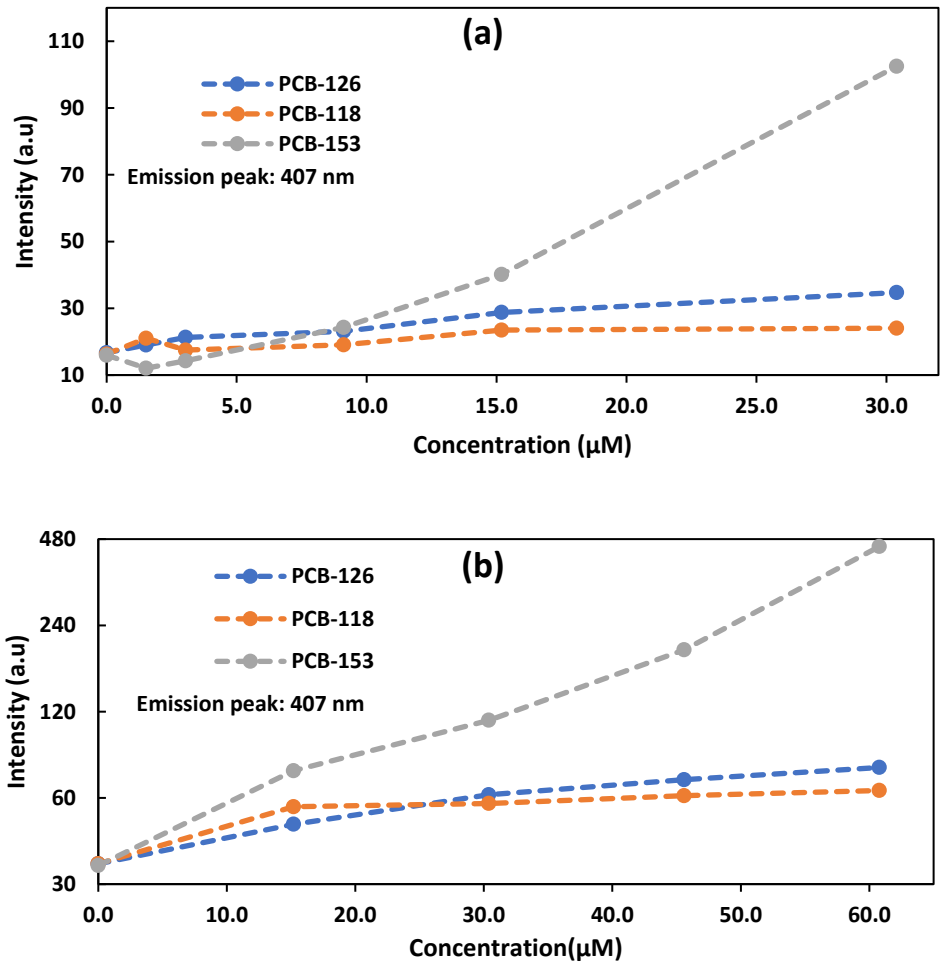

Figure 3.20: (a)- BaP displaced by different molecules in 5% DMSO solvent. The peak intensity is recorded at 407nm. (b)- BaP displaced by different molecules in 10% DMSO solvent. The peak intensity is recorded at 407nm.

intensity of BaP for 5% DMSO. However, this increase is more promising for both PCBs in 10% DMSO. PCB-153 has a different story, it shows very high displacement of BaP from the poly(curcumin) MPs and these signals are very high as compared to the other two PCBs. It is suggesting that PCB-153 is more active in pushing BaP out of the poly(curcumin)MPs in both solvent systems, it might be because of the high octanol-water constant of PCB-153. Figure 3.21 shows that PCB-153 background signals are

almost negligible; indicating that signals are coming from the BaP displaced from the poly(curcumin) MPs and not from PCB-153. This section successfully demonstrates the detection of PCBs in water using BaP incubated poly(curcumin) MPs.

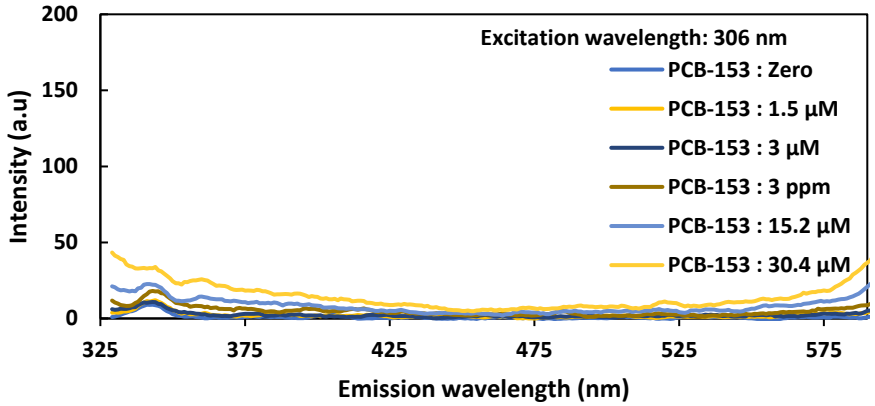

Figure 3.21: PCB-153 fluorescence spectra in 5%DMSO, excited at 306 nm.

3.3.10 BaP-displaced calibration and detailed analysis

Fluorescence spectra of BaP displaced by PCB-153 is shown in figure 3.22(a,b) for both 5% and 10% DMSO. BaP is forming an excimer shape in both solvent systems, but the spectra as a whole are going upward with increasing the concentration of PCB-153. The concentration of BaP that is being displaced is calibrated to relate the PCBs concentration that is causing this displacement. The calibration spectra of BaP in 5% and 10% DMSO are shown in figure 3.23(a,b). Whereas peak intensities for these plots are shown in figure 3.23(c,d), it covers three BaP peaks, first peak at 407nm, second peak at 432nm and third excimer peak at 494 nm. The calibration resulted in unexpected outcomes that BaP's displacement curve from poly(curcumin) MPs with PCB-153 and its calibration curve in

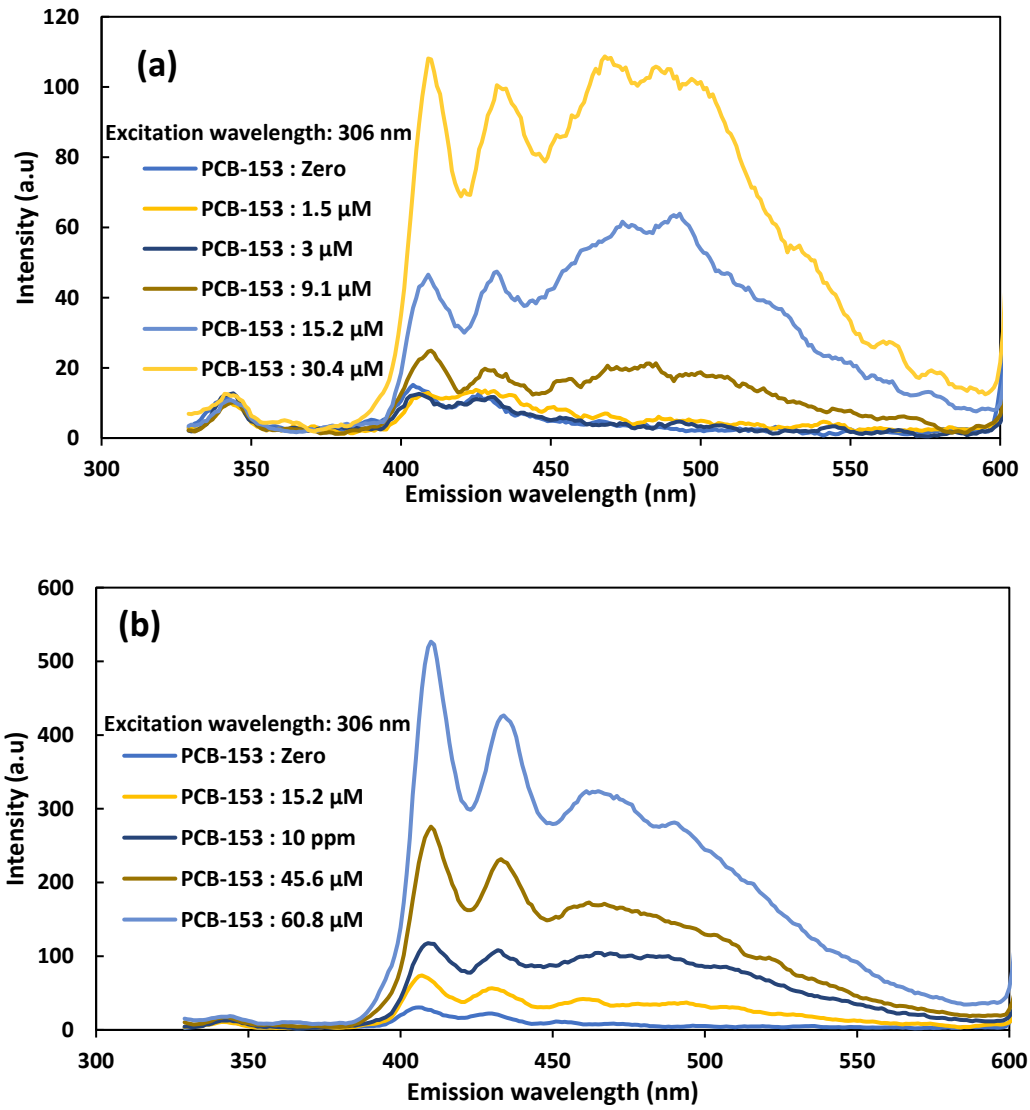

Figure 3.22: (a)- BaP being displaced from the poly(curcumin) MPs with PCB-153 in 5% DMSO. (b)- BaP being displaced from the poly(curcumin) MPs with PCB-153 in 10% DMSO.

DMSO based solvent are not identical. Both curves are un-relatable in terms of spectral shape and intensity. At low concentration, BaP shows both peaks at 407nm and 423 nm and the formation of excimer around 494 nm is in accordance with the results to match with 3.22(a,b). However, as the concentration of BaP is increased in the calibration system, peak at 407 stops increasing and peaks at 423 and at 494nm begin to increase as

shown in figure 3.23(c,d). Both other PCB-126 and PCB-118 show very low displacement, their concentration might be related to the BaP calibration curve. However, if PCB-153 is affecting BaP's stability in DMSO based solvent then other PCBs might be doing the same thing with low strength. This system was further analyzed to find out the problem. The system involves different components that include curcumin, DMSO, polymer(PEGDA), BaP and PCBs in it.

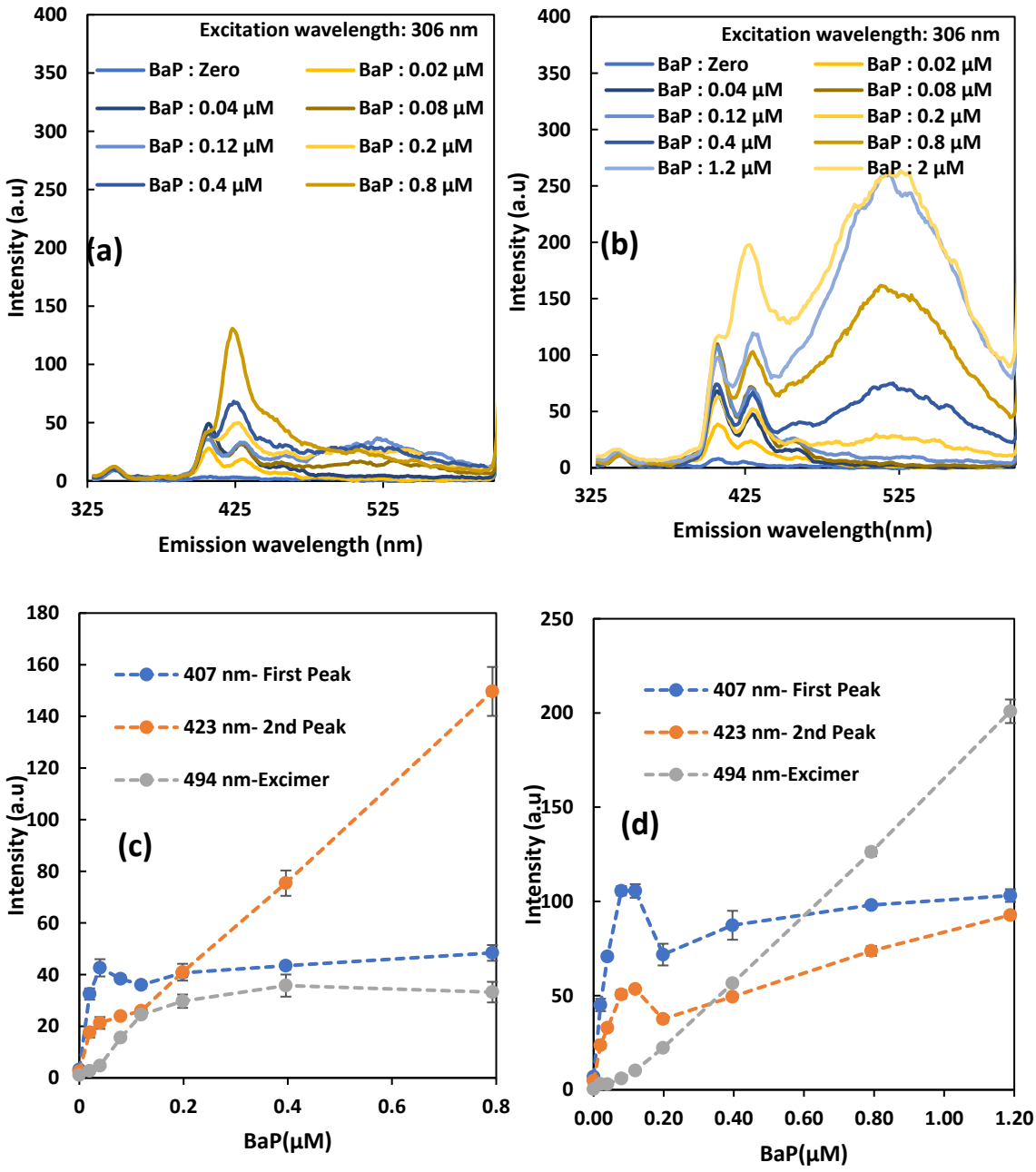

Figure 3.23: (a)- BaP calibration curve in 5% DMSO solvent. (b)-BaP calibration curve in 10% DMSO solvent. (c)- BaP peaks intensity in 5% DMSO solvent. (d)- BaP peaks intensity in 10%DMSO solvent.

Since poly(curcumin)MPs are being separated and only supernatant is being analyzed here, curcumin and polymer were ruled out. Whereas, DMSO is fluorescently inert

solvent. It left with BaP and PCB in the system that can cause strange fluorescent behavior. For this purpose, BaP concentration of 0.08 µM was selected, as it does not form an excimer in 10% DMSO calibration curve. This BaP concentration was mixed with various concentrations of PCB-153 in 10% DMSO to see the effect of PCB-153 on BaP in the solvent. The mixture was excited at 306 nm and the spectra obtained are shown in figure 3.24(a), whereas, change in peak intensity at 407nm is shown in figure 3.24(b). It is surprising to see that PCB-153 and BaP are interacting in the solvent and BaP's intensity is increasing in 10% DMSO. The increase in intensity is higher than the highest soluble concentration of BaP in 10% DMSO. BaP peak intensity is touching a plateau at a high concentration of PCB but still, no excimer is forming. There are two possibilities that inferred from the poly(curcumin) MPs based displacement assay, one that PCB-153 is displacing BaP from the poly(curcumin)MPs and free PCB-153 is interacting with the displaced BaP in the solvent. Second, PCB-153 is not displacing BaP but it is attracting BaP to the solvent to interact with it and behave differently.

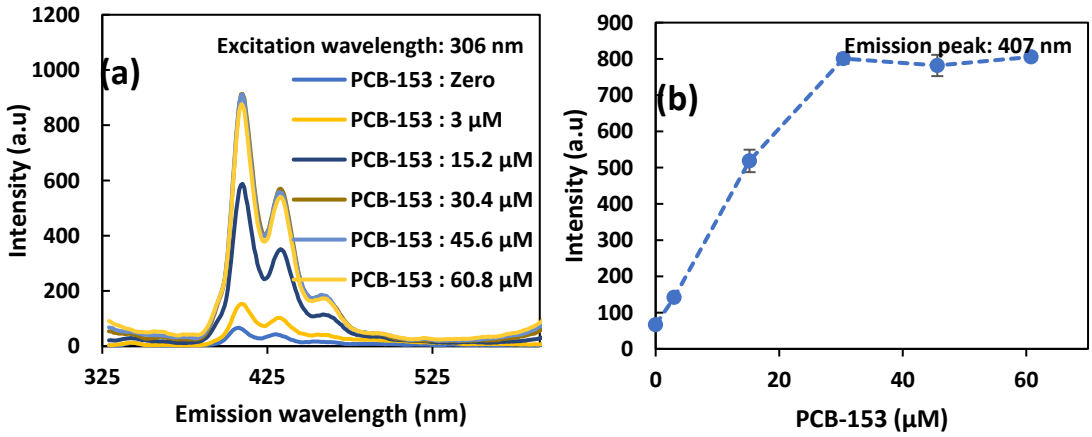

Figure 3.24: (a)- BaP (0.08 µM) interaction with PCB-153 in 10% DMSO, excited at 306 nm. (b)- BaP peak intensity at 407 nm with PCB-153.

3.4 Conclusions

In this work, different fluorescent molecules were screened to finalize BaP/curcumin as a quenching pair used in the displacement assay. curcumin was successfully converted to curcumin multiacrylate using an existing protocol. This CMA was incorporated into the PEGDA chain using free radical polymerization to obtain non-degradable polymer particles. Poly(curcumin) MPs loaded with 6 mol% CMA showed very good binding of BaP to the MPs using π-π interaction. The control MPs also showed the presence of non-specific binding for BaP. However, BaP showed a stable binding to Poly(curcumin) MPs in 25% DMSO solvent. The interaction of BaP incubated Poly(curcumin) MPs with PCBs showed the signs of PCBs presence in the solvent. There might be displacement in the system, however, these signals are dominantly representing the interaction of BaP and PCBs in the solvent. This interaction is further evaluated in chapter 4.

CHAPTER 4. DETECTION OF PCBs IN WATER USING HYDROPHOBIC INTERACTION

Based on the research article:

> **Ahmad, Irfan**, Jiaying Weng, A. J. Stromberg, J. Z. Hilt, and T. D. Dziubla. "Fluorescence based detection of polychlorinated biphenyls (PCBs) in water using hydrophobic interactions." Analyst 144, no. 2 (2019): 677-684.

4.1 Introduction

Fluorescence spectroscopy is a highly sensitive, rapid and simple to employ detection method.[219] This technique is already being used for environmental and bio applications in terms of sensing precious metal ions [220], explosives [221], hazardous gas molecules [222], cancer biomarkers, cells, and tissues [223]. While other methods and techniques are limited by the cost, time and sample handling, the ubiquitous use of fluorescence techniques in a wide range of industries, make their application to environmental pollutant detection plausible.

In this chapter, it was hypothesized that PCBs can make a hydrophobic complex with other fluorescent molecules in water that can alter their fluorescent properties. BaP fluorescence signal is strongly enhanced in non-polar environments. It was found that BaP intensity increases in water beyond the highest intensity in organic solvent through interaction with PCBs, potentially providing a rapid sensing technique for the detection of PCBs. Furthermore, this work demonstrates that hydrophobic sensor can sense PCBs in water in the presence of freshwater conditions such as pH, ionic strength and humic acid.

4.2 Experimental section

4.2.1 Materials

Unless otherwise stated, chemicals and reagents were used as received without any additional purification. 3,3',4,4',5-Pentachlorobiphenyl (PCB-126), 2,2',4,4',5,5'-hexachlorobiphenyl (PCB-153), 2,3',4,4',5-pentachlorobiphenyl (PCB-118) and biphenyl (BiP) were purchased from AccuStandard Inc.,(New Haven, CT). 4,4-dihydroxy biphenyl (Di-OH BiP) was purchased from Sigma Aldrich,(St.Louis, Mo). Sodium hydroxide was purchased from fisher scientific,(Hampton, NH). Sodium chloride was obtained from VWR,(Radnor, PA). Humic acid (H.A) and benzo[a]pyrene (BaP) were purchased from Alfa Aesar,(Haverhill, MA). Dichloromethane (DCM), iso-octane, n-hexane and dimethyl sulfoxide (DMSO) was purchased from Pharmaco (Brookfield, CT). Deionized (DI) water was obtained from Milli-Q water purification system.

4.2.2 Method

4.2.2.1 BaP fluorescence properties in organic solvents

In order to determine the relationship between fluorescence intensity and solvent hydrophobicity, BaP fluorescence was measured in five organic solvents (n-hexane, DMSO, chloroform, DCM and isooctane). Stock solutions of BaP were prepared in each organic solvent and then it was diluted to 0.08 µM of BaP with the respective organic solvent and analyzed the fluorescence spectra using excitation wavelength of 294 nm.

4.2.2.2 BaP interaction with PCBs, biphenyls and humic acid in water

The stock solution of BaP, PCBs, biphenyls were prepared in DMSO. Whereas, the stock solutions for humic acid and 4,4-dihydroxy biphenyl were prepared in water. First BaP (0.08 µM) was introduced to the DI water and then it was spiked with the analyte. Glass syringes were used to transfer the analytes for minimum loss. Solutions were mixed on the vortex mixer for 5 seconds to homogenize them. Once the solution is completely mixed, it was then analyzed for the fluorescence signals. Total DMSO in the solvent was kept constant at 1.6 vol%.

4.2.2.3 BaP interaction with PCBs and other molecules in the organic solvent

BaP, PCBs biphenyls, and 4,4-dihydroxybiphenyl were dissolved in the organic solvent (DMSO). The same procedure was repeated as in section 4.2.2.2, with DMSO as the solvent instead of DI water.

4.2.2.4 Effect of ionic strength on BaP and PCBs interaction

Sodium chloride stock solution was prepared in water. Using the method form the section 4.2.2.2, BaP and PCBs were mixed in DI water with ionic strength varying from 1mM to 20mM.

4.2.2.5 Effect of pH on BaP and PCBs interaction

DI water of an un-buffered pH of 8.5 was used as a solvent for samples preparation. Both BaP and PCBs were mixed in the unbuffered pH solvent as described in section 4.2.2.2 and then characterized.

4.2.2.6 Effect of natural organic matter on BaP and PCBs interaction

Humic acid stock solution was prepared in water. After introducing BaP, the solution was spiked with PCBs and humic acid both. Humic acid concentration was varied from zero to 20 ppm in the sample.

4.2.3 Characterization

All the samples were characterized using Cary Eclipse spectrophotometer. It has a maximum spectra intensity of 1000 a.u. All the samples were scanned at medium scanning rate (600nm/min) with medium voltages (600 volts) of the PMT detector. Samples were introduced to the spectrophotometer using a quartz micro fluorometer cell of 0.7 ml volume and 10 mm path length from Starna Cells, Inc.

4.3 Results and Discussion

4.3.1 BaP fluorescence properties in organic solvents

Various properties of organic solvents potentially affecting BaP fluorescence are shown in table 4.1. These solvents are divided into three groups, non-polar solvents (n-hexane and isooctane), polar aprotic solvents (DCM and DMSO), polar protic solvents (water) and chloroform was tagged as a slightly polar solvent. Since BaP is an unsubstituted aromatic hydrocarbon, it is less sensitive to the solvent polarity.[212]

As shown in Figure 4.1, the fluorescence intensity of BaP increases with increasing solvent hydrophobicity. The maximum fluorescence intensity of BaP is evaluated in five organic solvents (n-hexane, DMSO, chloroform, DCM and isooctane). BaP

concentration is constant at 0.08 µm in all solvents. The change in fluorescence spectra for each organic solvent is analyzed that is displayed in figure 4.1(a,b).

Table 4.1: Organic solvents with their dipole moment, viscosity, dielectric constant and BaP intensity in the solvents. BaP (n=3 with standard deviation)

Solvent	Dipole moment (D) [224–226]	Viscosity (mPa.s) [227,228]	Dielectric constant(ϵ) [229,230]	Polarity Index	Solubility parameter	BaP fluorescence intensity (a.u)
n-hexane	0.00	0.29	1.9	0.1	14.9	10.79 ± 0.33
Isooctane	0.00	0.47	2.2	0.4	15.1	18.18 ± 0.50
Chloroform	1.04	0.54	4.8	4.1	18.7	44.28 ± 0.38
DCM	1.62	0.42	9.1	3.1	20.2	66.97 ± 2.30
DMSO	3.96	2.0	47.24	7.2	26.4	84.71 ± 1.40
water	1.58	0.89	80.1	9.0	48.0	17.14 ± 0.7

Based on solvents types, non-polar solvents show very low intensity of BaP and polar aprotic solvents are showing an increase in the intensity of BaP. If only organic solvents are considered, then the intensity of BaP is higher for solvents with a higher dipole moment. Since the intensity levels vary in each organic solvent, this indicates the presence of specific solvent-fluorophore interaction. This interaction takes places due to the presence of one or more nearby molecules and it is determined by the chemical properties of the solvent and fluorescent molecules.[231,232]

As BaP is non-polar at the ground state, it is polarized at the excited state and this excited state is interacting uniquely with each solvent. For non-polar solvents, there is very low interaction for solute and solvent that is why the intensity for n-hexane and isooctane is

very low. Since chloroform is slightly-polar, it interacts with the excited state based on its low dipole moment and increases BaP intensity.

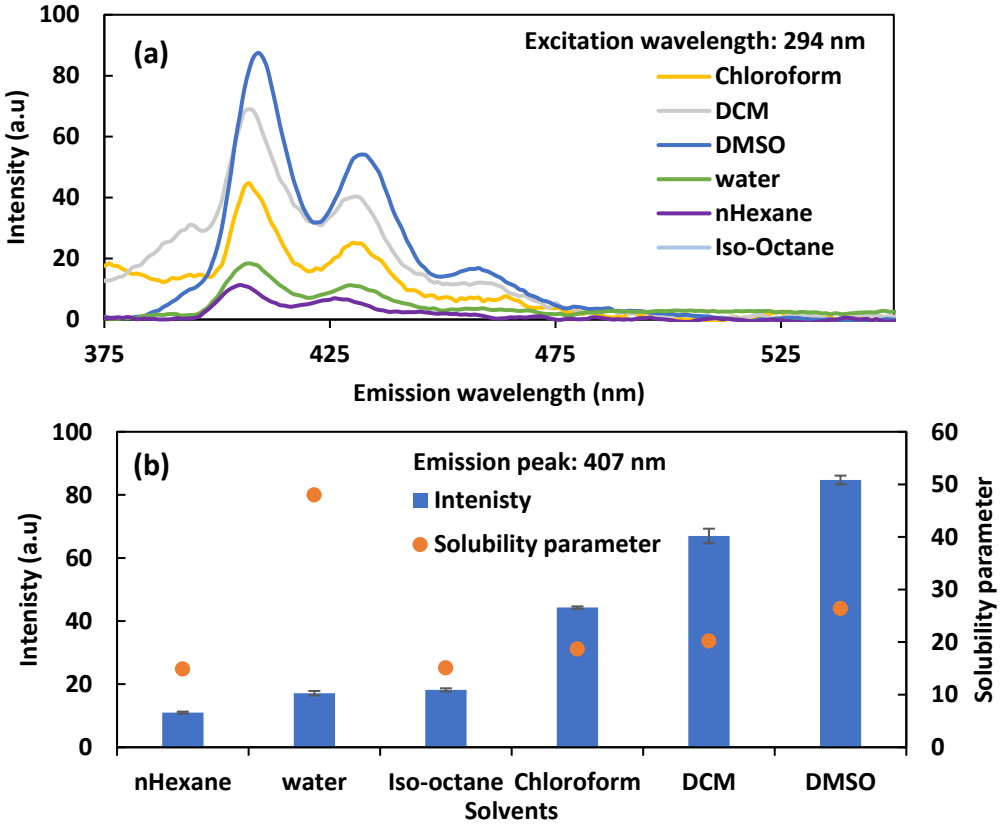

Figure 4.1: BaP fluorescence signals in organic solvents.
(a)- BaP (0.08µM) fluorescence spectra in organic solvents. Excited at 294 nm, (b)- BaP (0.08µM) peak intensity at 407nm in organic solvents and in water, excited at 294 nm. The bar graph represents the fluorescence intensity and the dotted curve represents the solubility parameter.

Whereas, for polar aprotic solvents, the intensity is higher for DMSO as it has a high dipole moment, viscosity and solubility parameter. There might be one or more than one factor (e.g. dipole moment, solvent-solute interaction at excited state and viscosity for the local environment) that are active here for enhancing BaP intensity. As water is a unique polar protic solvent with the presence of hydrogen bonding, it is behaving opposite to the listed

organic solvents. Its dipole moment is close to DCM, but BaP intensity in water is closer to isooctane. This indicates the absence of solvent-solute interaction at the excited state of BaP. The presence of hydrogen bonding suggests water molecules are very strong, and they are not letting water interact with the excited state BaP. There is one more possibility that BaP is not very strongly polarized by the incident light that can break the hydrogen bonding and interact with the water molecules based on their dipole moment. Here, the interaction of individual organic solvent with BaP is not evaluated in detail. As the focus of to detect PCBs in water to display the intensity of BaP changes with the surrounding environment including PCBs.

4.3.2 BaP interaction with PCBs, biphenyls and humic acid in water

For sensing evaluation, BaP interaction is studied with PCBs, biphenyls and humic acid. BaP concentration was kept at 0.08 µm while analytes concentration was varied from zero to 30 µM. The change in BaP spectra in the presence of PCB-126 is displayed in figure 4.2(a). BaP intensity is increasing with increasing the concentration of PCB-126 in water. Whereas, PCB-126 control in water has a very low intensity as shown in figure 4.2(b). Figure 4.2(c) illustrates the peak intensity of BaP in the presence of all three PCBs(PCB-126, PCB-118, and PCB-153). Similarly, biphenyl, 4,4-dihydroxy biphenyl, and humic acid were studied with BaP in water as control molecules. Peak intensities of BaP with these three molecules are given in figure 4.2(d).

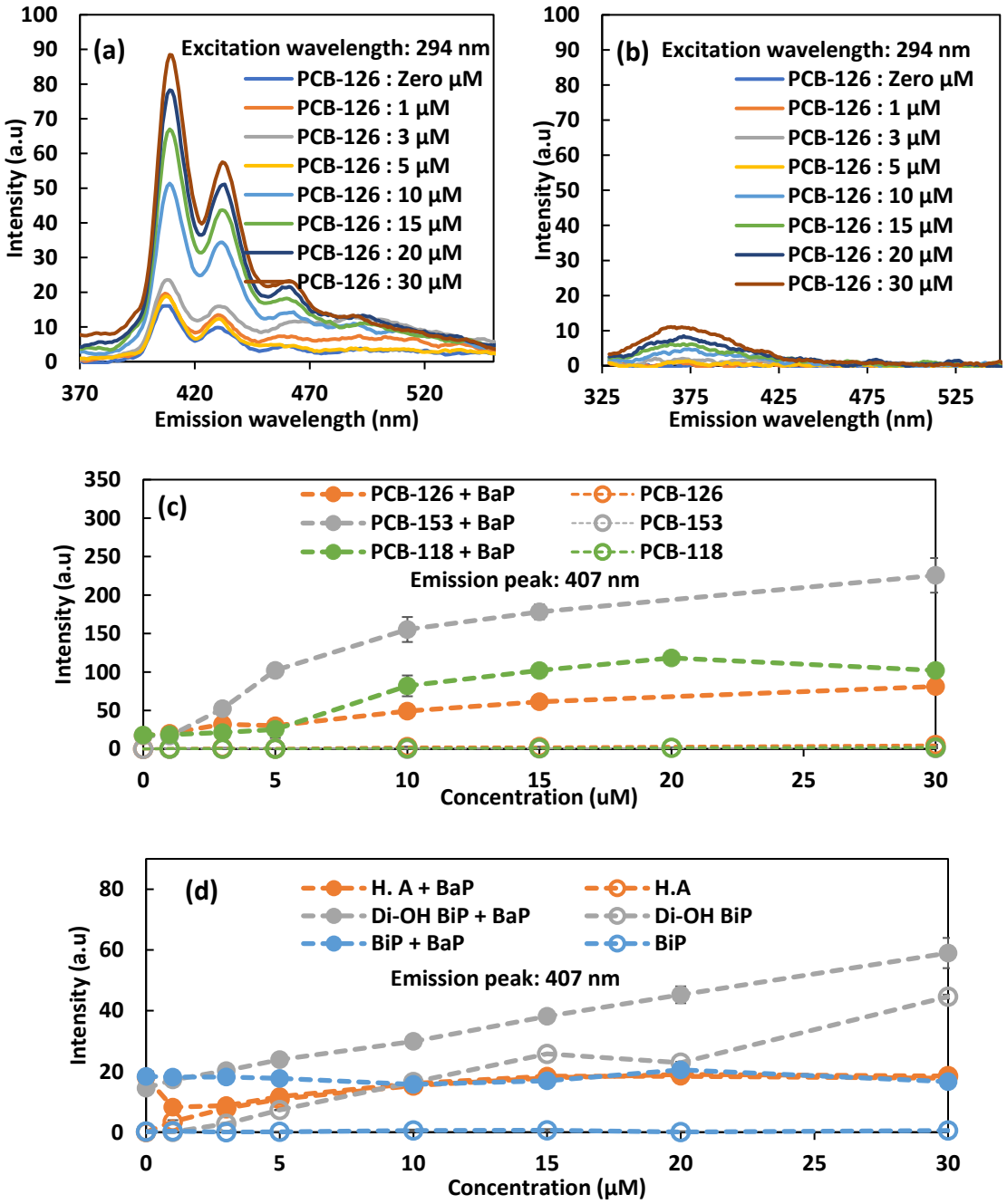

Figure 4.2: BaP with PCBs and other molecules in water.

(a)- Increase in BaP (0.08µM) fluorescence intensity with PCB-126 in water, (b)- PCB-126 control fluoresces spectra in water, (c)- Peak intensity of BaP in the presence of three PCBs and the peak intensities of PCBs control in water,(d)- Change in intensity of BaP with the addition of humic acid, biphenyl (BiP) and 4, 4-Dihydroxy biphenyl (Di-OH BiP) and their control in water

Biphenyl does not show any change in the intensity, whereas, 4,4-dihydroxy biphenyl and humic show an increase in the intensity with BaP and without BaP in water. Humic acid molecular weight was calculated using average chemical formula $C_{187}H_{186}O_{89}N_9S_1$.[233] PCBs have low solubility in pure water, ranging from 0.0012 to 4830 µg/L.[234] PCB-126, PCB-153 and PCB-118 solubility in water is 7.4 µg/L (0.023 µM), 0.91 µg/L (0.003 µM) and 13.4 µg/L (0.04 µM), respectively.[235,236] Solubility of PCBs in water depends on both the number of chlorine atoms with their positions.[237] Sometimes PCBs can be exceeded in water than excepted solubility [238] due to the dissolved solids and humic acid. PCB-126 and PCB-118 have five chlorine atoms and both have unlike solubilities based on the position and geometry of the molecule, whereas, PCB-153 has the highest chlorine atoms (six) among these PCBs and its solubility is lower than other two PCBs. However, the absence of chlorine atoms in biphenyls increases its solubility to 7.48 mg/L.[239] These PCBs showing high solubility as compared to the literature data because of two possible reasons. One, the stock solution of reagents is prepared in DMSO and each sample contains around 1.6 % DMSO in it, which is changing the solubility values in water. Secondly, the presence of two hydrophobic molecules (BaP and PCBs) are providing pockets to each other for the hydrophobic interaction and their solubility in water. If PCB is increased beyond the max solubility in water, then they should make white precipitates. The solution was centrifuged at 4500 rpm for 30 min to see if there is any precipitate that is separating from the solution, however, there were no visible precipitates present in the samples. Furthermore, the intensity interaction between BaP and PCB should reach a plateau, as a constant concentration of PCB will be available in solution and the rest will be settling

down. However, BaP intensity is increasing with increasing the PCBs concentration suggesting the absence of precipitations of PCBs in the solution. Although, there are other factors discussed in the next sections that dramatically affect the solubility of PCBs in water. When BaP is introduced in water, water's hydrogen bond is broken to accommodate BaP by forming a clathrate cage (hydrophobic hydration) around the molecule as exposed in figure 4.3(a). BaP concentration of 0.08μM is the maximum concentration in water with a minim excimer peak as revealed in figure 4.2(a). Increasing the concentration of BaP beyond 0.08 μM starts to increase the excimer peak (around 494 nm). In organic solvents, the intensity of BaP was increased to higher values as a function of BaP concentration without forming the excimer, it is because of the hydrophobic nature of the organic solvents. These organic solvents provide hydrophobic pockets for BaP that result in an increase in its solubility. Similarly, hydrophobic pockets are provided in water that results in an increase in the intensity of BaP. When PCB and BaP are introduced in water, the water molecules surround the individual analyte molecule forming the clathrate hydrates. When the concentrations of hydrophobic molecules (BaP and PCBs) increase in water, they start to interact with each other and make their own cage forming the hydrophobic complex that leads to hydrophobic interaction, figure 4.3(b), this hydrophobic complex possesses its own unique properties that differ from both PCBs and BaP. BaP/PCB complex might be showing high polarity that is breaking the hydrogen bond and interacting with the solvent and causing the solvent-solute interaction effect to enhance the quantum yield of BaP in water.

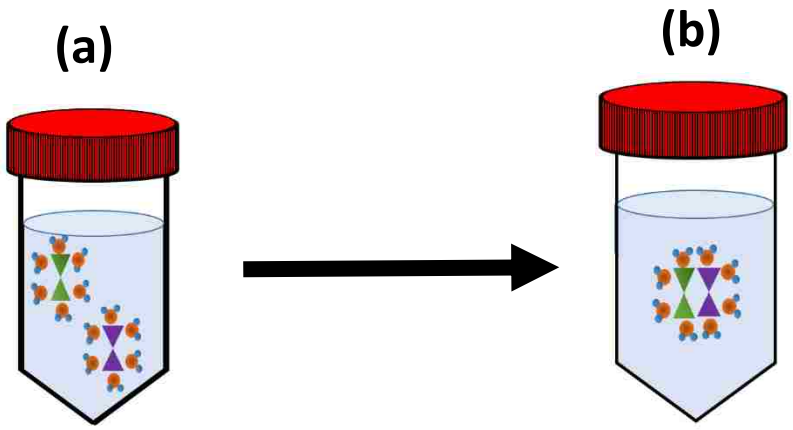

Figure 4.3: (a) Water forms the clathrate cage to accommodate the hydrophobic molecule, (b)- if there are two unique hydrophobic molecules surrounded by the water then these two molecules can stick together to make a complex based on their hydrophobicity and affinity.

PCBs have two benzene rings and chlorine atoms at different locations. The number of chlorine atoms, their location and coplanar and non-coplanar geometry of PCBs determine the degree of hydrophobicity, PCBs and BaP structures are shown in figure 4.4. Higher the number of chlorine atoms higher the hydrophobicity that will lead to more interaction with BaP and increase fluorescence signals.

BaP has the same spectral structure and an increasing trend for PCB-153 and PCB-118 as for PCB-126. PCBs were distinguished in the order of high to low intensity as PCB-153, PCB-118, and PCB-126, respectively. PCB-153 might be making more suitable interaction with BaP based on its structure for maximum increase in quantum yield as compared to coplanar PCB-126 and mix-planar PCB-118. The *log* K_{ow} values of PCB-126, PCB-118 and PCB-153 are 7.09, 7.26 and 7.79, respectively [214], indicating that PCB-153 has the highest hydrophobicity among these PCBs and hence highest change in intensity.

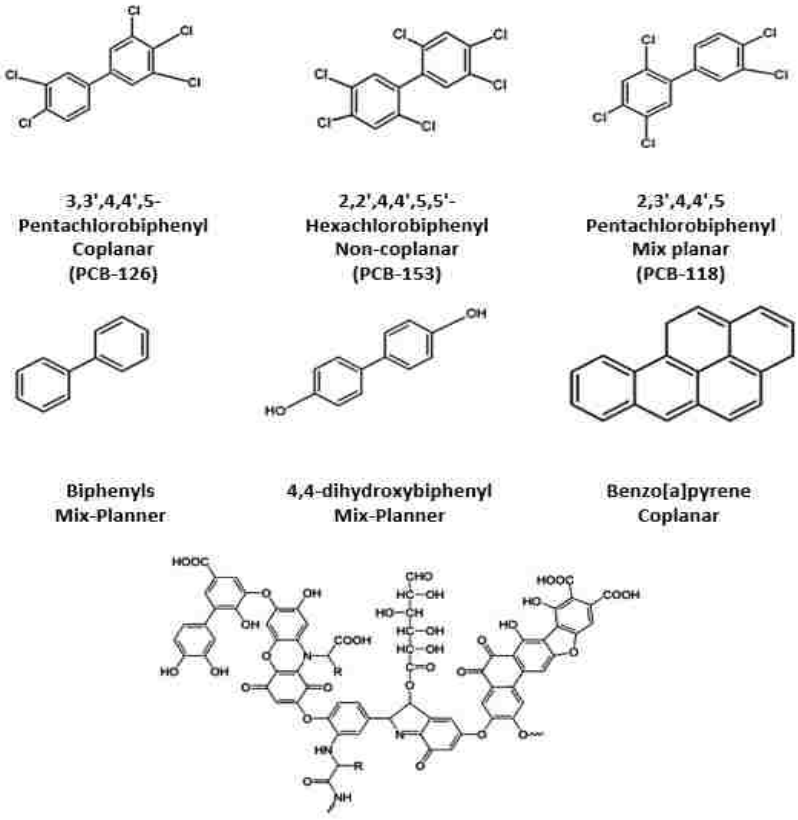

Humic acid structure [258]

Figure 4.4: Structure of PCBs and other molecules used in this work.

Other non-planar PCBs, PCB-206 (2,2',3,3',4,4',5,5',6-nonachlorobiphenyl) and PCB-209 (2,2',3,3',4,4',5,5',6,6'decachloro-biphenyl) has *log* K_{ow} of 9.63 and 10.83 [214], respectively. Since non-planar PCB(PCB-153) gave the highest intensity and has high hydrophobicity due to the higher number of chlorine atoms. Based on the observed trend and keeping the geometry and hydrophobicity in mind, it can be inferred that PCB-209 will give the highest intensity for BaP as all its sides are filled with chlorine atoms.

Figure 4.2(d) displays the interaction of BaP with humic acid (H.A), biphenyl (BiP) and 4, 4-Dihydroxy biphenyl (Di-OH BiP). These molecules are selected as control molecules to compare them with PCBs, the absence of chlorine atoms makes them highly soluble in

water than PCBs. H.A is selected, as it is one of the main impurities in the freshwater. It is noted that BiP does not show any change in the signal in the presence of BaP. Whereas, both H.A and Di-OH BiP show an increasing trend with BaP. Di-OH BiP indicates a high increasing trend than other molecules. Both H.A and Di-OH BiP in water have autofluorescence and their spectra fall in the same region as of BaP. The autofluorescence of both molecules is adding the signal with BaP, it is seen in figure 4.5 and figure 4.6. H.A control intensity in water and its respective intensity with BaP in water show that as H.A's concentration goes beyond 3 μM, fluorescence signals are completely shadowed by the H.A alone and BaP does not play any role beyond this concentration of H.A. Similarly, for Di-OH BiP the variance between the intensity with BaP and without BaP indicates net difference in intensities bounce around 17nm, it represents no actual increase in the signal with BaP. In case of BiP, the absence of chlorine atoms makes it less hydrophobic and more solubilize in water as compared to PCBs. Due to the low hydrophobicity of BiP, it is not interacting with BaP. Di-OH BiP has hydroxyl groups that provide it with the hydrophilic region and the absence of chlorine atoms further reduces its hydrophobicity. Di-OH-BiP is more likely to solubilize in water based on the hydrogen bonding instead of hydrophobic hydration. Whereas H.A is an amphiphilic molecule, the presence of carboxyl and hydroxyl groups helps it to dissolve in the water and aromatic rings provide pi-pi interaction for aromatic molecules.

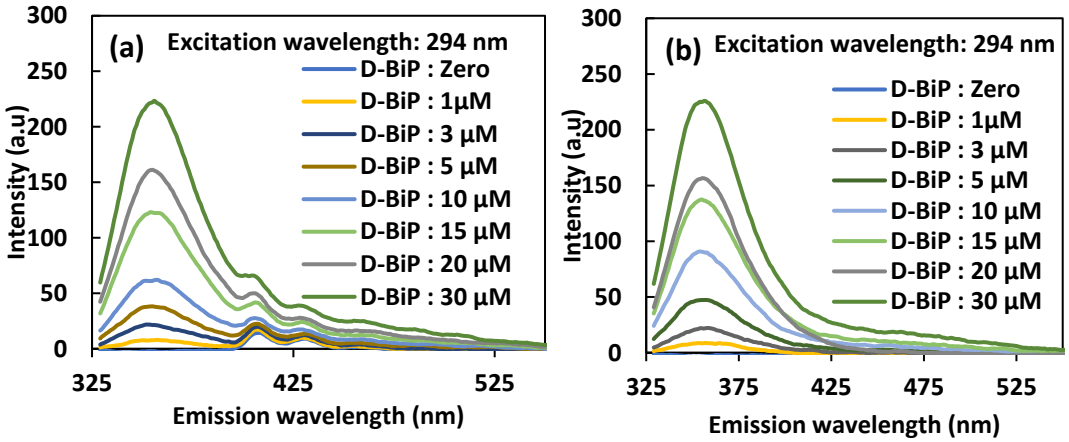

Figure 4.5: (a)-4, 4-dihydroxy biphenyl interaction with BaP in water. (b)- 4, 4-dihydroxy biphenyl control in water.

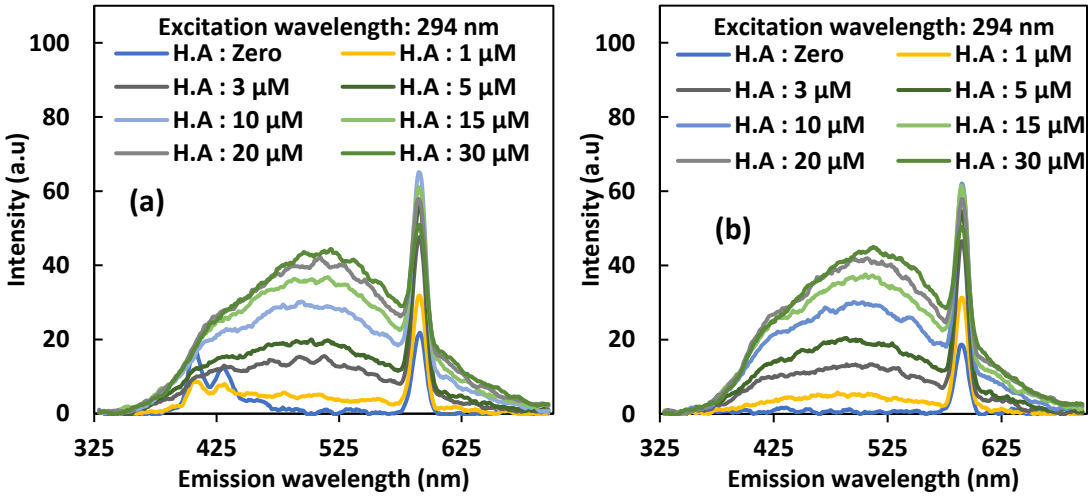

Figure 4.6: (a)-Humic acid (H.A) interaction with BaP in water. (b)- Humic acid control in water.

Based on PCBs, BiP, Di-OH BiP and H.A study with BaP it can be derived that this interaction is a function of the presence of chlorine atoms in the biphenyl family. More types of PCBs can be studied with low chlorine to high chlorine atoms to develop the relationship between the number of chlorine atoms and hydrophobicity.

4.3.3 BaP interaction with PCBs and other molecules in the organic solvent

Hydrophobic interaction is unique and exists only in non-organic solvent (water) and not in the organic solvent. In order to confirm this, BaP/PCBs interaction was studied in DMSO. It is selected as a model organic solvent based on its non-volatility, which makes it easy to handle. Moreover, it does not have any background fluorescent signal that can interact with the signals from PCBs and BaP. The peak intensity of BaP with PCB-126, PCB-118, and PCB-153 is shown in figure 4.7. The interaction of BaP/PCB is being inhibited in an organic solvent. BaP baseline intensity is higher in DMSO than in the water but there is no dose-dependent effect on BaP intensity within the concentration range. Biphenyl and 4,4-Dihydroxy biphenyl were also studied with BaP in DMSO, it was also noted that these two molecules do not have any interaction with BaP in the organic solvent.

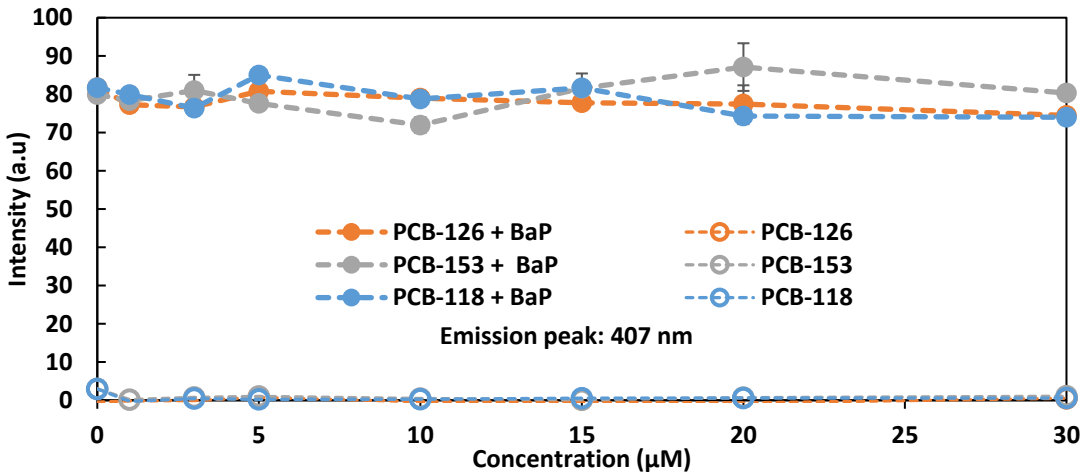

Figure 4.7: PCBs interaction with BaP in an organic solvent.

BaP and PCBs are easily dissolved in most of the organic solvents, they make their own pockets (figure 4.8) because of their high solubility, unlike water where they stick together (figure 4.3(b)) within their water cage to form a hydrophobic complex. Figure 4.7 indicates the max peak intensity around 407 nm for all three PCBs with BaP and without BaP in DMSO. Figure 4.9(a) and 4.9(b) show PCB-126 spectra with and without BaP in DMSO. There is no change in spectral intensity or shape. Similarly, no interaction was observed for BiP and Di-OH BiP in DMSO, their behavior was found to be the same in both organic solvent and in water. As discussed in the previous section, in water, both molecules have low solubility and strive for hydrophobic pockets, which is a driving force in bringing both molecules closer to each other.

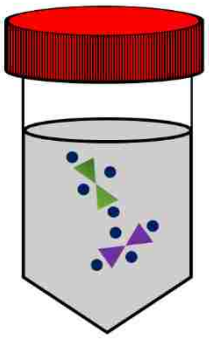

Figure 4.8: Hydrophobic molecules staying apart in an organic solvent and not making and complex for change in energy.

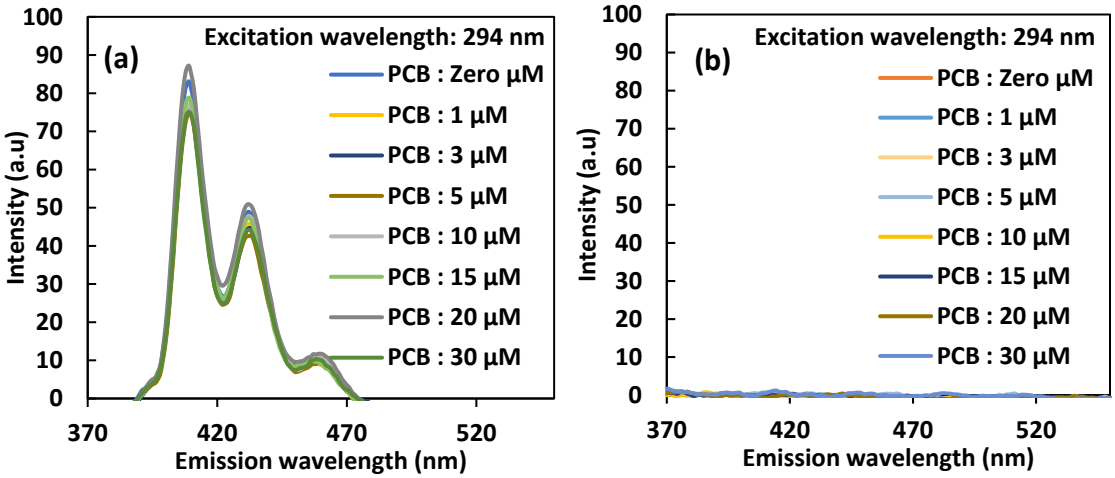

Figure 4.9: (a)- PCB-126 interaction with BaP in DMSO, (b)- PCB-126 control in DMSO.

4.3.4 Effect of water properties and environmental contaminants on BaP/PCB interaction

BaP is successfully detected in the DI water, but freshwater has altered conditions than DI water, these affect the detection system. The factors that are studied along with BaP and PCBs interaction include pH, humic acid and ionic strength. Temperature is also one of the factors as temperature directly linked to the kinetic energy of the molecules. The temperature change can affect the viscosity of the solution that can change the kinetic energy of the molecules [240] and hence changing the fluorescence properties. This problem is easy to handle by using a thermostatted cuvette cell or letting the sample reach the room temperature before analyzing it. Temperature effects are not mentioned here as all the samples are studied at room temperature.

4.3.4.1 pH effects

pH is an important factor in water as a slight change in pH can radically influence the fluorescence intensity.[241] pH can also change the solubility of the solute in water making it either more soluble or precipitating it out of the water and in both cases, the fluorescence signals will change. Groundwater pH falls in range ~6 to 8.5 and freshwater pH varies from 6.5 to 8.5.[242] DI water has an unbuffered pH of 5.8, which is close to the lower limit of pH of 6. The solvent pH is changed to the higher end and its effects on sensing are studied. Figure 4.10(a,b and c) illustrate the interaction of BaP with PCB-126, PCB-153, and PCB-118, respectively in pH 5.8 (DI water pH) and in pH 8.5. The change in pH affects each PCBs in a unique way. PCB-126 and PCB-153 intensities decrease as the pH is changed from 5.8 (DI water) to 8.5. Whereas, the intensity for PCB-118 increases with increasing the pH of water. The intensity of BaP control (zero µM PCBs) is almost the same (around 16 a.u) in both 8.5 and 5.8 pH, this means the change in fluorescence intensity is due to the change in properties of PCBs at 8.5. pH might be affecting the solubility of PCBs in water, pushing the molecules closer to each other for enhanced interaction or relaxing them for low interaction. This interaction is different for each PCB, making it a characteristic of PCBs type. Another possible reason is the interference in the interaction of BaP and PCBs(PCB-126 and PCB-153), it might be based on the orientation of chlorine atom's sensitivity to pH as PCB-126 and PCB-118 has the same number of chlorine atoms but at distinctive locations and both PCBs demonstrate opposite effect with the change in pH. pH 8.5 is changing the spectral shape of PCB-126 as shown in figure

4.10(d) by lifting the part of the curve around 490 nm, whereas spectra shape for PCB-153 and PCB-118 are not changing except their intensities.

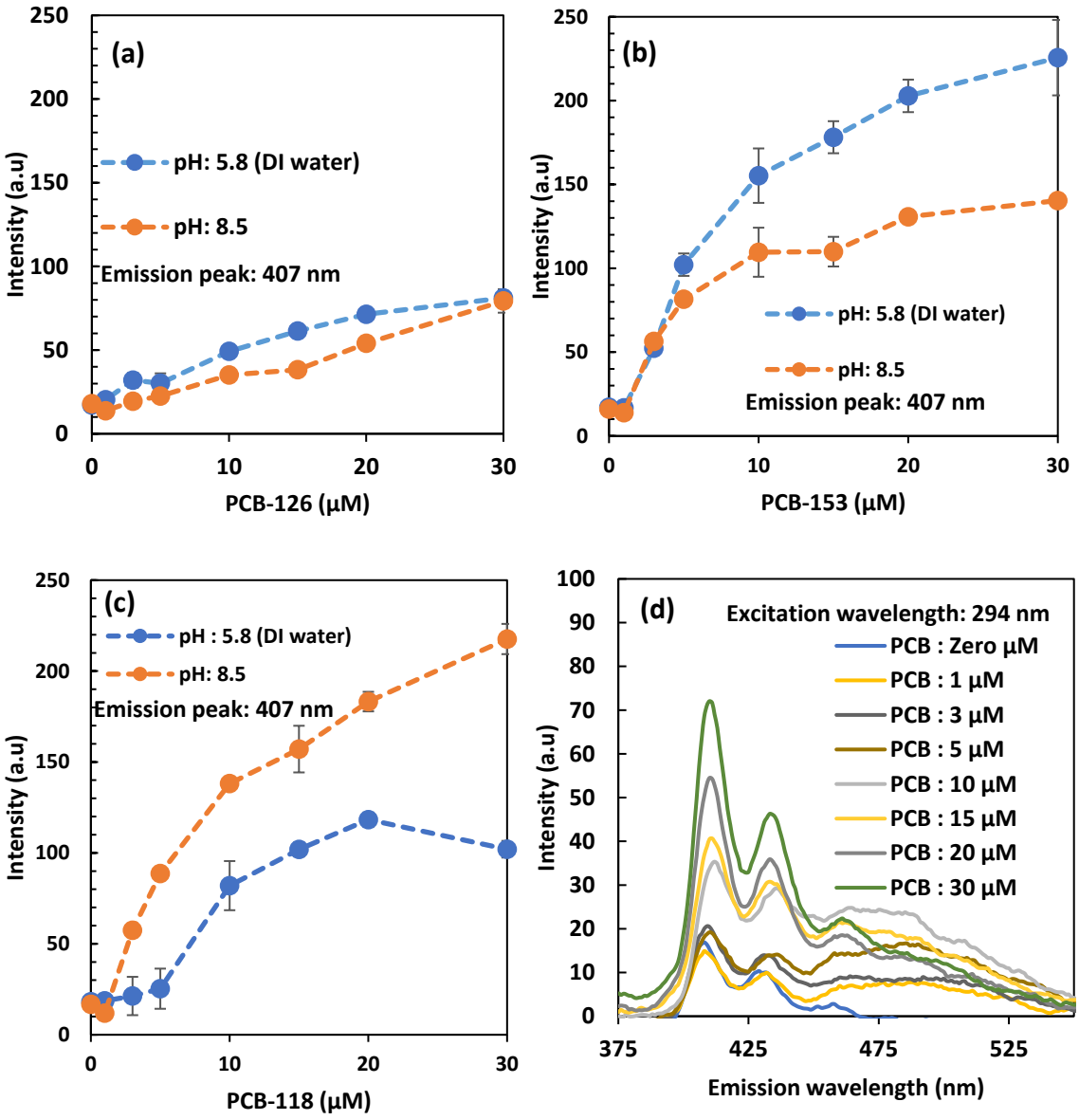

Figure 4.10: BaP and PCBs in different pH solutions.
(a)- BaP and PCB-126 interaction in DI water with unbuffered pH of 5.8 and 8.5, (b)- BaP and PCB-153 interaction in DI water with unbuffered pH of 5.8 and 8.5, (c)- BaP and PCB-118 interaction in DI water with unbuffered pH of 5.8 and 8.5, (d)- PCB-126 in water with BaP at pH 8.5

As pH 8.5 is towards the basic range, it might be the presence of OH^- ions that are increasing the specific solvents effects on the hydrophobic complex of PCB-118 and BaP. These ions might be interacting with the charge on the hydrophobic molecule or interacting with the induced dipole moment caused by the electronic excitation. For the other two PCBs, this effect is more profound in the presence of H^+ ions i.e. pH 5.8. For 10 µM of PCBs, the signal drops by 28% and 29% for PCB-126 and PCB-153, respectively. However, for PCB-118, it increases by 59%. The pH value of 8.5 is the highest for freshwater that confirms the change in the fluorescence signal of BaP with PCBs, but PCBs are still detectable if the pH of water is varied between 6 and 5.8.

4.3.4.2 Effect of Natural organic matters (NOM)

The concentration of natural organic matter (NOM) in freshwater ranges from 0.1 ppm to 20 ppm and mainly comprises of humic acid substance.[243] It can give light brown to dark brown color to water based on its concentration. To evaluate the impact of these compounds on PCBs detection, five concentrations of humic acid (0.1, 3,5,10 and 20 ppm) were selected here to study the change in fluorescence signals of BaP and PCBs. Since humic acid has background fluorescence, in order to get the BaP specific intensity in the presence of humic acid, background signals of humic acid were subtracted from the respective intensity. Figure 4.11(a,b and c), represents the interaction of BaP/PCBs in the presence of humic acid in the solvent.

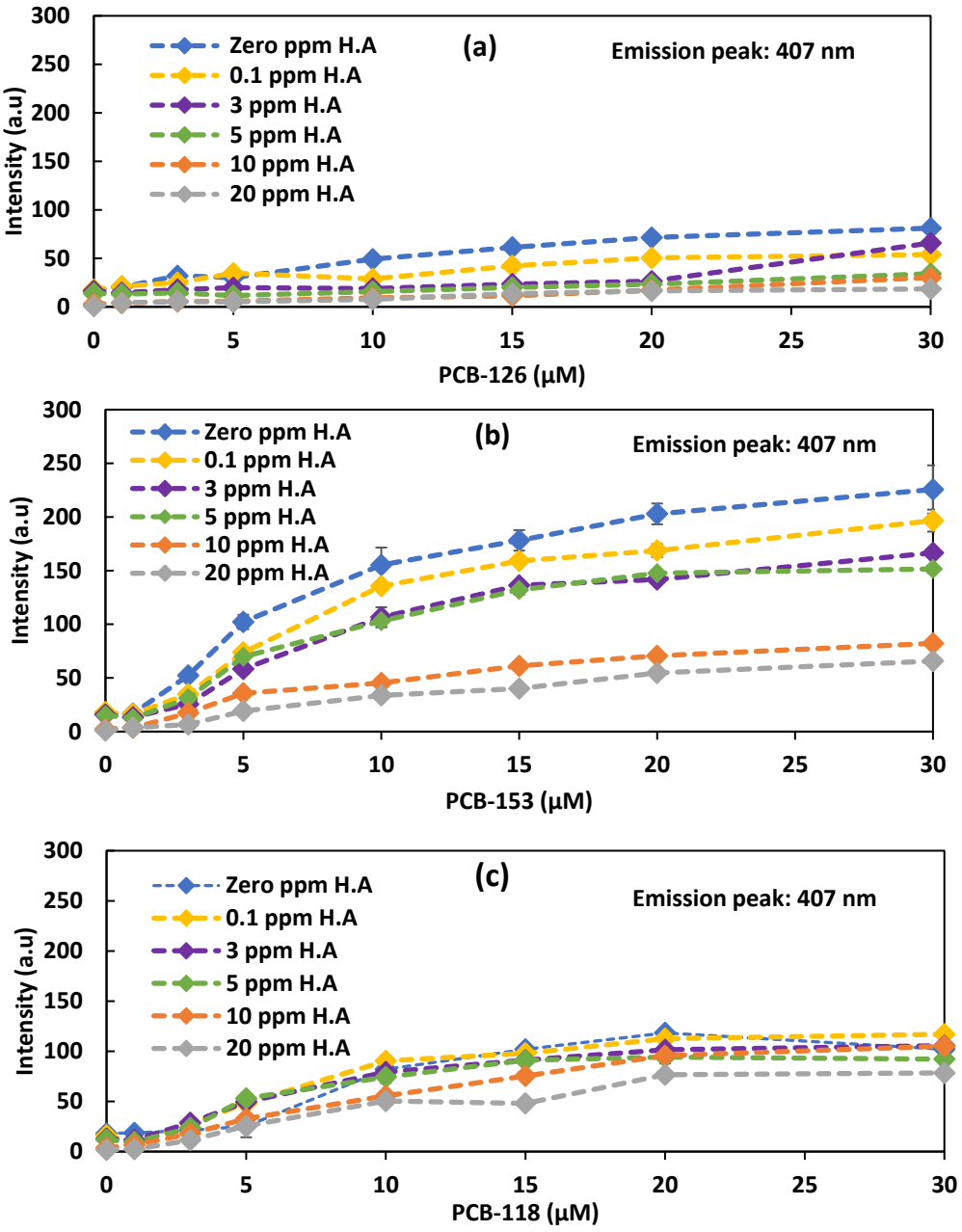

Figure 4.11: BaP and PCBs in water in the presence of humic acid.
(a)- BaP/PCB-126 interaction in the presence of humic acid in water, (b)- BaP/PCB-153 interaction in the presence of humic acid in water, (c)- BaP/PCB-118 interaction in the presence of humic acid in water.

Humic acid is an amphiphilic molecule. It has carboxyl and hydroxyl groups that make it partially hydrophilic. Hydrophobic pockets in the humic acid are ideal for pollutants in water and soil. Humic acid can control the acidity of the soil, it can remove hazardous compounds and its amphiphilic properties are affecting the environment.[244] Humic acid's critical micelles concentration is 10g/L (10,000 ppm) which is a much higher concentration used in this work. Humic acid is the reason PCBs and other pollutants are soluble in water and in soil due to its hydrophobic pockets. Humic acid causes a decreasing trend in the intensity of BaP with PCB-126 and PCB-153. Whereas, for PCB-118, there is not much change in the intensities of BaP. Effect of humic acid is not the same for each PCB, for example, in the presence of 10 ppm of humic acid, signals are reduced to 19 %, 29% and 67% for PCB-126, PCB-153, and PCB-118, respectively and this decrease is 15.7%, 21.7% and 61.5% for 20ppm of humic acid. PCB-126 and PCB-153 show a profound effect on the BaP signal in the presence of humic acid, whereas, PCB-118/BaP has a very low effect in the presence of humic acid. There are two possibilities for interaction. Either both molecules (PCB and BaP) are sticking at the same location on the humic acid or they are still in the water cage and interacting without sticking to the humic acid.

The presence of humic acid is challenging for PCBs sensing in water as it is decreasing the signal due to its hydrophobic pockets, but the hydrophobicity of PCBs is stronger than humic acid that is why BaP is still producing signals in the presence of PCBs. This system is strong enough to sense and develop a trend for PCBs in the maximum possible concentration of humic acid in freshwater.

4.3.4.3 Effect ionic strength

Freshwater's ionic strength typically varies from 1mM to 5mM. Whereas, groundwater has ionic strength ranges from 1mM to 20mM. The sensing interaction of BaP and PCBs are studied using three ionic strength values of 1 mM, 5 mM, and 20 mM. Since the electrolyte solutions deviate from the ideality, here salt ionic strength is converted to the activity coefficient to study the effect of deviation from ideal behavior. Sodium Chloride(NaCl) is selected to control the ionic strength of the water, as its molar concentration is equal to the ionic strength (1:1 electrolyte) of water, it is calculated using the following equation [245]

$$I = \frac{1}{2}\sum_{i=1}^{n} c_i \, z_i^2$$

Where

I = ionic strength (M, mol/L)

c_i = Molar concentration of ions *i* (M, mol/L)

Z_i = Charge number of the ion

Since the highest ionic strength in this work is 20 mM (<1M), Extended Debye-Hückel equation can be used to calculate the ionic activity coefficient of each ion

$$\log \gamma = \frac{-0.51 z^2 \sqrt{I}}{1 + \left(\alpha \sqrt{I}/305\right)}$$

Where,

γ = Activity coefficient

α = Ion size parameter (400 Picometer for Na^+, and 300 Picometer for Cl^-)

Solution properties depend on both cations and anions in the water, for which, single-ion activity coefficients can be linked to the activity coefficient of the dissolved salt as if undissociated. The mean stoichiometric activity coefficient ($\gamma_{\pm}$) of NaCl can be calculated with the following equation.

$$\gamma_{\pm} = \sqrt{\gamma_{+}\gamma_{-}}$$

Where

γ_{+} and γ_{-} are the activity coefficients of cations and anions

The ionic activity coefficient of Na^{+} and Cl^{-} ions and the stoichiometric activity coefficient of the salt are calculated in the following table.

Table 4.2: Ionic activity coefficient of individual ions and stoichiometric activity coefficient.

Ionic Strength (mM)	$\boldsymbol{\gamma_{+}}$	$\boldsymbol{\gamma_{-}}$	$\boldsymbol{\gamma_{\pm}}$
0	1	1	1
1	0.96	0.96	0.96
5	0.93	0.93	0.93
20	0.87	0.86	0.87

Figure 4.12(a,b and c) expresses the interaction of BaP and PCBs in the presence of activity coefficients of salt in water. Under the dilute electrolyte conditions, the activity coefficient is 1. However, as the ionic concentration increases the solution behaves non-ideally resulting in a decrease in the activity coefficient below 1, shown in table 4.2. There are two reasons for the activity coefficient to be below 1.

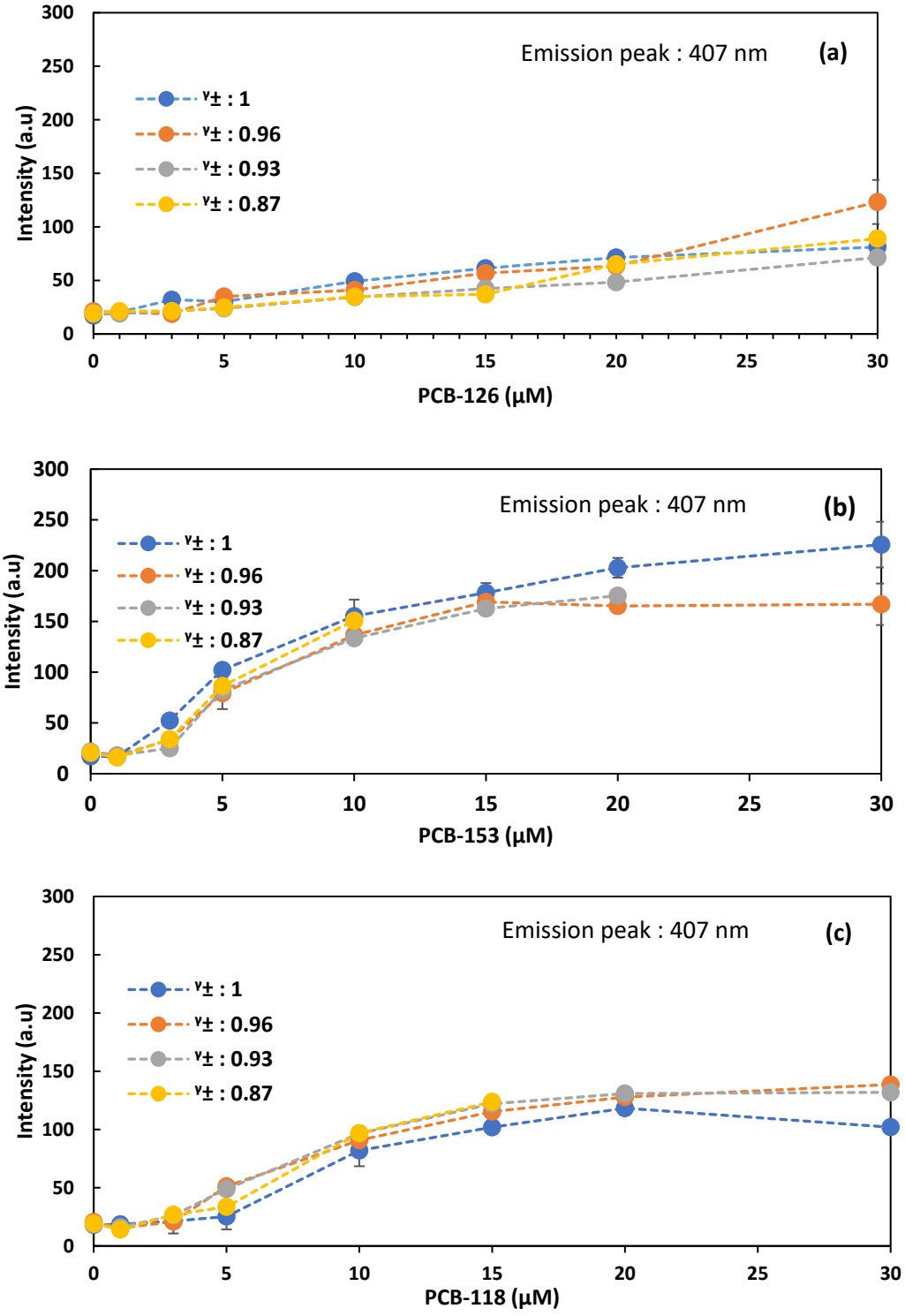

Figure 4.12: BaP and PCBs in water with different salt activity coefficients.
(a)- BaP and PCB-126 interaction. (b)- BaP and PCB-153 interaction. (c)- BaP and PCB-118 interaction.

First, the ionic dipole interaction with a water molecule that leads to solute-solvent interaction. Secondly, the ion paring, in which Na^+ ions paired with Cl^- ions in water and are less active, it results in the solute-solute interaction.

The presence of sodium chloride is affecting the interaction of BaP and PCB. Since water molecules form a clathrate cage around the BaP/PCB pair. The existence of ions in water is causing the dipole interaction with water molecules and fewer water molecules are available for the hydrophobic pair. As the solution deviates from ideality (increase in salt concentration) the interaction of BaP and PCBs decreases, it is shown for both PCB-126 and PCB-153. However, PCB-153 has high hydrophobicity and at lower activity coefficient fewer water molecules are around BaP/PCB-153, it is causing PCB-153 to crash out of water. PCB-118 has opposite effects in the presence of salt as compared to the other two PCBs. The decrease in the activity coefficient is increasing the hydrophobic interaction of BaP and PCB-118. The presence of ions might be increasing this interaction. However, like PCB-153, PCB-118 is also crashing out of the water at higher concentration. Electrolytes also cause “salting-in” or “salting-out” of non-electrolytes in water and salting-in or salting-out coefficients can be calculated using Setschenow equation. Nevertheless, the application of the Setschenow equation is outside the scope of this work, and it is not discussed here.

4.3.5 BaP with real-world samples

Benzo[a]pyrene (BaP) was also evaluated for real-world PCB samples. Samples were obtained from Arcadis, (Highlands Ranch, CO) using the Super Research Program (SRP) group platform. The water samples were used as obtained without any further

characterization. According to the Arcadis analysis, the sample contains Aroclor 1248 from 30 to 100 µg/l. Moreover, the literature indicates that Aroclor 1248 is dominated with PCB-52, followed by PCB-44 and PCB-66 and other PCBs in small fractions. The upper limit of Aroclor 1248 in the sample is not high enough to be successfully detected by BaP. In order to overcome this problem, another PCB of known relationship to BaP was mixed with the real sample, and the interaction of PCB/BaP was observed in the presence of Aroclor 1248. For this purpose, PCB-153 was selected with three solvent samples (3 ml each), one the lab DI water, second the contaminated water and third the treated water from the remediation site. PCB-153 and BaP were added and mixed well for the interaction. The spectra for these interactions are displayed in figure 4.13(a,b and c). The changes in the intensity of BaP around an emission peak of 407nm are shown in figure 4.13(d). BaP/PCB-153 is behaving the same way at a lower concentration of PCB-153 for DI water and contaminated water. They do show a unique behavior at 3µM and at the higher concentration of PCB-153 in the two solvents. Whereas, in treated water, this interaction is different from the contaminated water system. It might be because of the leftovers from the treatment system that Arcadis is using to treat the water. It is interacting with both PCB-153 and BaP and the concentration of PCB-153 goes higher than 6 µM in the treated water, the spectra starts to go down. It is because of the decrease in the solubility of BaP/PCB-153.

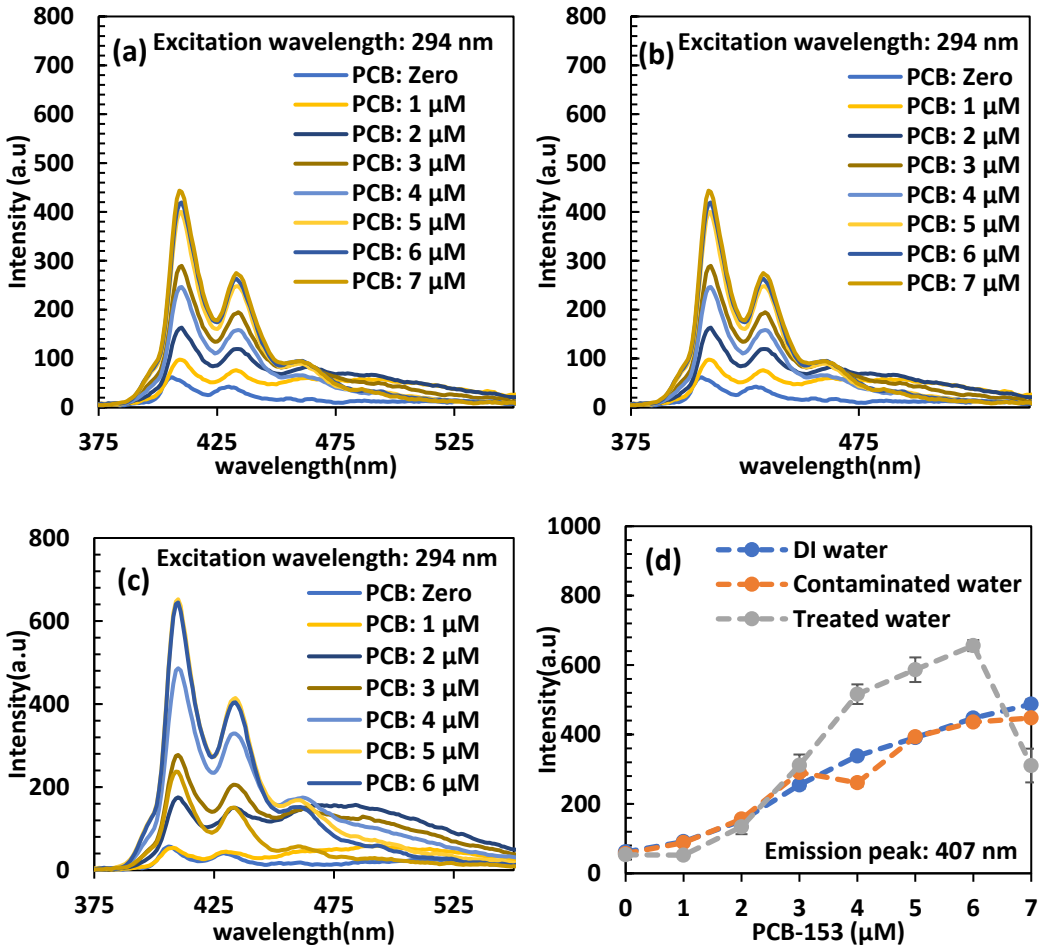

Figure 4.13: BaP interaction with real-world samples.
PCB-153 with BaP in (a)- DI water, (b)- the presence of Aroclor1248 contaminated water, (c)- the treated water from the contaminated site. (d)- BaP peak intensity with PCB-153 in three water solvents.

4.4 Conclusions

Three different PCBs, PCB-126(Coplanar), PCB-118 (Mix-coplanar) and PCB-153 (Non-coplanar) were successfully detected in water using hydrophobic interaction between PCBs and BaP. The interaction is diverse for each PCB molecule that depends on the numbers of chlorine atoms, their orientation and the geometry of the molecule. It is also found that this interaction is unique to non-organic solvent and does not exist in an organic solvent. PCB-153 demonstrates higher hydrophobic interaction in water than PCB-118 and PCB-126. Furthermore, presences of impurities affect the sensing of PCBs in terms of intensity and shape of spectra, but the dose-dependent trend exists despite the impurities. The increase in pH decreases the BaP intensity for PCB-126 and PCB-153, whereas it increases for PCB-118. Humic acid being an impurity for fluorescence also decreases BaP intensity for PCB-126 and PCB-153 but PCB-118 interaction with BaP does not change as much as the other two PCBs. Moreover, changing the ionic strength of water causes the sating-in or salting-out behavior of the PCBs/BaP complex. Increase ionic strength decreases the intensity for both PCB-126 and PCB-153 but for PCB-118, the intensity of BaP increases due to the salting-out phenomenon. PCB-126 and PCB-153 produce the same trends but have opposite intensities levels. Whereas, PCB-118 is very contrasting compared to the other two PCBs. Based on the intensity trends, it is possible to detect each PCBs in water with allowable limits of impurities. BaP didn't show promising results with the real-world samples due to the very low concentration of PCBs. This fluorophore can be immobilized on the particles to enhance the sensitivity and efficiency of the sensing system.

CHAPTER 5. EVALUATION, DESIGN, AND SYNTHESIS OF PYRENE FUNCTIONALIZED POLYMER PARTICLES

5.1 Introduction

Polymers have been widely used to improve the quality of human life. Polymers are large molecules, called macromolecules, consist of many simple repeated units.[247] Artificial polymers have an advantage over natural polymers, they are reproducible under controlled conditions with a wide range of tailored properties such as degradation, pore size, chemical, physical and mechanical properties.[248,249] Polymers can be organized with multiple components to harness novel properties.[250] Polymer-based materials have been reported for environmental contamination sensing including gases, heavy metal ions, anions, organic compounds, and explosives.[251,252]

In this work, it was hypothesized that the fluorescence dye from chapter 4 can be incorporated within the polymer network to enhance the sensitivity and the reusability of the sensing system. For this purpose, poly(acrylic acid) was selected as a polymer backbone due to its high hydrophilicity and controllable swelling. Water and hydrophilic polymer will push PCBs towards hydrophobic dye, and it will produce the same response as in chapter 4.

Here, Pyrene was selected as a model fluorescent probe instead of BaP, because of the commercial availability of functionalized pyrene. Crosslinked poly(acrylic acid) microparticles were synthesized with pyrene molecules in the network. Poly(acrylic acid)

MPs swell above pKa 4.26 and let more analyte move into the polymer chains. These MPs are evaluated for the detection of polychlorinated biphenyls (PCBs) in water.

5.2 Experimental section

5.2.1 Material

Unless otherwise stated, chemicals and reagents were used as received without any additional purification. 2,2',4,4',5,5'-hexachlorobiphenyl (PCB-153) and 2,3',4,4',5 pentachlorobiphenyl (PCB-118) were purchased from AccuStandard Inc., (New Haven, CT). Mono-2-(methacryloyloxy)ethyl succinate, boric acid, 2,2'-azobisisobutyronitrile (AIBN) and pyrene were purchased from Sigma Aldrich, (St.Louis, Mo). 1-pyrenemethanol was purchased from TCI (Portland, OR). Polyethylene glycol diacrylate (400 MW) (PEGDA) was purchased from Polysciences, Inc. (Warrington, PA). N,N'-dicyclohexylcarbodiimide, 4-dimethylaminopyridine, and acrylic acid were purchased from Acros Organics (Pittsburg, PA). Sodium hydroxide, acetic acid, toluene, and phosphoric acid were purchased from Fisher Scientific (Pittsburg, PA). Dimethyl sulfoxide-D6 was purchased from Millipore (Burlington, MA). Dimethyl sulfoxide (DMSO), dichloromethane (DCM), acetone, acetonitrile (ACN) and anhydrous tetrahydrofuran (aTHF) were purchased from Pharmaco, (Brookfield, CT). Molecular sieves of 3 angstroms were added to the organic solvents to keep them dry.

5.2.2 Method

5.2.2.1 Solvent selection for Pyrene monomer (PyMMA) synthesis

For the esterification reaction, four solvents were selected (acetonitrile, dichloromethane, acetone, and tetrahydrofuran). Mono-2-(methacryloyloxy)ethyl succinate (MMES) was kept at 1 mole equivalent to pyrene methanol (PyMeOH). For Steglich esterification reaction, N,N'-dicyclohexylcarbodiimide (DCC) was kept at 5 molar equivalents to PyMeOH and 4-dimethylaminopyridine(DMAP) at 1 molar equivalent to PyMeOH. Four reagents were dissolved in the solvent in the round bottom flask equipped with a magnetic stirrer and mixed the solution 24 hours under room temperature conditions. The flask was covered with aluminum foil to avoid light contact with PyMeOH. After a few hours, DCC started converting to white precipitates of dicyclohexylurea (DCU). After 24 hours, free DCC was converted to DCU by adding water in equivalent concentration to the total DCC. The mixture was stirred an additional 30 minutes for maximum conversion of DCC to DCU. White precipitates were separated using syringe filters. The clear solution was characterized.

5.2.2.2 Synthesis and purification of PyMMA

Based on the characterization results of PyMMA, ACN was selected as a solvent for the esterification reaction. Similar steps were repeated as in section 5.2.2.1 the synthesis of PyMMA. Water was added after 24 hours and white precipitates were separated using a syringe filter to obtain a clear solution. In order to remove the DMAP and unreacted pyrene methanol, around 8 volume times cold water was added to the solution to crash

out the product in the form of white precipitates. The mixture was placed in the refrigerator an additional 3 hours for maximum separation of the PyMMA. After that, the white particles of PyMMA were separated using centrifugation at 13000 rpm for 30 min. The supernatant was separated while the product was washed with water multiple times to analyze the DMAP to find the number of washes needed. Precipitates of PyMMA from the centrifuge were separated and dried in the freeze dryer. Dried PyMMA was redispersed in DCM and syringe filtered again to remove any remaining impurity. DCM was evaporated using a rotary evaporator. The final pure product was stored in the refrigerator until further use.

5.2.2.3 Copolymerization of PyMMA and acrylic acid

Acrylic acid was copolymerized with PyMMA in the presence of PEGDA as a crosslinker and AIBN as a free radical initiator. Two solvents mixtures were used in this work, DMSO/DCM and DMSO/toluene. First PEGDA (1 mole %) and PyMMA(1 mol%) were introduced in the glass vial and dissolved with DCM or toluene. After this, DMSO and acrylic acid in a volume ratio of 1:1 were added to the glass vial. Nitrogen was purged from the monomer's solution for 15 minutes then AIBN (1 wt.% of total monomers) was introduced and stirred until AIBN was completely dissolved. A glass template was prepared using two glass plates separated by the Teflon spacer. Sides and bottom of the template were covered with parafilm to avoid any leakage. In addition, binder clips were used to hold the plates together. The monomer solution was introduced to the glass plate's template and placed in a preheated oven at 60 ^{o}C for 3 hours. The film was

separated from the parallel glass template. It was first washed with DCM/toluene based on the initial solvent combination. Second, wash with DMSO and then third wash with DI water. Each wash lasted 20 minutes. Films were submerged in the solvent and placed on a plate shaker at low speed. Films were then separated and placed in the vacuum oven at 50 ^{o}C for one day to remove the water.

5.2.2.4 Py-PAA film cryomilling to the MPs

The dried polymer film was then cryomilled to obtain microparticles using a SPEX Sample Prep 6875D Freezer/Mill using liquid nitrogen. The film was cut to fit within the stainless-steel milling tubes. It was subjected to four milling cycles of 5 minutes each at 15 cycles per second CPS (max), with 5 minutes pre-cool and cooling in between each cycle. Microparticles were then collected and dried overnight in the freeze dryer and stored in a dark cold place.

5.2.2.5 PCB detection using Py-PAA MPs

PCBs detection system, a stock solution of PCB was prepared in DMSO. PyMPs with a concentration of 0.1 mg/ml were dispersed in the DI water at altered concentrations levels of PCB being introduced into the solution. The interaction of pyrene from the MPs and PCBs was studied using fluorescence spectroscopy under stirring conditions to keep the MPs suspended in the solvent.

5.2.3 Characterization

5.2.3.1 High-Performance Liquid Chromatography (HPLC)

In order to confirm the esterification reaction, the filtered product solutions from different solvents were diluted to 0.05 mg/ml (based on the initial Py-MeOH used) and analyzed using reverse-phase HPLC (Water Phenomenex C18 column, 5 µm, 250 mm (length) x 4.6 mm (ID) on a Shimadzu Prominence LC-20 AB HPLC system. The sample was introduced to the HPLC with an injection volume of 50 µl. The isocratic elution method was used with 30% water concentration along with ACN for 30 minutes run. The chromatogram was recorded at 240 nm.

5.2.3.2 Proton Nuclear Magnetic Resonance (^{1}H-NMR) Spectroscopy

Esterification reaction was also studied using ^{1}H-NMR spectroscopy. Reagents were dissolved in DMSO-D6 at a concentration of 10 mg/ml. Solution was transferred to the NMR tubes and analyzed using 400 MHz Varian 400-MR equipped with an ATB Probe using s2pul plus sequence. The obtained data was analyzed using TopSpin 4.02 software from Bruker.

5.2.3.3 Fourier-transform infrared spectroscopy (FTIR)

The new bonds in the product were also confirmed using FTIR spectroscopy. A Varian Digilab stingray FTIR system with a 7000e stepscan spectrometer was used. Powder and liquid samples were placed on the crystal and software methods were used to produce their spectra.

5.2.3.4 UV-Visible spectroscopy

The absorbance spectra of the resultant product was analyzed using Varian Cary 50 Bio UV-Visible spectrophotometer. Samples were introduced in the holder using a quartz cuvette.

5.2.3.5 Particle size analysis

The particle size distribution was analyzed using Shimadzu SALD-7101 UV particle size analyzer operated using WingSALD software (ver. 1.02, Shimadzu). The refractive index was set to 1.4. First, the instrument was filled with the buffer solution for blank calibration. Second, MPs suspended in buffer solution were analyzed. MPs were dispersed 24 hours before the size analysis for equilibrium swelling. Last, the sample was introduced into the instrument and measured under stirring. Each sample was measured into triplicate.

5.2.3.6 Fluorescence spectroscopy

Fluorescence spectroscopy was performed using a Cary Eclipse spectrophotometer. It has a maximum spectral intensity of 1000 a.u. Samples were introduced into the spectrophotometer using a quartz cuvette from Starna Cells, Inc., (Atascadero, CA). The instrument was equipped with “Cary Single Cell Peltier Accessory” for temperature control and stirring facility. MPs samples were analyzed under continuous stirring.

5.3 Results and Discussion

5.3.1 Selection of Pyrene as a potential fluorophore for PCBs sensing

In the previous chapter, PCBs were detected using BaP. While it is preferable to study BaP conjugated into polymer networks, BaP with reactive groups is not commercially available. As an alternative, pyrene was used in this study. To confirm the ability of pyrene as BaP analog, it was hypothesized that pyrene will behave in the same fashion as BaP in the organic solvents and with PCBs. For this purpose, the fluorescence spectra of pyrene was first studied in a range of organic solvents to evaluate its response to the surrounding environment. Pyrene in a concentration of 1 µM was dissolved in water, EtOH, DMSO, ACN, ethyl acetate, toluene, and nHexan. Pyrene excitation and emission spectra in EtOH are shown in figure 5.1. The emission spectra of pyrene have five distinctive emission band peaks. Here, only focus at I_1 (375 nm) and 1_5 (394 nm), the ratio of I_5/I_1 intensity increases with a decrease in the polarity of the local environment around pyrene. [220,253,254] The trend is seen in figure 5.2 (a). Whereas, pyrene peak intensity of I_1 (375 nm) in different solvents is given in figure 5.2 (b). Pyrene peak intensity is decreasing with decreasing the polarity index of the solvents. Similarly, to BaP, pyrene has the ability to react to the change in the surrounding environment.

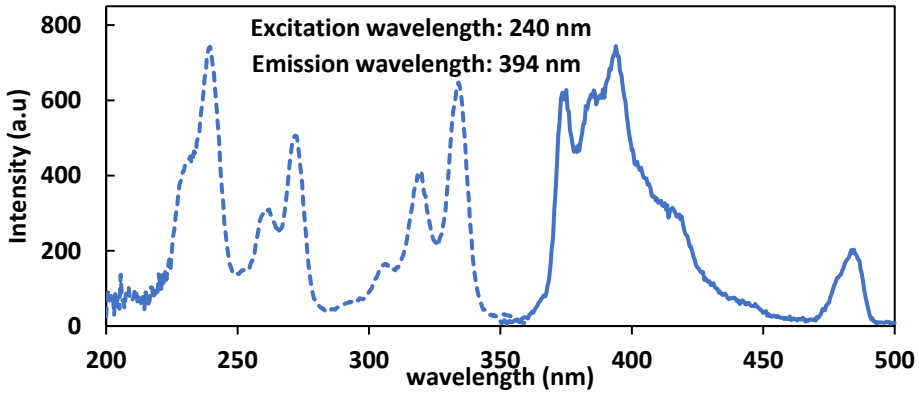

Figure 5.1: Pyrene excitation and emission spectra in ethanol.

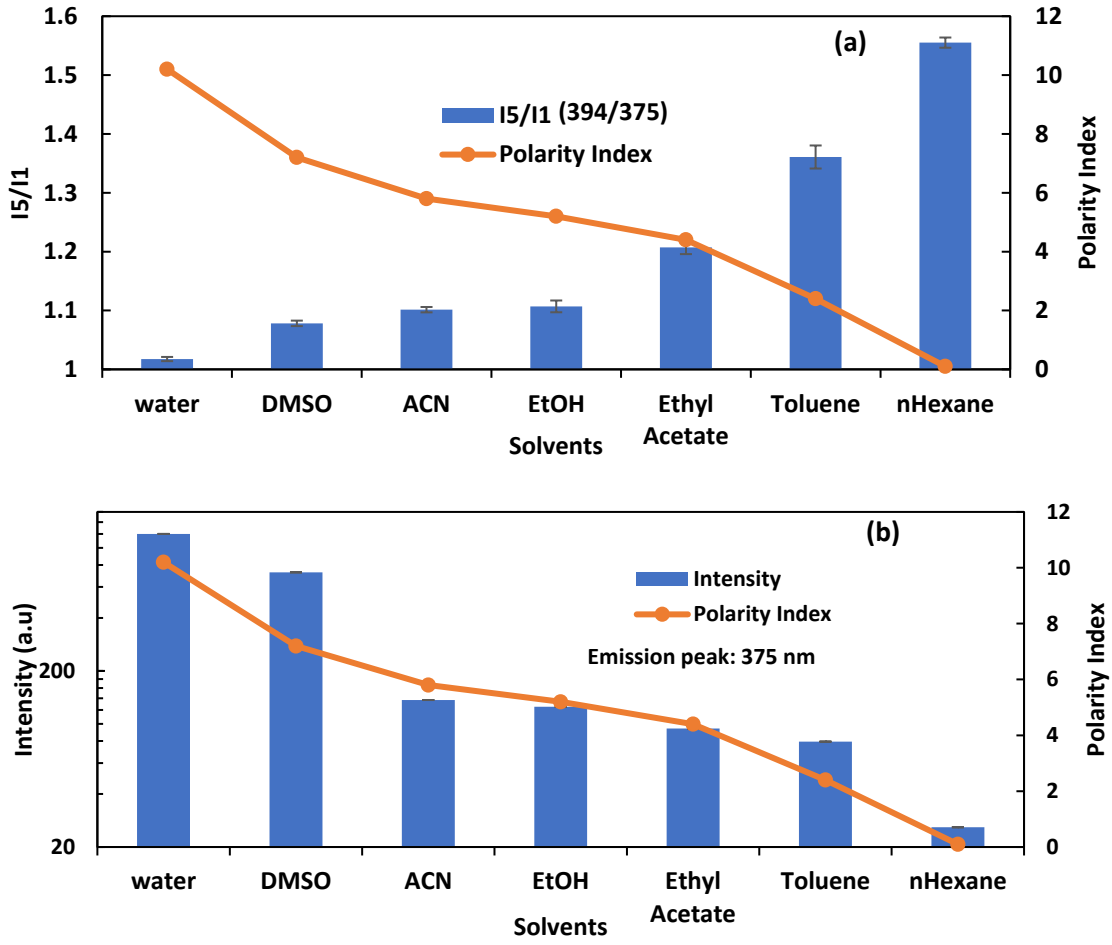

Figure 5.2: (a)- Pyrene I5 and I1 peak ratio in different solvents and its relation to the polarity index of the solvent. Solution was excited at 334nm. (b)- Peak intensity of pyrene at 375 nm in different solvents and its relation to the polarity index of the solvent.

The peak ratios(I_5/I_1) of pyrene remained unaffected in water in the presence of PCBs. However, pyrene emission and excitation spectra intensity changes in the presence of PCB-153 in water. The excitation spectra of Pyrene/PCB-153 and PCB-153 are shown in figure 5.3(a) and 5.3(b), respectively. The spectra show that pyrene fluorescence intensity and shape are sensitive to the presence of PCBs in water. Pyrene fluorescence response to the surrounding environment and to PCBs confirms that it is an excellent analog to BaP for contaminant detection. Pyrene/PCB-153 are excited at three wavelengths of 237nm, 282nm, and 334 nm to see the change in the first peak of pyrene around 375 nm. The emission spectra of Pyrene/PCB-153 and PCB-153 control are shown in figure 5.4. Pyrene intensity is changing at these three excitation wavelengths, whereas, PCB-153 control remains unchanged at all the excitation wavelengths. The intensity ratios for pyrene are plotted in figure 5.5.

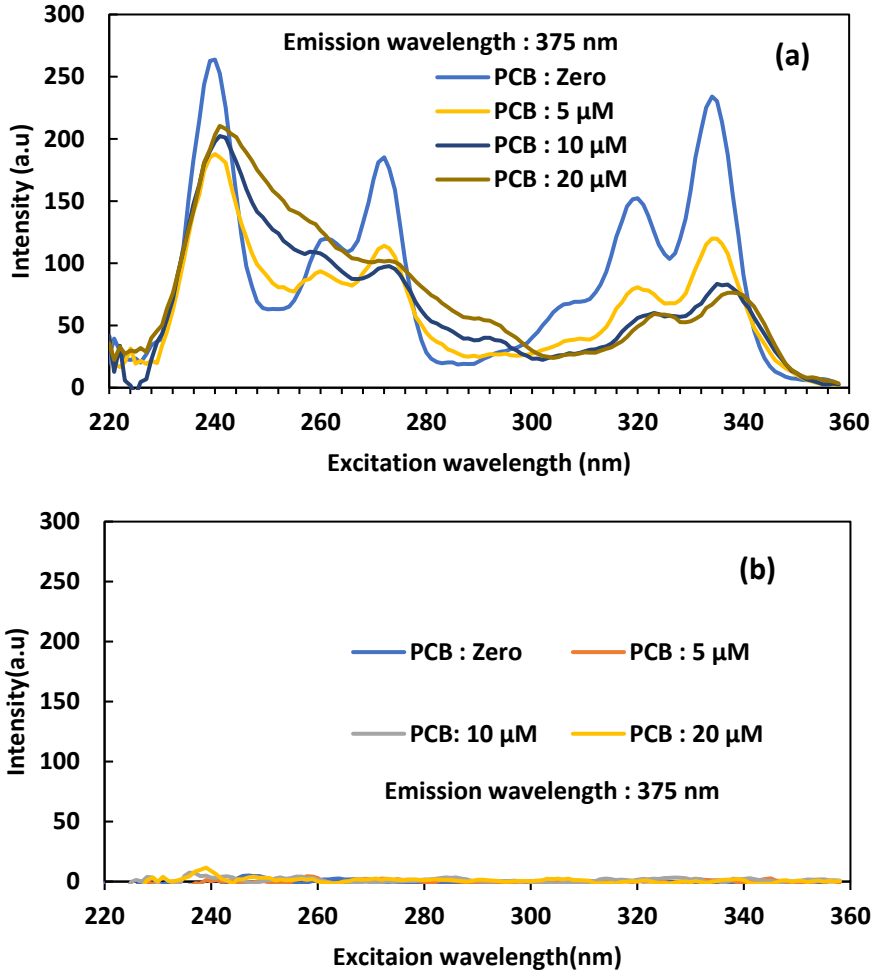

Figure 5.3: (a)- Excitation spectra of Pyrene with PCB-153 in water, (b)- Excitation spectra of PCB-153 control in the water. Emission wavelength of 375nm.

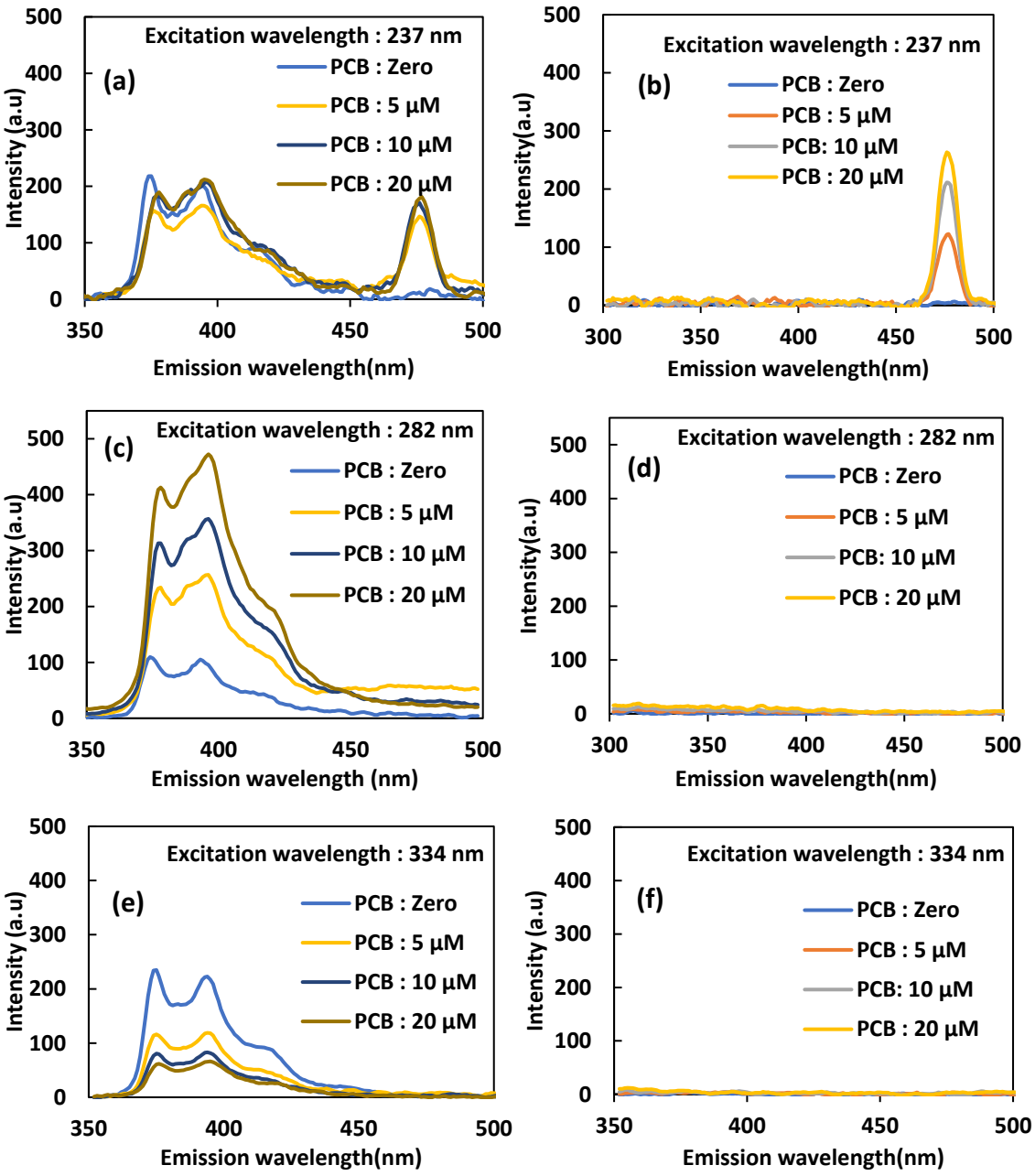

Figure 5.4: Pyrene and PCB-153 interaction in water.

(a)-Emission spectra of Pyrene with PCB-153 in water. Excitation wavelength of 237nm.

(b)- Emission spectra of PCB-153 control in water. Excitation wavelength of 237nm.

(c)- Emission spectra of Pyrene with PCB-153 in water. Excitation wavelength of 282 nm.

(d)- Emission spectra of PCB-153 control in water. Excitation wavelength of 282 nm.

(e)- Emission spectra of Pyrene with PCB-153 in water. Excitation wavelength of 334 nm.

(f)- Emission spectra of PCB-153 control in water. Excitation wavelength of 334 nm.

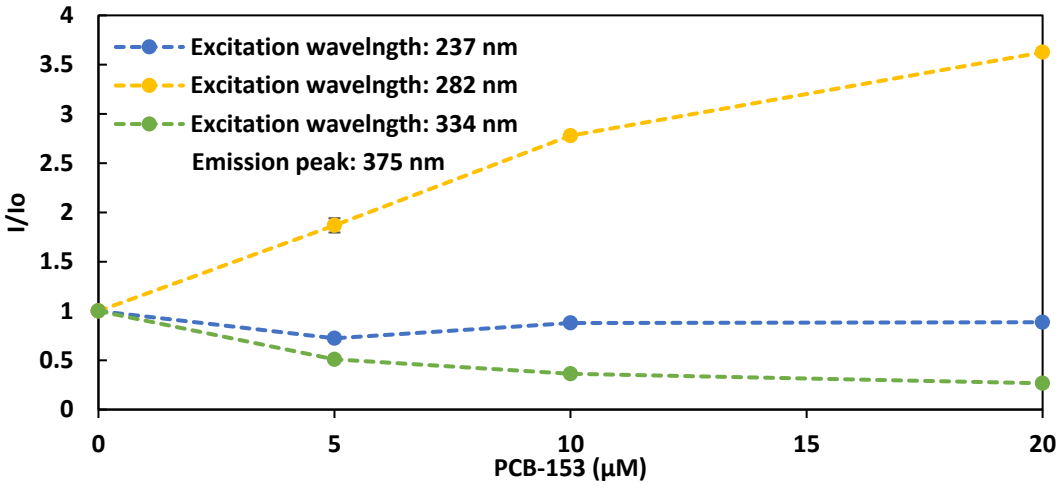

Figure 5.5: Pyrene peak intensity at 375 nm with PCB-153 at three excitation wavelengths.

5.3.2 Preparation of pyrene monomer

Since pyrene showed an interaction with PCB-153. It was incorporated into the polymer particles. For this purpose, hydroxy-pyrene was selected. It was reacted with Mono-2-(methacryloyloxy)ethyl succinate (MMES) using an esterification reaction as shown in figure 5.6. This reaction synthesized the pyrene with methyl methacrylate group. This mechanism can also be applied to functionalized BaP to incorporate into the polymer network.

5.3.3 Solvent selection and HPLC spectroscopy

The esterification reaction was initially carried out in ACN, DCM, acetone, and THF to find out the appropriate solvent. MMES was 1.5 molar equivalent, DCC was 5 molar equivalents and DMAP was 1 molar equivalent to PyMeOH.

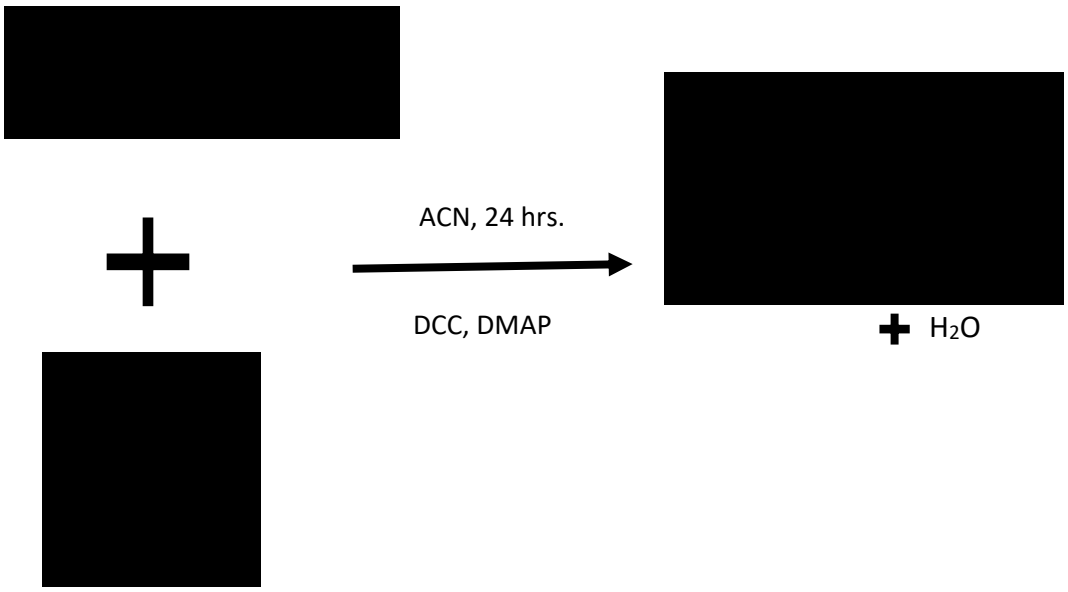

Figure 5.6: Steglich esterification reaction of PyMeOH and MMES in the presence of DCC and DMAP for 24 hours.

The solution was stirred for 24 hours in aluminum covered round bottom flask. Unused DCC was converted to DCU precipitates and separated. Samples were analyzed using HPLC to find out the peaks of PyMeOH and PyMMA in each solvent. HPLC spectra are shown in figure 5.7. Samples were syringe filtered prior to the injection to the HPLC column. An injection volume of samples was 50µl and the temperature kept constant at 40 ^{o}C during the elution time. Due to the presence of OH in PyMeOH, it is eluding very early around 6.45 min. Whereas, the ester product PyMMA, does not have any hydrophilic group (-OH or –COOH) and the presence of extra carbons in the chain makes it more hydrophobic and eluding very late around 16.6 min. Two solvents DCM and ACN indicate a very good peak of PyMMA. Whereas, acetone HPLC spectroscopy in figure 5.7(b) displays a broader peak of PyMMA between 15 min and 18 min.

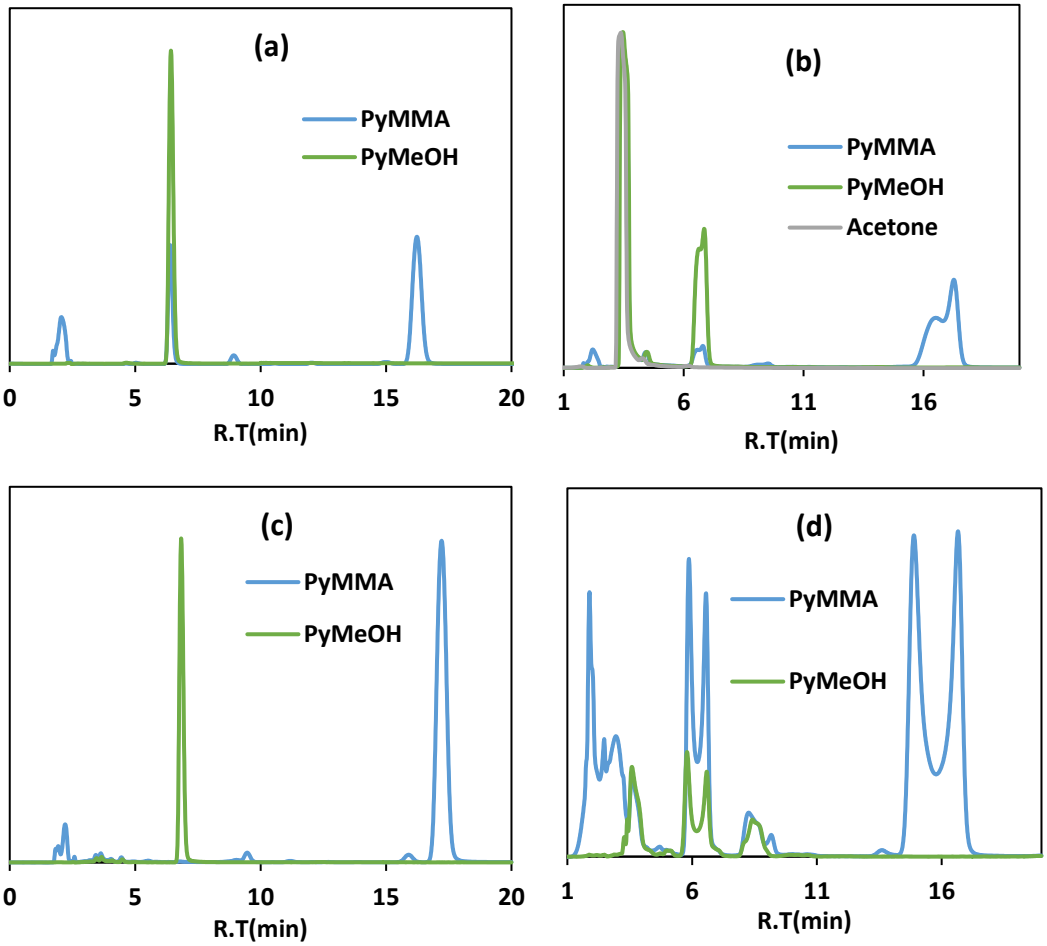

Figure 5.7: Esterification reaction in solvents.
Esterification reactions were carried out in (a)- DCM. (b)- acetone. (c)- ACN. (d)- THF. All the HPLC samples were analyzed using 30% water in ACN and absorbance recorded at 240 nm.

Similarly, THF has unique peak shapes for both PyMeOH and PyMMA. Both molecules are making two peaks that are difficult to analyze. Solvents were screened based on the PyMMA peak shape and the presence of unreacted PyMeOH in the product. DCM, acetone, and THF have unreacted PyMeOH with the product. Whereas, ACN displays almost no sign of PyMeOH with the product. Based on the HPLC spectroscopy analysis,

ACN is the one giving the maximum conversion. Hence, ACN was selected as the reaction solvent.

5.3.4 Purification of the reaction product

Samples analyzed in figure 5.7 have only DCC removed. It is because DCC converts to DCU in the presence of water. DCC needs to be removed before injecting the sample to the HPLC for the column safety. As observed in the HPLC chromatogram, the sample contains DMAP and trace amounts of MMES. DMAP acts as a catalyst in the acyl transfer reaction in the esterification and it needs to be removed from the product. DMAP appears at around 1.9 min in the HPLC analysis. Products were precipitated into cold water around 8 times the volume of the solvent and supernatant was separated using centrifuging and analyzed for DMAP peak in the HPLC. Washing was repeated four times to remove DMAP completely from the product. HPLC analysis of supernatant from each washing step is shown in figure 5.8(a). DMAP gradually goes away with each washing step and after four cycles the product was pure. The spectra illustrate the absence of DMAP peak. DMAP intensity in terms of (mV) is plotted in figure 5.8(b). DMAP in the sample decreases after each wash. It is very important to carefully consider the number of washes as each wash causes the product lost. In order to avoid the product lost it is wise to do only one wash as maximum DMAP is being removed after a single wash.

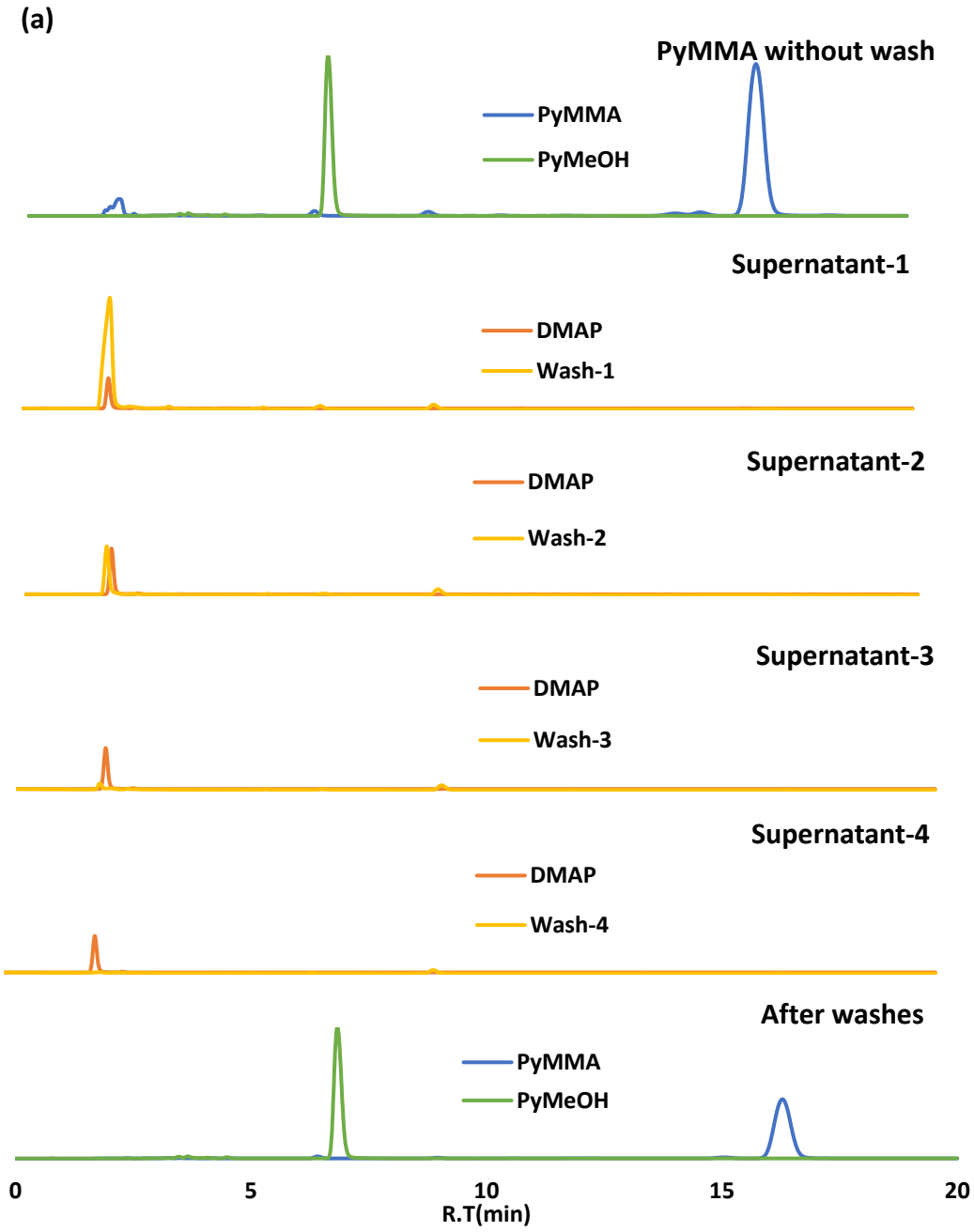
(a)
PyMMA without wash
PyMMA
PyMeOH
Supernatant-1
DMAP
Wash-1
Supernatant-2
DMAP
Wash-2
Supernatant-3
DMAP
Wash-3
Supernatant-4
DMAP
Wash-4
After washes
PyMMA
PyMeOH
0
5
10
15
20
R.T(min)

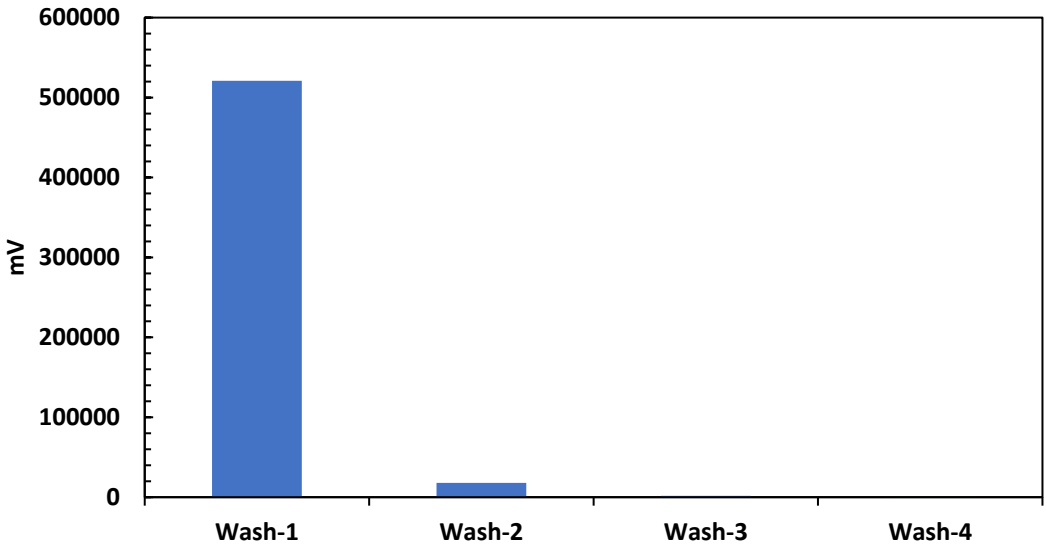

Figure 5.8: Number of washing steps for the purification of the product.
(a)- HPLC spectroscopy of esterification product without washing. DMAP peak falls around 1.9 min. The supernatant obtained from washing steps shows the removal of DMAP and the final pure product. DMAP is absent from the purified product. (b)- DMAP coming out in the supernatants.

5.3.5 Characterization of PyMMA

5.3.5.1 Proton Nuclear Magnetic Resonance (^{1}H-NMR) Spectroscopy

The esterification was further confirmed using ^{1}H-NMR. All the reagents and the product were dissolved in the DMSO-D6 at a concentration of 10 mg/ml. The ^{1}H-NMR spectra are shown in figure 5.9. MMES has five distinguish peaks (C,C,E,F,d).[255] Four peaks (c, f, d) of MMES are present in PyMMA. Similarly, peaks (R, a) from PyMeOH are also present in the PyMMA. The presence of all the peaks from both reagents and the absence of peak (b) from the PyMeOH indicates the reaction has been carried out successfully. The absence

of any additional peak in the product also suggests the product is pure and there is no impurity (DMAP/DCC/DCU) present in the final product.

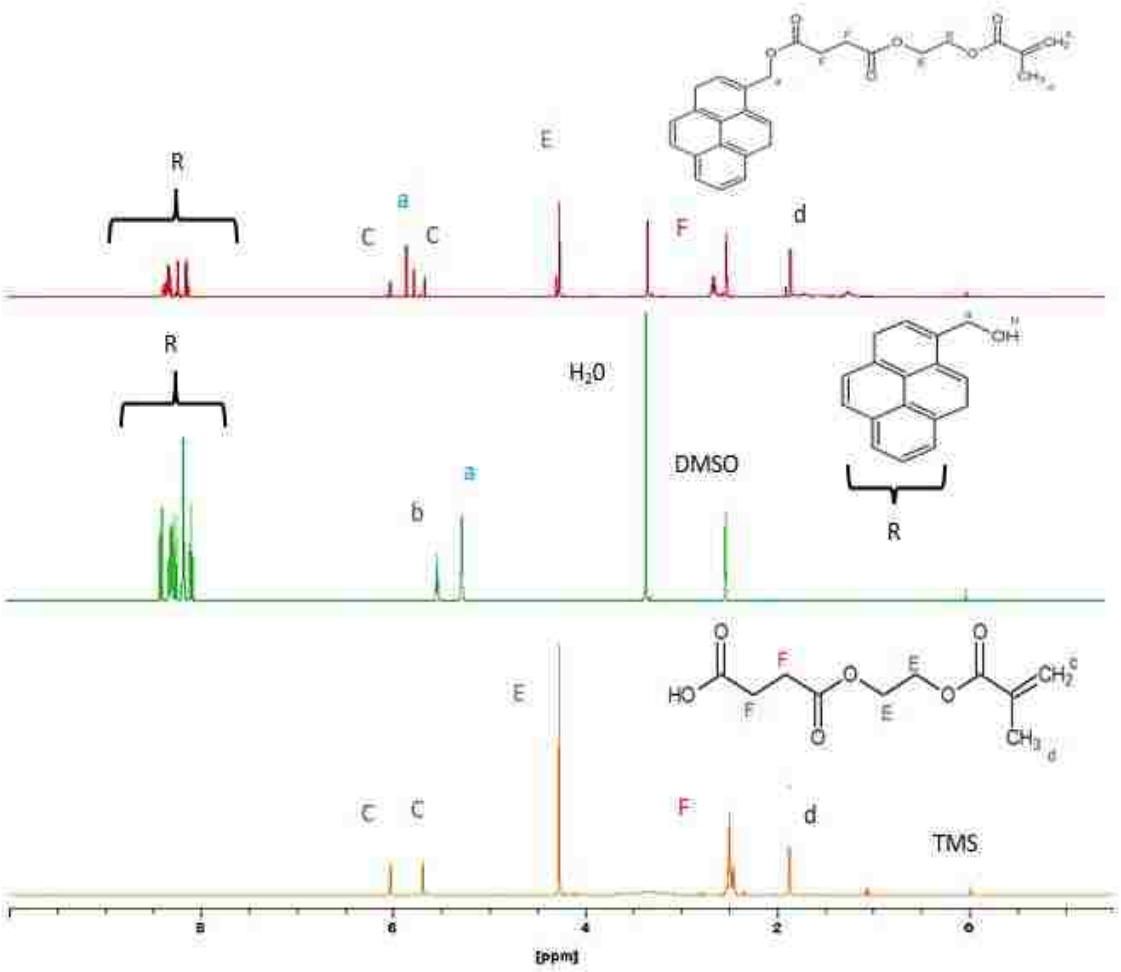

Figure 5.9: ^{1}H-NMR spectroscopy analysis of PyMeOH, MMES and PyMMA using 400 MHz Varian 400-MR NMR spectrophotometer.

Presence of high electronegative oxygen in PyMMA closer to the –CH group (peak a) from PyMeOH, decreases the electron density. It deshields the protons (peak a) from the external magnetic field and moves the peak to the left as shown in figure 5.9.

5.3.5.2 UV-Visible spectroscopy

The absorbance properties of PyMMA and reagents were analyzed using the UV-Vis spectroscopy. The spectra are shown in figure 5.10. These reagents were analyzed in ACN, first ACN blank was run to obtain the background signal of the solvent and then all four samples were analyzed. PyMeOH absorbance spectra is very close in shape to that of pure pyrene. Except for the position of the peaks at 275 nm, 326 nm, and 342 nm, these peaks are little to the right as compared to the pure pyrene. Whereas, PyMMA spectra is distinctive from pyrene or PyMeOH spectra. The presence of an additional long chain is changing the absorbance properties of PyMMA. It has peaks around 240 nm and 275 nm, which are in the same spot as PyMeOH peaks but with low intensity. The extra dome-shaped region falls between 248nm and 269nm. It is because of the additional chain group in PyMMA. Moreover, the other two peaks at a higher wavelength of 326 nm and 342 nm fall at the same place as for PyMeOH.

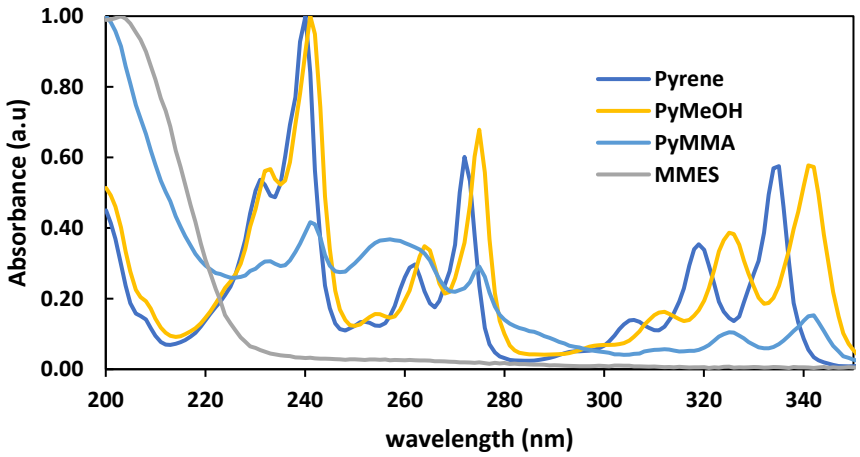

Figure 5.10: UV-Vis absorbance spectra of PyMeOH, Pyrene, PyMMA, and MMES in acetonitrile (ACN).

5.3.5.3 Fourier-transform infrared spectroscopy (FTIR)

FTIR spectra of the reagents used in this reaction and the product (PyMMA) are shown in figure 5.11. DCC and DMAP peaks are missing in PyMMA which, indicates the purity of the product. The peak around 1720 cm^{-1} is the C=O stretch that is the part of the ester bond and peaks at 1145 cm^{-1} is the C-O stretching that also indicates the presence of the MMES chain in the product. Whereas the peak around 1590 cm^{-1} represents the C=C stretching, it endorses the presence of aromatic ring in the product, which is the part of the pyrene molecule. Peak around 2980 cm^{-1} indicates the aliphatic C-H stretching. FTIR confirms the purity of the product and the reaction of the reagents.

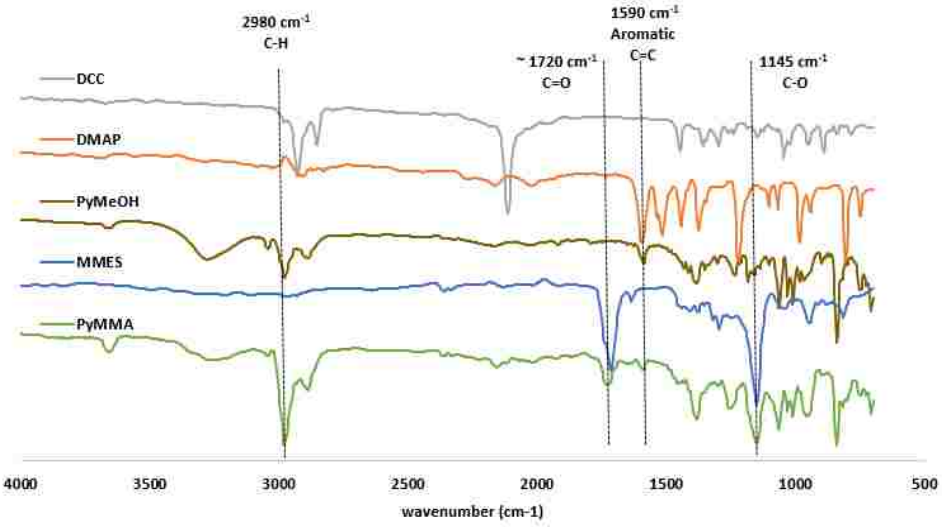

Figure 5. 11: FTIR spectra of reagents and the product. DCC and DMAP peaks are missing from the PyMMA spectra that show the purity of the product.
Peaks at 1720 cm^{-1}, 1145 cm^{-1}, and 1590 cm^{-1} confirm the reaction and product formation.

5.3.6 Interaction of PyMMA with PCBs in water

Since pyrene reveals prominent interaction with PCB in water. Keeping that interaction in mind PyMMA was prepared to incorporate it into the polymer network. Before moving to the polymer-based particle system, it is very important to make sure the modification of pyrene with MMES is not making PyMMA inert to PCB in an aqueous system. PyMMA stock was prepared in DMSO and then introduced into the water along with PCB-153. The excitation and emission spectra of PyMMA with PCB-153 are shown in figures 5.12(a) and 5.12(b). The spectra at 282 nm are shown here, it resembles with pyrene spectra. The intensity ratios are plotted in figure 5.12(c). PyMMA alone has a very weak fluorescence response in water but these signals increase in the presence of PCB-153. The intensity ratio of pyrene at 282 nm goes beyond 3.5, whereas for PyMMA it is beyond 500. Both pyrene and PyMMA are behaving differently in water in the presence of PCB-153. PyMMA exposes way higher sensitivity than pyrene. The presence of an additional chain is making PyMMA more hydrophobic and enhancing its interaction with PCB-153 in water. Since PCB-153 has chlorine atoms that are electron-withdrawing groups. It is possible that the presence of an ester chain in pyrene making it an electron-donating molecule. This electron-donating and accepting combination is inducing a strong effect in enhancing the interaction (attractiveness) and quantum yield of PyMMA.

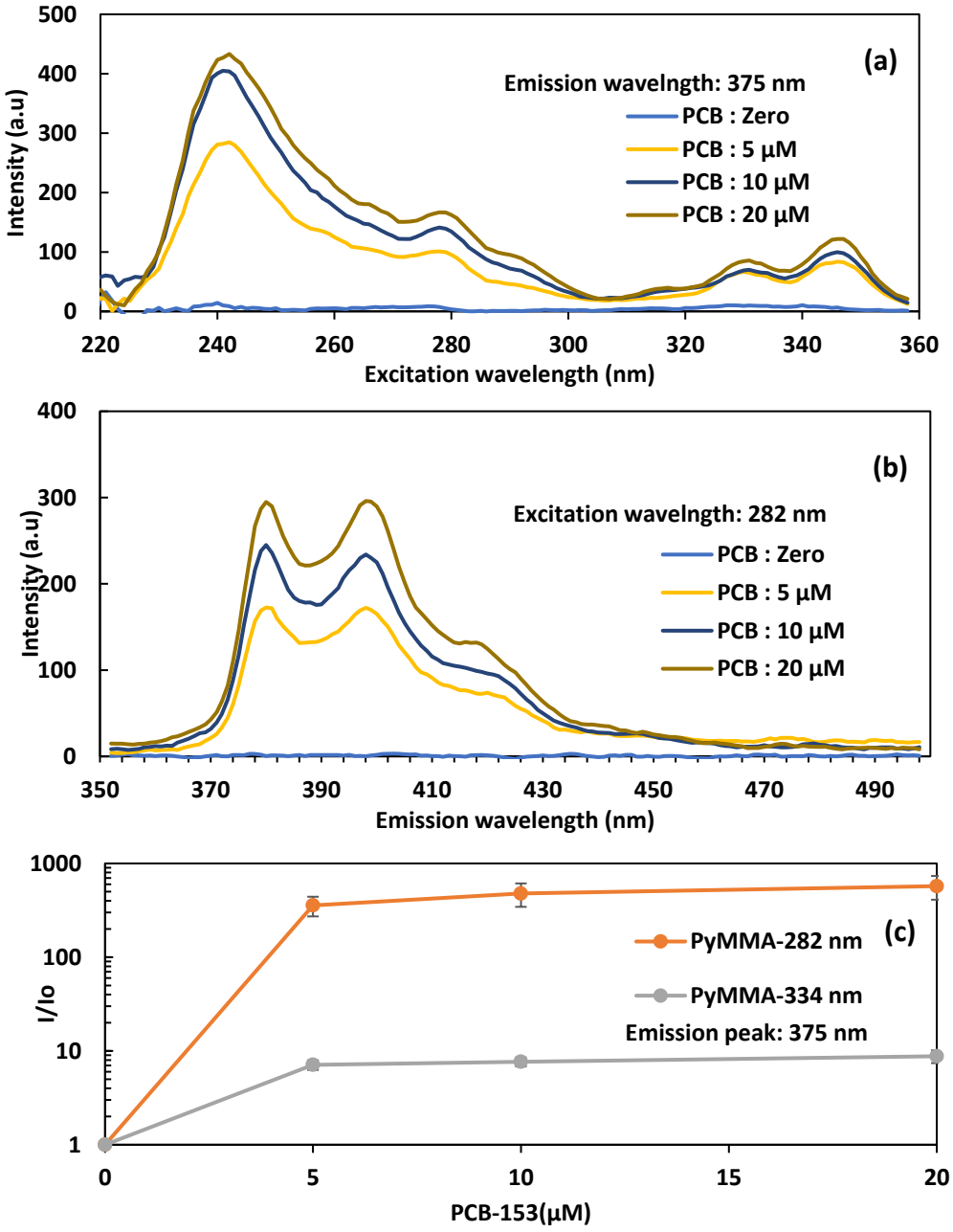

Figure 5.12: PyMMA emission and excitation spectra with PCB-153 in water.
(a)- Excitation spectra of PyMMA with and without PCB-153 in water. PyMMA (0.2 ppm), emission wavelength of 375 nm. (b)- Emission spectra of PyMMA with and without PCB-153 in water. PyMMA (0.2 ppm), Excited at a wavelength of 282 nm. (c)- PyMMA intensity ratio in the presence of PCB-153 excited at 282 nm and 334 nm. The emission peak is around 382 nm.

5.3.7 Polymerization and size reduction analysis

PAA was polymerized with PEGDA and PyMMA. DMSO was selected because of the high polymerization temperature. However, PyMMA was unable to solubilize in DMSO at higher concentrations. For polymerization two solvent system was selected. PyMMA was solubilized in four organic solvents, toluene, ACN, DCM and methyl ethyl ketone (MEK). Then PyMMA solution was mixed with DMSO and other monomers for polymerization. Polymerization was not very successful in MEK/DMSO and ACN/DMSO solvents. However, toluene/DMSO and DCM/DMSO successfully polymerized the polymer film. The film shape and appearance for different steps are shown in figure 5.13. These films have only 1-mole percent loading of PyMMA along with 1-mole percent PEG400DA for crosslinking. The crosslinking ratio is low so that the MPs can swell more and let more and more PCB interact with pyrene. Cryomilled MPs are shown in figure 5.13(d). These MPs were freeze-dried overnight to remove any trapped moisture within the polymer network. Since PAA is rich with carboxyl groups, it dissociates in water, which makes it a pH-responsive polymer. PAA has a pKa value of 4.2. When the pH increases beyond pKa, it causes the dissociation of carboxylic groups in PAA and releases the protons in water. The proton acceptor from the base at higher pH accepts these protons. It left PAA negatively charged side chains (COO-) that have strong repulsion. This repulsion of the charges and increase affinity towards water causes the swelling of the polymer at higher pH. For experimental purposes, it is very important to analyze these MPs in buffered pH instead of DI water. For this purpose, Britton-Robinson buffer solutions of pH 3,5 and 7 were used.[256]

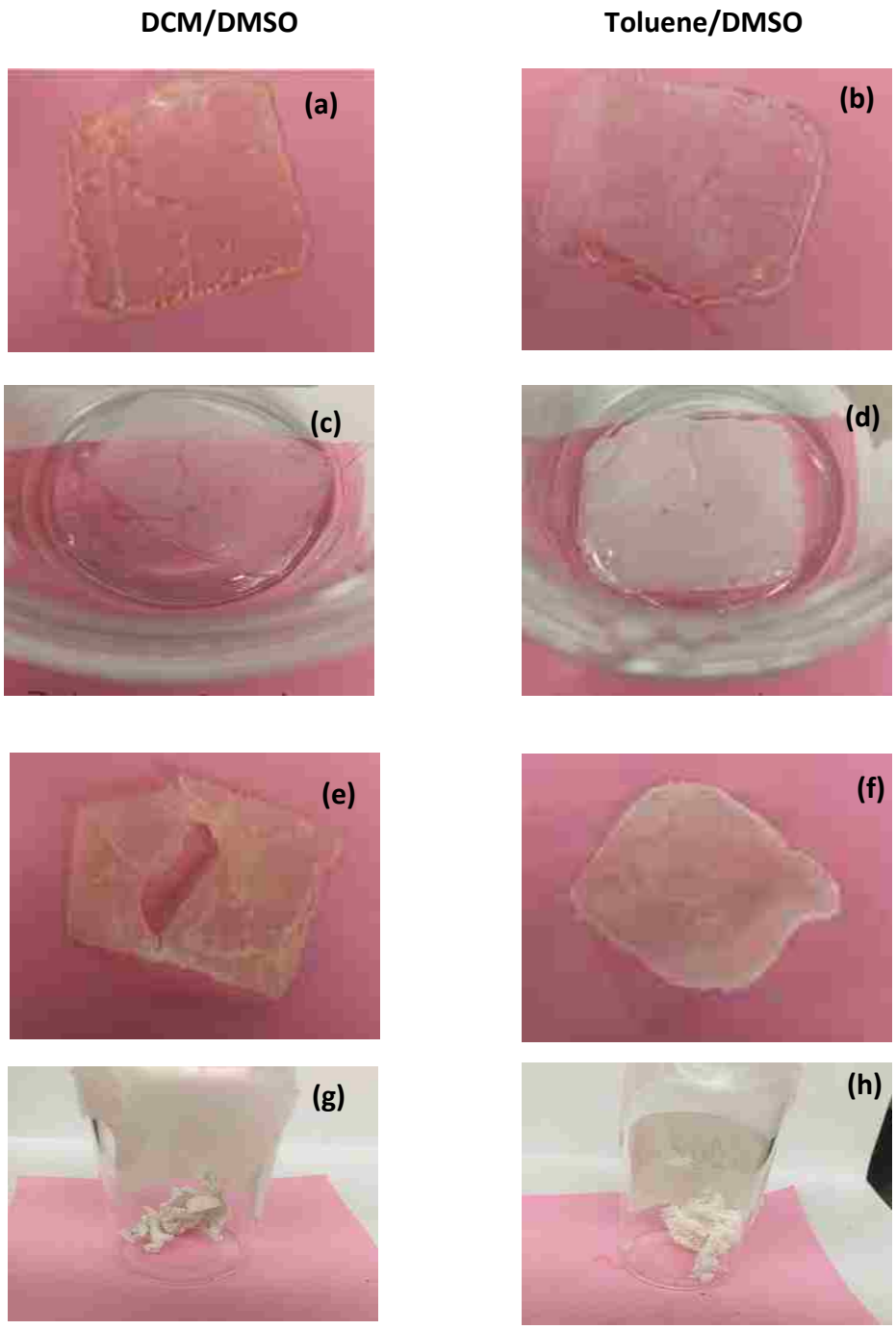

Figure 5.13: Polymer films after synthesis in (a)- DCM/DMSO,(b)- toluene/DMSO. (c,d)- Polymer films after washing. (e,f)- Polymer films after drying. (g,h)- PyMPs after cryomilling. Left-hand side figures present DCM/DMSO solvent system and right-hand side figures present toluene/DMSO system.

The diameter size is shown in figure 5.14. PyMPs show a very good response to the pH. At low pH, PyMPs are collapsed, and their size is very small. As pH increases, PyMPs swell, and their diameter increases. DMSO is studied to analyze the effect of organic solvent. Since side-chains of PAA do not deprotonate in DMSO and it does not swell. The high value of diameter is due to the agglomeration of MPs.

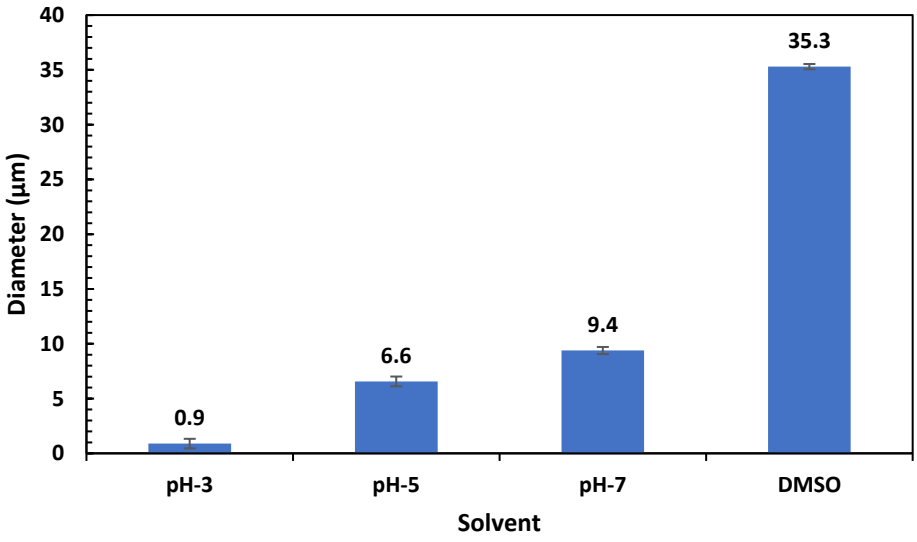

Figure 5.14: MPs diameter in the buffer and in DMSO. The diameter is increasing with increasing the pH of the water. The high diameter size in DMSO is not the swelling, it is because of the aggregation of the MPs.

5.3.8 Characterization of PyMPs

5.3.8.1 Fluorescence properties of PyMPs

PyMPs mainly consist of PAA that has very good swelling properties in water. This swelling also changes the pyrene fluorescence properties. The fluorescence spectra of PyMPs is shown in figure 5.15 for three pH levels. At a lower pH value of 3, PyMPs are not

deprotonated and do not have any repulsion within the polymer network, most of the pyrene is not exposed to the light. Only surface pyrene is being prone to the light that's why PyMPs have very low fluorescence spectra at lower pH. When the pH increases to the higher value (pH 5), it starts to swell due to deprotonation the more pyrene is exposed to the light. The excimer part of pyrene is still very close to each other at that swelling and pH value. However, at a pH of 7, there is a lot of swelling of PyMPs that is shown in figure 5.14 with higher diameter. At this pH, higher swelling increases the distance between pyrene molecules that not only decreases the excimer part but also exposes more pyrene to the light. PyMPs have the highest fluorescence spectra at pH-7. These MPs were also dispersed in DMSO to dissolve any free form of pyrene from the MPs. Supernatants of three buffer solutions and DMSO are shown in figure 5.16. There is almost no sign of PyMMA molecules in the supernatant.

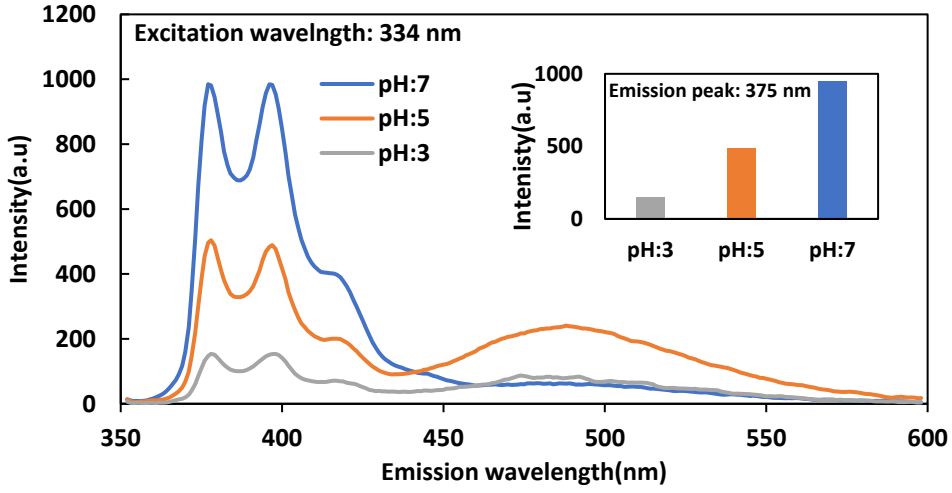

Figure 5.15: Change in shape and peak intensity of PyMPs in pH. PyMPs were loaded with 4 mol% PyMMA and excited at 344 nm.

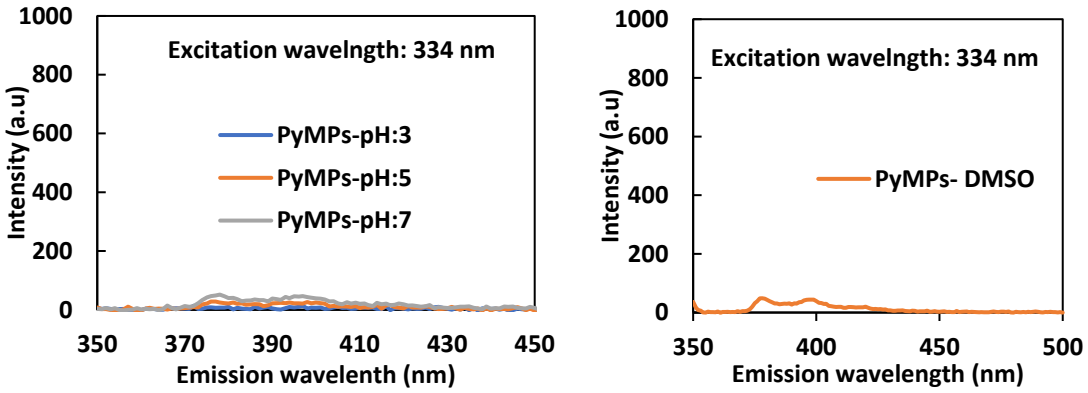

Figure 5.16: Supernatant of MPs from buffer solution and DMSO to analyze if there is free PyMMA associated with the PyMPs.

5.3.8.2 UV-Visible spectroscopy of MPs

The absorbance properties of PyMPs were analyzed using the UV-Vis spectroscopy. The spectra of pyrene, PyMMA, and PyMPs are shown in figure 5.17. Pyrene and PyMMA were analyzed in ACN and PyMMA in a buffer (pH-5). First blanks were run to obtain the background signal of the solvent and then all three samples were analyzed. Pyrene in all three forms has distinguished spectra. In between 300 nm to 360 nm, all three forms have the same shape but distinctive intensity and separate peak location. The last peak of pyrene is at around 315 nm, whereas these peaks shift to 342nm and 344nm for PyMMA and PyMPs, respectively. The incorporation of PyMMA in the polymer network is causing the bathochromic (redshift) in the wavelength of the last two peaks in the absorbance spectra.

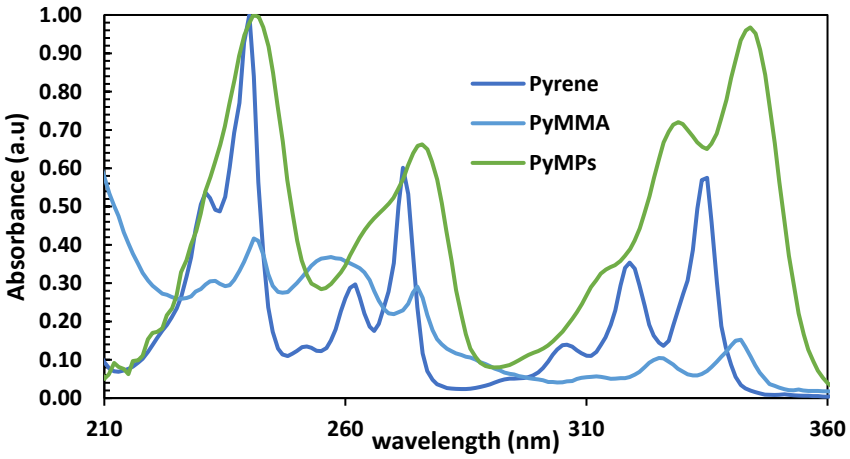

Figure 5.17: UV-Vis absorbance spectra of PyMMA and Pyrene in acetonitrile (ACN).

5.3.9 PyMPs interaction with PCBs

After the characterization of PyMPs, their interaction with PCBs was evaluated. PyMPs were dispersed in 3 ml of buffer solution in glass vials and then PCBs were introduced. These glass vials were covered with aluminum foil to avoid the light exposure to pyrene molecules in the PyMPs and placed on the plate shaker for 24 hours for maxim absorption and contact between pyrene and PCB. The mixture was then placed in a quartz cuvette and placed in the cell holder with magnetic string arrangements, inside the fluorescence spectroscopy instrument as shown in figure 5.18. This stirring is vigorous enough to keep the PyMPs suspended in the buffer solution but gentle enough to avoid the formation of any vortex that can affect the incident light.

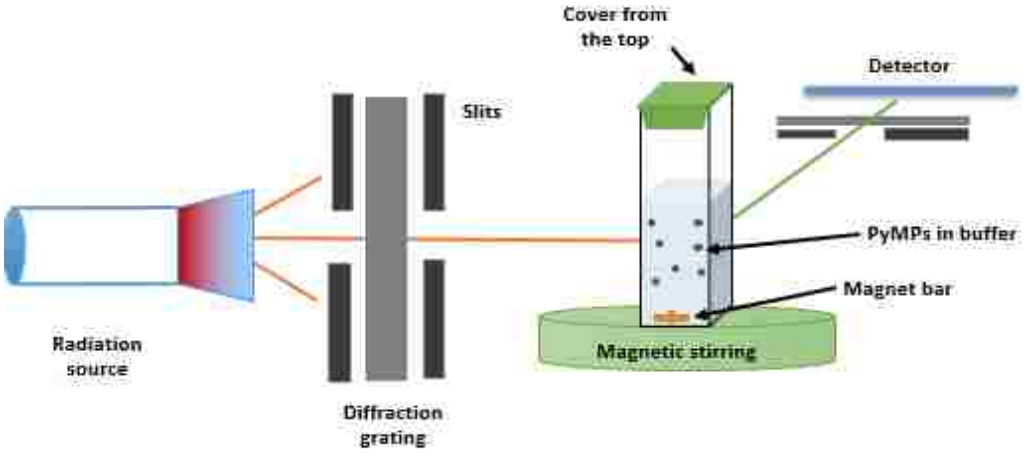

Figure 5.18: Quartz cuvette placed inside the fluorescence instrument fitted with a magnetic stirring arrangement. A magnetic bar is used to keep the MPs suspended in the pathway of the light.

The fluorescence spectra for PCB-118 with PyMPs and with PAA MPs control in three pH of 3,5 and 7 are shown in figure 5.19. Whereas, the change in the peak intensity of PyMPs with PCB-118 and PCB-153 in the buffer solutions are shown in figures 5.20(a and b). Pyrene and PyMMA interacted with PCBs in water but pyrene in bound form is not interacting with PCBs in water. These PyMPs have only 1 mol% PyMMA loading. PyMPs of different loadings were also studied with PCB-153 to investigate if the interaction depends on the Pyrene concentration within the PyMPs. The peak intensity ratios of PyMPs in three pH with PCB-153 are plotted in figure 5.21. The system was excited at two excitation wavelengths of 242 nm and 344 nm. The excitation wavelength of 242 nm reveals the presence of interaction of PCB-153 and PyMPs. It is still unknown whether it is shielding or quenching effect. However, the higher excitation wavelength is the main

focus. PyMPs in pH-3 express the presence of some sort of interaction for PyMMA loading of 0.1, 1 and 4 moles %. But the ratios are small with high error bars.

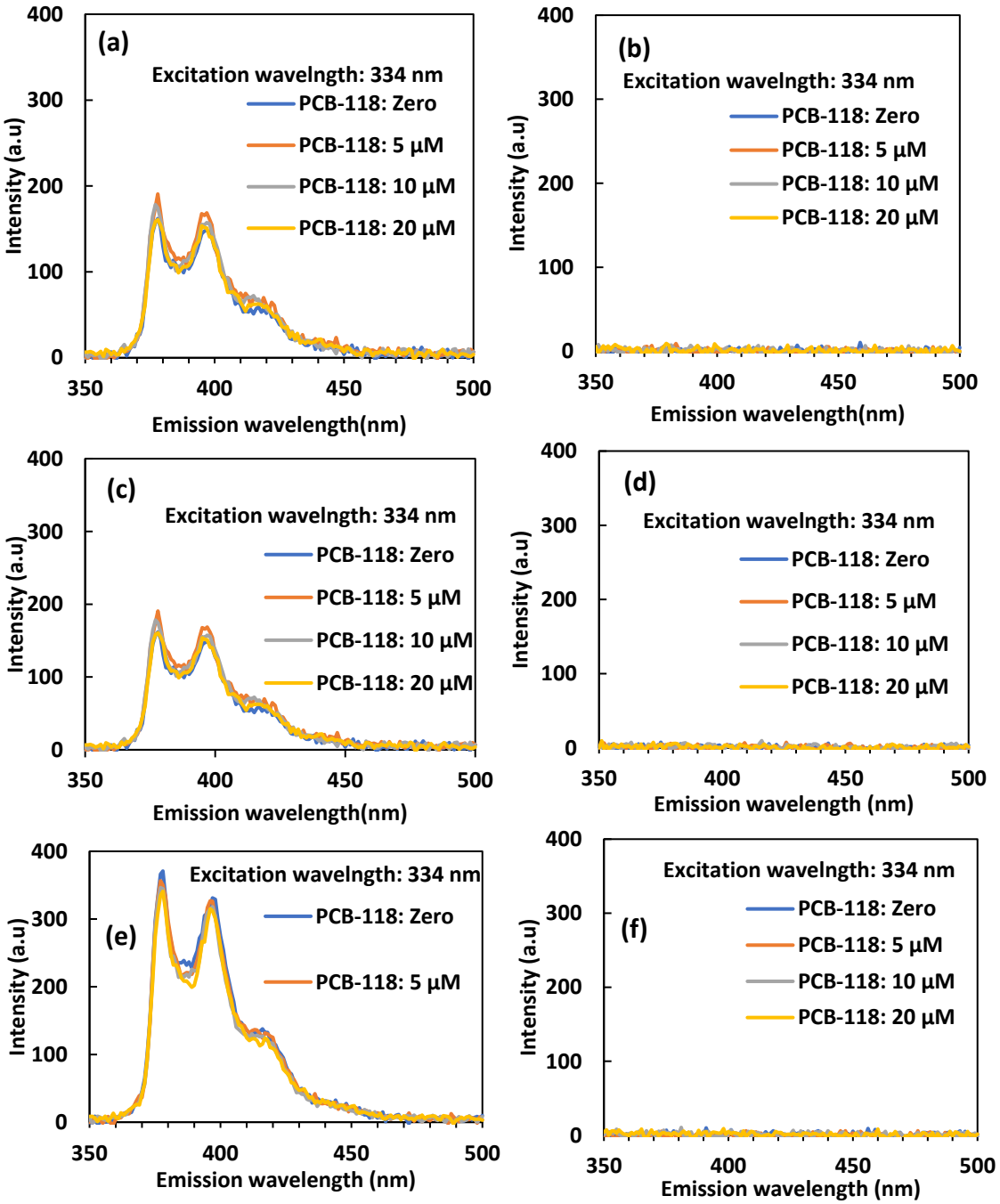

Figure 5.19: (a): PCB-118 with PyMPs (0.05 mg/ml) in three pH, (a)-pH-3, (c)- pH-5 and (e)- pH-7. PyMPs control in three pH, (b)- pH-3, (d)- pH-5 and (f)- pH-7. The system was excited at 334 nm.

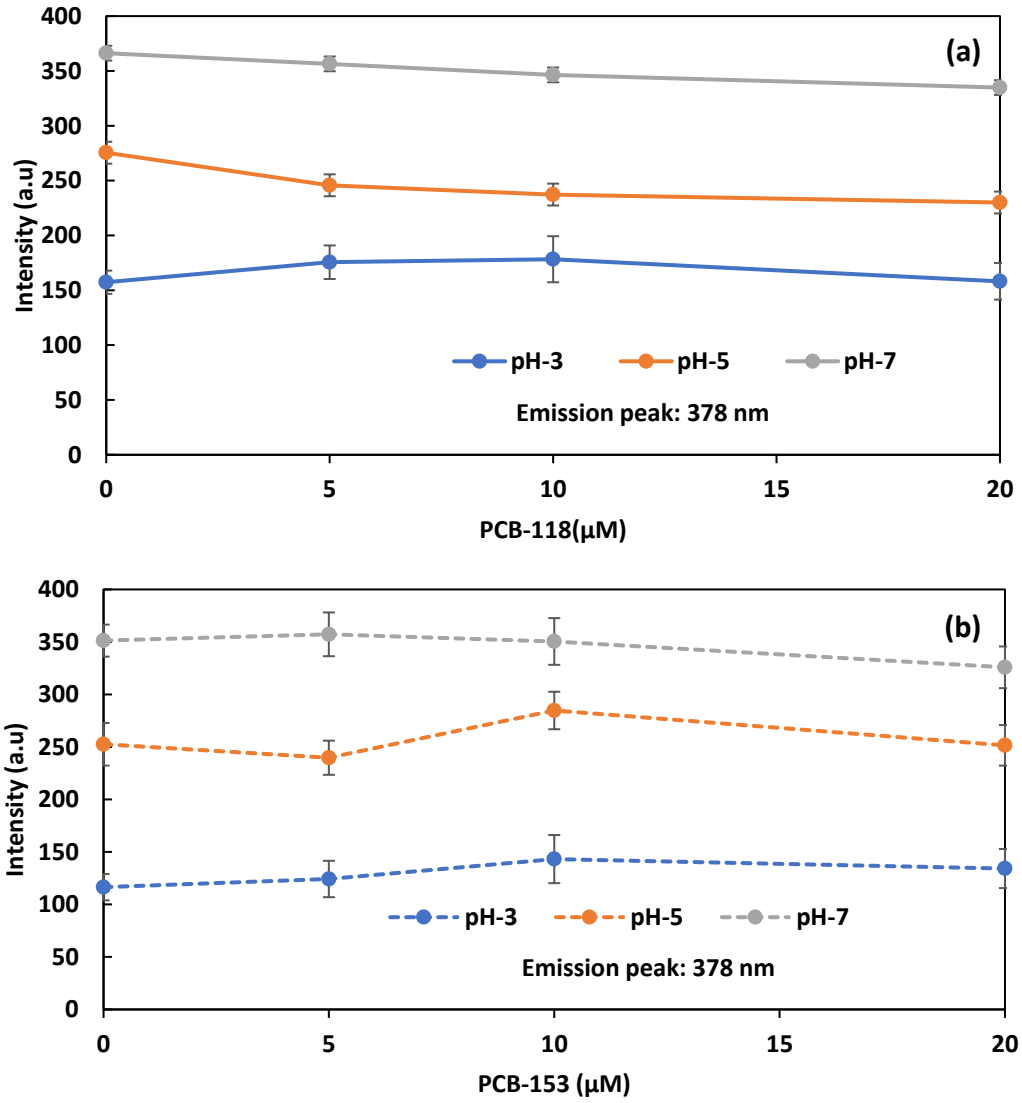

Figure 5.20: (a)- PyMPs peak intensity around 378 nm with PCB-118 in three buffer solutions. (b)- PyMPs peak intensity around 378 nm with PCB-153 in three buffer solutions. Both systems were excited at 334 nm with PyMPs concentration of 0.05 mg/ml and 1 mol% PyMMA loading.

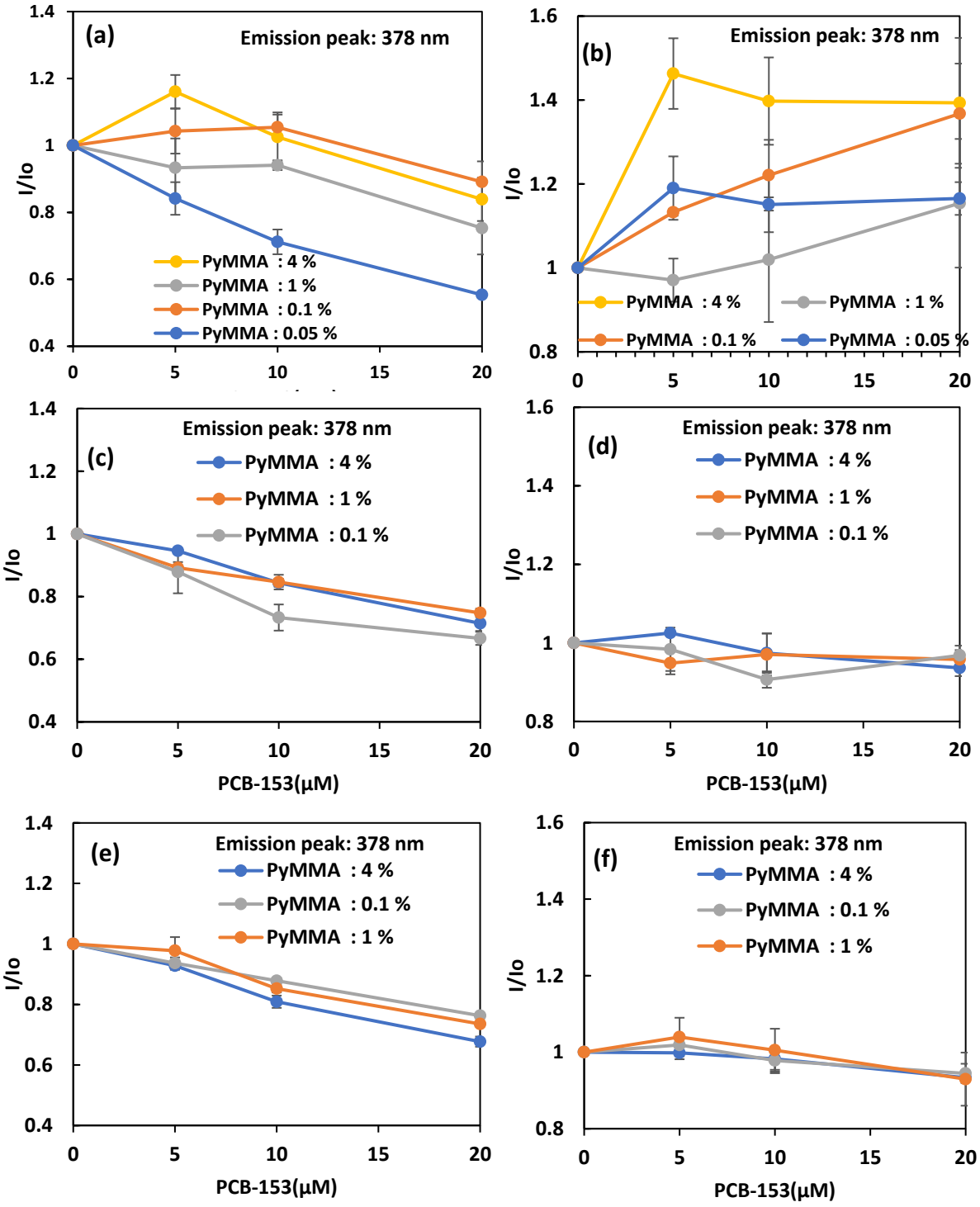

Figure 5.21: PyMPs (0.1 mg/ml) with different PyMMA loading with PCB-153 excited at 242 nm in three pH, (a)-pH-3, (c)- pH-5 and (e)- pH-7. All the systems excited at 344 nm in three pH, (b)- pH-3, (d)- pH-5 and (f)- pH-7.

At pH-5 only PyMMA (4 mole %) has little interaction, showing the decrease in the intensity ratio, but this ratio is very small. pH-7 has a decreasing trend for all PyMMA loadings, but this decrease in intensity ratio is very small for the high concentration of PCB-153 in the system. Apparently, PyMPs are not interacting with PCBs as initially anticipated from Pyrene and PyMMA's interaction with PCBs. Even Pyrene was analyzed with PAA MPs to investigate if PAA is changing pyrene's fluorescence properties. Figure 5.22 illustrates peak intensity kinetics of pyrene with and without PAA MPs in various buffer solutions. Fluorescence signals of free pyrene in the buffer solution are not being affected by the PAA MPs. Pyrene is staying away from PAA MPs, as it is hydrophobic and PAA MPs are hydrophilic. In case of PyMPs, either pyrene properties are being changed after polymerization with PAA or it is also possible that due to the high hydrophilicity of PAA, PCB is not even going close to the PyMPs. Since PAA does not dissociate at lower pH-3. It is possible that PCB is interacting with pyrene in PyMPs but due to the compact structure of PyMPs at pH-3, only a few pyrene(surface) molecules are accessible for the interaction and that's why there is a change in the intensity ratio at this pH.

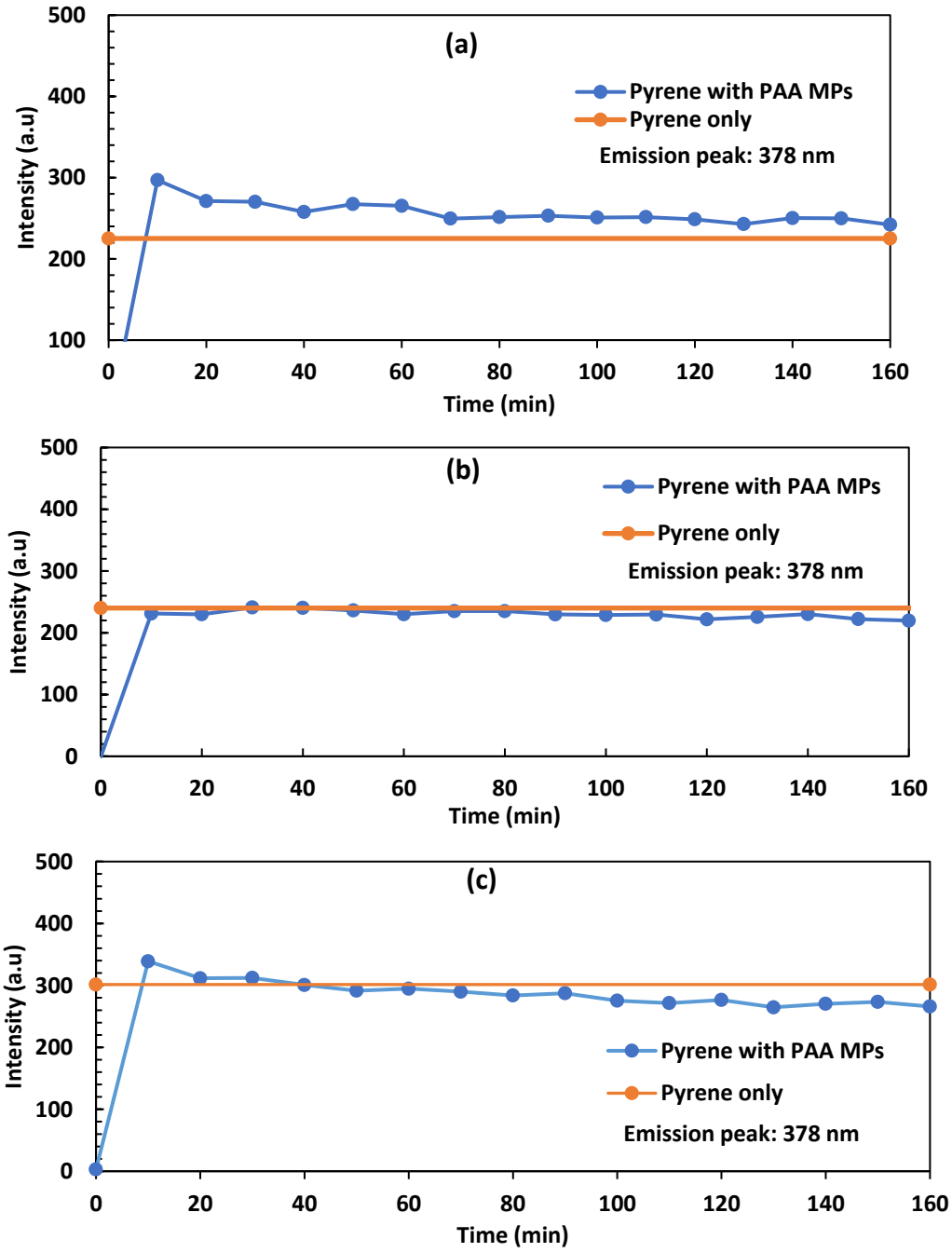

Figure 5.22: Pyrene with and without PAA MPs excited at 334 nm and intensity recorded sat emission 378 nm in three buffer solutions, (a)- pH-3, (b)- pH-5 and (c)- pH-7.

5.4 Conclusions

In this work, pyrene and PCBs interaction was successfully studied to show that it is an analog of BaP. This interaction was also successfully observed in the branched pyrene monomer(PyMMA). The interaction of PyMMA/PCB-153 showed more prominent sensitivity to the presence of PCBs than pyrene. This monomer was successfully polymerized with PAA and crosslinked with PEGDA. Due to the presence of carboxylic acid in PyMPs, these MPs showed pH-dependent swelling and fluorescence intensity signals. As the swelling increases with increasing the pH more pyrene was exposed to the incident light and increases the emission intensity. PyMPs presented weak interaction with PCB-153 at a lower pH value of 3, it is because of the low hydrophilicity of the PyMPs. At higher pH (5 and 7) PAA is deprotonated in PyMPs that led to the increase in hydrophilicity of the PyMPs that repels PCBs away from the PyMPs. This research shows that more studies are needed to investigate the absence of PyMPs and PCBs interaction in the water.

CHAPTER 6. CONCLUSIONS AND FUTURE STUDIES

In this work, fluorescence method was utilized for the detection of PCBs in water. Since PCBs have very weak fluorescence properties, they were studied using indirect fluorescence detection techniques. First, various fluorophores were screened based on the fluorescence quenching mechanism to finalize a potential displacement pair for PCBs detection. The quenching pair was utilized by conjugating the curcumin to polymer microparticles(MPs) and allowing BaP to freely absorb for displacement. Poly(curcumin) MPs displayed a high uptake of BaP from the solvent. Moreover, based upon the displacement studies, it was found that the predominant signals observed resulted from the direct interaction of BaP and PCBs in the solution phase. Additionally, it was also observed that BaP fluorescence spectra was sensitive to the surrounding environment (nature of the solvents). BaP's fluorescence sensitivity was exploited to successfully detect PCB-126(Coplanar), PCB-118(Mix-coplanar) and PCB-153(Non-coplanar) in water. The interactions for each PCB resulted in a unique response with BaP, which is a function of numbers of chlorine atoms, their orientation, and the geometrical shape of the molecule. As PCB-153 revealed the greatest interaction to BaP it also has the highest hydrophobicity, of the PCBs studied. Furthermore, the presence of impurities and water quality affect the sensing of PCBs in terms of intensity and shape of spectra, but dose-dependent trend exists under allowable water conditions.

Pyrene was studied as an alternative to BaP, comparing its fluorescence in different organic solvents to observe the sensitivity to the surrounding environment. Pyrene displayed a very good interaction with PCBs in water like BaP. Pyrene methanol (PyMeOH)

was successfully converted to pyrene methacrylate monomer, PyMMA. This monomer also disclosed a very good interaction with PCB-153 that was superior to the pyrene. PyMMA was polymerized with PAA and crosslinked with PEGDA using free radical polymerization and cryoground to the MPs. The presence of carboxylic acid side chains in PAA made PyMPs a pH-sensitive network. These PyMPs showed pH-responsive swelling determined through the size analysis and pH-dependent fluorescence intensity. However, PyMPs did not show the interaction with PCBs as initially predicted. Pyrene and PyMMA interacted with PCBs at pH (3,5 and 7). Only pH-3 exhibited some interaction, that might be because of the lower hydrophilicity of PyMPs attracted the PCBs to the surface pyrene in PyMPs. Nevertheless, at pH 5 and 7, high hydrophilicity of PyMPs kept PCBs away from the MPs that hindered the PyMPs interaction with PCBs in water.

6.1 Future studies

Pyrene demonstrated an effective alternative to benzo(a)pyrene(BaP) for PCBs sensing in water. Even the functionalization of pyrene to pyrene monomer denoted promising results with PCB-153. The research revealed the existence of the polymer inhibited the PCBs interaction with pyrene. There might be two possibilities of this hindrance. One, availability and/or orientation of pyrene within the PyMPs network. Second, PCB is being repelled by the polymer to keep it away from pyrene. To test what is the root cause of this inhibition. I would recommend two studies for future work.

6.1.1 Evaluation of the polymer backbone

Pyrene bounded to the polymer network is not able to detect PCBs in water. PAA is repelling PCBs from the hydrophilic core due to the presence of carboxylic acid chain groups, creating highly charged core. This repulsion force can overcome the attraction force between pyrene and PCB. PyMPs first dispersed in PCBs aqueous system for 24 hours for equilibrium. The PyMPs will be spun down and the supernatant will be analyzed for the remaining PCBs in the water using the protocol from chapter 4 as shown in figure 6.1. The resultant spectra/intensity can be compared with the control. In this way, it'll be easy to find out if PAA is the problem for PCBs repulsion from the PyMPs, and it will help in the selection of a more appropriate polymer backbone.

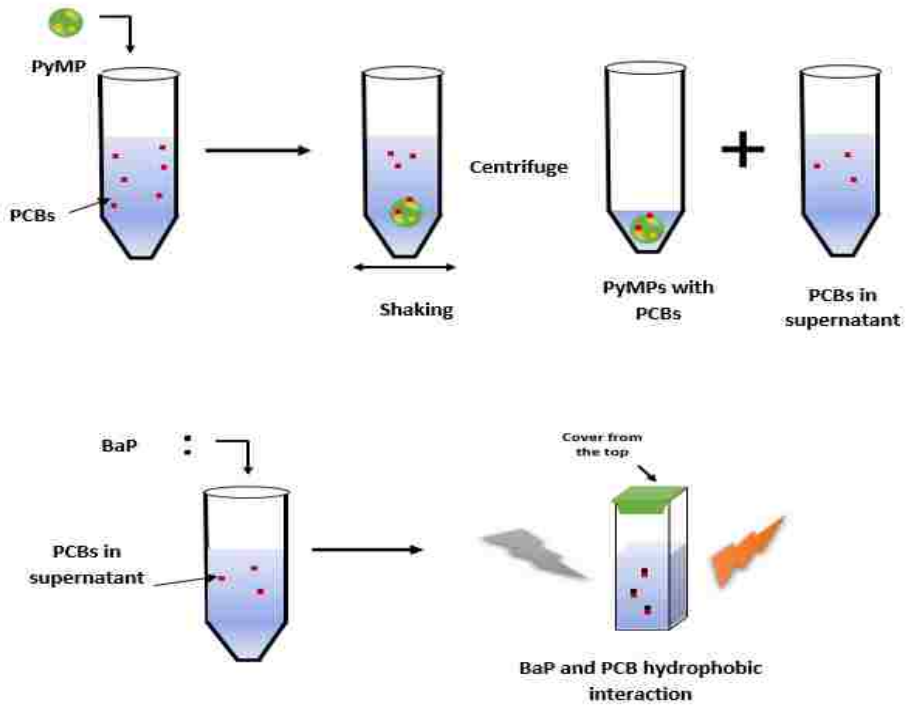

Figure 6.1: PyMPs capability of binding the PCBs to pyrene sites can be analyzed using the binding study. The remaining un-attached PCBs in the supernatant can be analyzed using the protocol in chapter 4 with the help of BaP.

It is also possible that the polymerization of PyMMA within the PAA network is causing the steric hindrance or geometrical orientation problem of the complex. These impediments are not letting the pair(pyrene/PCB) to transfer energy as in case of hydrophobic interaction. If this is the case then the experiment in figure 6.1, should display a low value of PCB in the supernatant, indicating that PCB is bounding to pyrene, but no energy transfer is taking place.

6.1.2 Pyrene distance from the nanoparticles

It is also possible that the polymer network is not letting the pyrene molecule adjust to a degree that is required for the hydrophobic interaction of PCB and pyrene. This problem can be solved by keeping the pyrene molecule away from the particle core using nanoparticles instead of microparticles. The sensitivity of the pyrene molecule can be further enhanced by using electron-donating groups. Since chlorines in PCBs are electron-withdrawing groups. Pyrene with the electron-donating group can be analyzed for electron-donating and withdrawing combination for enhanced interaction. Different functional groups have diverse properties, for example, hydroxyl (-OH), amino ($-NH_2$), and acetylamino ($-NHCOCH_3$) groups as electron-donating and cyano (-CN), carbamoyl ($-CONH_2$), ethynyl ($-C\equiv CH$), ethenyl ($-CH=CH_2$), and formyl (-CHO) functions as representative electron-withdrawing groups.[257]

One of the proposed combinations is shown in figure 6.2. Where the polymer is obtained in the form of functionalized NPs to attach amino-pyrene through a linker chain. This will

not only keep the pyrene away from the NPs to minimize the effect of polymer but also attract more PCB based on the electron-donating and accepting combination.

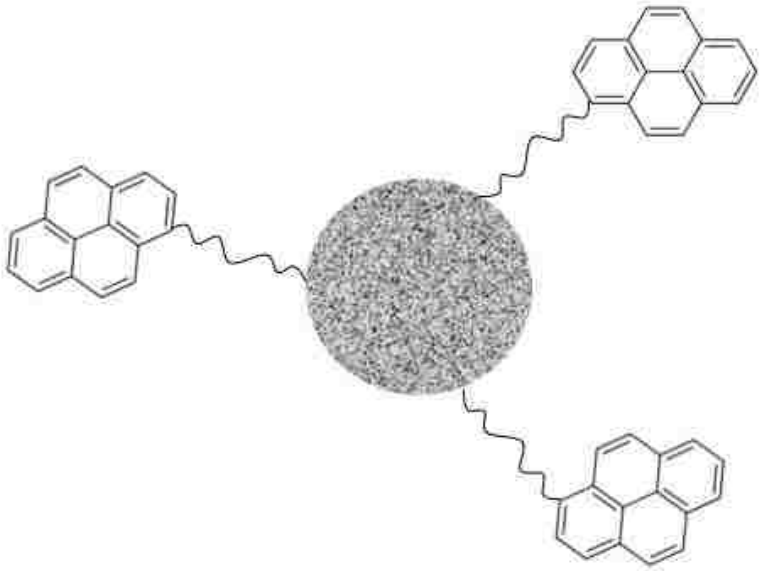

Figure 6.2: Polymer nanoparticles functionalized with pyrene molecule through long-chain linker using esterification/amidation combination reactions.

References:

1. Erickson, M. D. & Kaley, R. G. Applications of polychlorinated biphenyls. *Environ. Sci. Pollut. Res.* **18**, 135–151 (2011).
2. Lind, P. M., Eriksen, E. F., Sahlin, L., Edlund, M. & Örberg, J. Effects of the antiestrogenic environmental pollutant 3, 3', 4, 4', 5-pentachlorobiphenyl (PCB# 126) in rat bone and uterus: diverging effects in ovariectomized and intact animals. *Toxicol. Appl. Pharmacol.* **154**, 236–244 (1999).
3. UNEP. Ridding the world of POPs: A guide to the Stockholm Convention on Persistent Organic Pollutants, the Secretariat of the Stockholm Convention and UNEP's Information Unit for Conventions. (2005).
4. FAA. *Polychlorinated Biphenyls (PCBs) in the National Airspace System*.
5. ACSH. What's The Story? PCBs. (2003). Available at: https://www.acsh.org/news/2003/01/01/whats-the-story-pcbs.
6. Kucewicz, W. P. THE PUBLIC HEALTH IMPLICATIONS OF POLYCHLORINATED BIPHENYLS (PCBs) IN THE ENVIRONMENT. (2005). Available at: https://www.acsh.org/wp-content/uploads/2012/04/20050103_PCBs2005.pdf.
7. Hame, J. *PCBs in Caulking*. (CONNECTICUT'S OFFICIAL STATE WEBSITE, 2010).
8. US EPA, O. National Primary Drinking Water Regulations.
9. Voogt, P. & Brinkman, U. T. Production, properties and usage of polychlorinated biphenyls. *Halogenated biphenyls, terphenyls, naphthalenes, dibenzodioxins Relat. Prod.* 3–45 (1989).
10. AMAP. *PCB in the Russian Federation: Inventory and proposals for priority remedial actions.Oslo, Norway: Arctic Monitoring and Assessment Programme. Report 2000:3, ISBN 82–7971–008–6.* (200AD).
11. Drinker, C. K., WARREN, M. F. & Bennett, G. A. The Problem of Possible Systemic Effects from Certain Chlorinated Hydrocarbons. *J. Ind. Hyg. Toxicol.* **19**, 283–299 (1937).
12. Grunwald, M. Monsanto Hid Decades Of Pollution PCBs Drenched Ala. Town, But No One Was Ever Told. (2002).
13. IARC. *IARC Working Group on the Evaluation of Carcinogenic Risk to Humans. Polychlorinated Biphenyls and Polybrominated Biphenyls. Lyon (FR): International Agency for Research on Cancer; 2016. (IARC Monographs on the Evaluation of Carcinogenic Risks to Humans,*. (2016).
14. EPA. Toxic Substances Control Act (TSCA) and Federal Facilities. (2018). Available at: https://www.epa.gov/enforcement/toxic-substances-control-act-tsca-and-federal-facilities. (Accessed: 1st September 2019)
15. Masuda, Y. The Yusho rice oil poisoning incident. in *Dioxins and health* 633–659 (Springer, 1994).
16. Tatsukawa, R. PCB pollution of the Japanese environment. in *PCB Poisoning and Pollution* (ed. Kodansha, K. H.) 147–179 (Academic Press, 1976).
17. Korea, N. National Implementation Plan for the Stockholm Convention on Persistent Organic Pollutants. *The Democratic People's Republic of Korea* (2008). Available at: http://chm.pops.int/Implementation/NIPs/NIPSubmissions/tabid/253/Default.aspx.
18. Schlosserová, J. *Kontrolle ausgewählter Böden in der Tschechischen und Slowakischen Republik auf ihre Kontamination mit chlorierten Kohlenwassertstoffen*. (Schadstoffatlas Osteuropa. Ecomed Verlagsgesellschaft AG & Co. Germany, 3-609-69540-4, 1994).

19. Jiang, K., Li, L., Chen, Y. & Jin, J. Determination of PCDD/Fs and dioxin-like PCBs in Chinese commercial PCBs and emissions from a testing PCB incinerator. *Chemosphere* **34**, 941–950 (1997).
20. China, N. The People's Republic of China National Implementation Plan for the Stockholm Convention on Persistent Organic Pollutants. (2007). Available at: http://chm.pops.int/Implementation/NIPs/NIPSubmissions/tabid/253/Default.aspx.
21. Sulkoski, W.W., Izabela Kania-Korwel, and L. W. R. Polychlorinated biphenyls production in Poland. 152–157 (2003).
22. Panero, M., Boehme, S. & Muñoz, G. *Pollution prevention and management strategies for polychlorinated biphenyls in the New York/New Jersey harbor*. (New York Academy of Sciences New York, NY:, 2005).
23. Breivik, K., Sweetman, A., Pacyna, J. M. & Jones, K. C. Towards a global historical emission inventory for selected PCB congeners—a mass balance approach: 3. An update. *Sci. Total Environ.* **377**, 296–307 (2007).
24. Fryxell, G. E. & Cao, G. *Environmental applications of nanomaterials: synthesis, sorbents and sensors*. (World Scientific, 2012).
25. GS, S., CV, A. & Mathew, B. B. Biosensors: A Modern Day Achievement. *J. Instrum. Technol.* **2**, 26–39 (2014).
26. Gamba, J. M. The role of transport phenomena in whispering gallery mode optical biosensor performance. (2012).
27. Pandey, P. C. & Weetall, H. H. Evanescent fluorobiosensor for the detection of polyaromatic hydrocarbon based on DNA intercalation. *Appl. Biochem. Biotechnol.* **55**, 87–94 (1995).
28. Mecklenburg, M., Grauers, A., Jönsson, B. R., Weber, A. & Danielsson, B. A strategy for the broad range detection of compounds with affinity for nucleic acids. *Anal. Chim. Acta* **347**, 79–86 (1997).
29. Ferapontova, E. E., Olsen, E. M. & Gothelf, K. V. An RNA aptamer-based electrochemical biosensor for detection of theophylline in serum. *J. Am. Chem. Soc.* **130**, 4256–4258 (2008).
30. Chen, J. *et al.* A new aptameric biosensor for cocaine based on surface-enhanced Raman scattering spectroscopy. *Chem. Eur. J.* **14**, 8374–8382 (2008).
31. Breivik, K., Sweetman, A., Pacyna, J. M. & Jones, K. C. Towards a global historical emission inventory for selected PCB congeners—a mass balance approach: 2. Emissions. *Sci. Total Environ.* **290**, 199–224 (2002).
32. UN Environment. PCB - A FORGOTTEN LEGACY? *United Nations Environment Programme* (2016). Available at: http://web.unep.org/chemicalsandwaste/what-we-do/science-and-knowledge/persistent-organic-pollutants-pops/pcb-forgotten-legacy. (Accessed: 20th March 2018)
33. Breivik, K., Sweetman, A., Pacyna, J. M. & Jones, K. C. Towards a global historical emission inventory for selected PCB congeners — a mass balance approach 1 . Global production and consumption. **290**, 181–198 (2007).
34. Ballschmiter, K. & Zell, M. Analysis of polychlorinated biphenyls (PCB) by glass capillary gas chromatography. *Fresenius' Zeitschrift für Anal. Chemie* **302**, 20–31 (1980).
35. Safe, S. *et al.* PCBs: structure–function relationships and mechanism of action. *Environ. Health Perspect.* **60**, 47 (1985).
36. Murphy, M. O. The Role of Exercise in Polychlorinated Biphenyl Induced Cardiovascular Disease. (2014).

37. Grossman, E. Nonlegacy PCBs: pigment manufacturing by-products get a second look. *Environ. Health Perspect.* **121**, a86 (2013).
38. Hu, D. & Hornbuckle, K. C. Inadvertent polychlorinated biphenyls in commercial paint pigments. *Environ. Sci. Technol.* **44**, 2822–2827 (2009).
39. Abramowicz, D. A. & Olson, D. R. Accelerated biodegradation of PCBs. *Chemtech* **25**, (1995).
40. Abramowicz, D. A. Aerobic and anaerobic biodegradation of PCBs: a review. *Crit. Rev. Biotechnol.* **10**, 241–251 (1990).
41. Boyle, A. W., Silvin, C. J., Hassett, J. P., Nakas, J. P. & Tanenbaum, S. W. Bacterial PCB biodegradation. *Biodegradation* **3**, 285–298 (1992).
42. Yadav, J. S., Quensen, J. F., Tiedje, J. M. & Reddy, C. A. Degradation of polychlorinated biphenyl mixtures (Aroclors 1242, 1254, and 1260) by the white rot fungus Phanerochaete chrysosporium as evidenced by congener-specific analysis. *Appl. Environ. Microbiol.* **61**, 2560–2565 (1995).
43. EPA. Other Federal Statutes - PCBs | Region 9: Toxics | US EPA. (2017). Available at: https://www3.epa.gov/region9/pcbs/otherstatutes.html. (Accessed: 22nd May 2019)
44. EPA. Superfund: National Priorities List (NPL). (2018). Available at: https://www.epa.gov/superfund/superfund-national-priorities-list-npl. (Accessed: 1st September 2019)
45. Obaid Faroon, J. O. *TOXICOLOGICAL PROFILE FOR POLYCHLORINATED BIPHENYLS (PCBs)*. (2000).
46. Thomas, K. *Polychlorinated biphenyls (PCBs) in school buildings: sources, environmental levels, and exposures*. (US Environmental Protection Agency, National Exposure Research Laboratory …, 2012).
47. Herrick, R. F., McClean, M. D., Meeker, J. D., Baxter, L. K. & Weymouth, G. A. An unrecognized source of PCB contamination in schools and other buildings. *Environ. Health Perspect.* **112**, 1051 (2004).
48. EPA. Criminal Provisions of the Toxic Substances Control Act (TSCA). (2018). Available at: https://www.epa.gov/enforcement/criminal-provisions-toxic-substances-control-act-tsca. (Accessed: 1st September 2019)
49. US EPA. National Primary Drinking Water Regulations.
50. Dianyi Yu, M. *ATSDR Case Studies in Environmental Medicine Polychlorinated Biphenyls (PCBs) Toxicity*. 1–90 (2016).
51. FDA. Unavoidable contaminants in food for human consumption and food packaging material: Tolerances for polychlorinated biphenyls (PCBs). *U.S. Food and Drug Administration 21 CFR 109.30* (2017).
52. AAP. Polychlorinated Biphenyls, Dibenzofurans, and Dibenzodioxins. in *Handbook of Pediatric Environmental Health.(eds. Ruth Etzel and Sophie Balk) AAP, Elk Grove Village, IL* 215–22 (2003).
53. OSHA. *Occupational Safety and Health Administration. 1998a. U.S. Department of Labor. Code of Federal Regulations. 29 CFR 1910.1000.* (1998).
54. NIOSH. NIOSH POCKET GUIDE TO CHEMICAL HAZARDS. (2007).
55. EPA. *Polychlorinated Biphenyls (PCBs) TEACH Chemical Summary*. (2009).
56. ATSDR. *ATSDR Case Studies in Environmental Medicine Polychlorinated Biphenyls (PCBs) Toxicity*. 1–90 (2014).
57. Beyer, A. & Biziuk, M. Environmental fate and global distribution of polychlorinated biphenyls. in *Reviews of Environmental Contamination and Toxicology Vol 201* 137–158

(Springer, 2009).
58. Robertson, L. W. & Hansen, L. G. *PCBs: recent advances in environmental toxicology and health effects*. (University Press of Kentucky, 2001).
59. Zhu, Y. Polychlorinated biphenyl (PCB)-induced oxidative stress mediates cytotoxicity in human breast and prostate epithelial cells. (2011). doi:10.17077/etd.xkq4mi9d
60. Djien Liem, A. K., Furst, P. & Rappe, C. Exposure of populations to dioxins and related compounds. *Food Addit. Contam.* **17**, 241–259 (2000).
61. Statista. Major producers of cow milk worldwide in 2016, by country (in million metric tons). *The Statistics Portal* (2016). Available at: https://www.statista.com/statistics/268191/cow-milk-production-worldwide-top-producers/. (Accessed: 28th March 2018)
62. Schecter, A. *et al.* Intake of dioxins and related compounds from food in the US population. *J. Toxicol. Environ. Heal. Part A* **63**, 1–18 (2001).
63. FDA. Total Diet Study. (2018).
64. GreenFact. PCBs: 4. What happens to PCBs when they enter the body? Available at: https://www.greenfacts.org/en/pcbs/l-2/4-human-body.htm. (Accessed: 8th May 2019)
65. USDA. Dairy Data. (2018). Available at: https://www.ers.usda.gov/data-products/dairy-data/. (Accessed: 4th April 2018)
66. WDC. MARINE CHEMICAL POLLUTION. *WDC in Acion* Available at: http://us.whales.org/issues/marine-chemical-pollution. (Accessed: 30th April 2018)
67. USDA. Livestock, Dairy, and Poultry Outlook. (2018). Available at: https://www.ers.usda.gov/publications/pub-details/?pubid=88063. (Accessed: 4th April 2018)
68. EPA. Polychlorinated Biphenyls (PCBs). (2002). Available at: https://archive.epa.gov/epawaste/hazard/wastemin/web/pdf/pcb-fs.pdf. (Accessed: 4th April 2018)
69. OCEANA. Report Finds Dangerous Chemical Building Up In Marine Life And Arctic People. (2003). Available at: http://usa.oceana.org/press-releases/report-finds-dangerous-chemical-building-marine-life-and-arctic-people. (Accessed: 4th April 2018)
70. EPA. National Listing of Fish Advisories General Fact Sheet 2011. (2013). Available at: https://www.epa.gov/fish-tech/national-listing-fish-advisories-general-fact-sheet-2011. (Accessed: 4th April 2018)
71. León-Cava, N., Lutter, C., Ross, J. & Martin, L. Quantifying the benefits of breastfeeding: a summary of the evidence. *Pan Am. Heal. Organ. Washingt. DC* (2002).
72. Guo, Y. L., Chen, Y.-C., Yu, M.-L. & Hsu, C.-C. Early development of Yu-Cheng children born seven to twelve years after the Taiwan PCB outbreak. *Chemosphere* **29**, 2395–2404 (1994).
73. Stewart, P. *et al.* Assessment of prenatal exposure to PCBs from maternal consumption of Great Lakes fish: an analysis of PCB pattern and concentration. *Environ. Res.* **80**, S87–S96 (1999).
74. Rappolt, R. T. & Hale, W. E. p, p'-DDE and p, p'-DDT residues in human placentas, cords, and adipose tissue. *Clin. Toxicol.* **1**, 57–61 (1968).
75. Brown, J. F., Lawton, R. W. & Morgan, C. B. PCB metabolism, persistence, and health effects after occupational exposure: implications for risk assessment. *Chemosphere* **29**, 2287–2294 (1994).
76. Polishuk, Z. W., Wassermann, D., Wassermann, M., Cucos, S. & Ron, M. Organochlorine compounds in mother and fetus during labor. *Environ. Res.* **13**, 278–284 (1977).

77. Dekoning, E. P. & Karmaus, W. PCB exposure in utero and via breast milk. A review. *J. Expo. Sci. Environ. Epidemiol.* **10**, 285 (2000).
78. Nickerson, K. Environmental Contaminants in Breast Milk. (2006). Available at: https://www.medscape.com/viewarticle/522025_2. (Accessed: 30th April 2018)
79. Robertson, L. W. & Ludewig, G. Polychlorinated biphenyl (PCB) carcinogenicity with special emphasis on airborne PCBs. *Gefahrstoffe, Reinhaltung der Luft= Air Qual. Control. BIA und KRdL im VDI und DIN* **71**, 25 (2011).
80. Schwenk, M., Gabrio, T., Päpke, O. & Wallenhorst, T. Human biomonitoring of polychlorinated biphenyls and polychlorinated dibenzodioxins and dibenzofuranes in teachers working in a PCB-contaminated school. *Chemosphere* **47**, 229–233 (2002).
81. Kohler, M., Zennegg, M. & Waeber, R. Coplanar polychlorinated biphenyls (PCB) in indoor air. *Environ. Sci. Technol.* **36**, 4735–4740 (2002).
82. Singh, P. P. & Sharma, V. *Water and health*. (Springer, 2014).
83. Sun, P., Basu, I., Blanchard, P., Brice, K. A. & Hites, R. A. Temporal and spatial trends of atmospheric polychlorinated biphenyl concentrations near the Great Lakes. *Environ. Sci. Technol.* **41**, 1131–1136 (2007).
84. Doskey, P. V & Andren, A. W. Concentrations of airborne PCBs over Lake Michigan. *J. Great Lakes Res.* **7**, 15–20 (1981).
85. Martinez, A. *et al.* Atmospheric dispersion of PCB from a contaminated Lake Michigan harbor. *Atmos. Environ.* **122**, 791–798 (2015).
86. Steenland, K. *et al.* Polychlorinated biphenyls and neurodegenerative disease mortality in an occupational cohort. *Epidemiology* 8–13 (2006).
87. Stewart, P. W., Reihman, J., Lonky, E. I., Darvill, T. J. & Pagano, J. Cognitive development in preschool children prenatally exposed to PCBs and MeHg. *Neurotoxicol. Teratol.* **25**, 11–22 (2003).
88. Jacobson, J. L. & Jacobson, S. W. Intellectual impairment in children exposed to polychlorinated biphenyls in utero. *N. Engl. J. Med.* **335**, 783–789 (1996).
89. Tryphonas, H. Immunotoxicity of polychlorinated biphenyls: present status and future considerations. in *Dioxins and the Immune System* 149–162 (Karger Publishers, 1994).
90. Miyazaki, W., Iwasaki, T., Takeshita, A., Kuroda, Y. & Koibuchi, N. Polychlorinated biphenyls suppress thyroid hormone receptor-mediated transcription through a novel mechanism. *J. Biol. Chem.* **279**, 18195–18202 (2004).
91. Gauger, K. J. *et al.* Polychlorinated biphenyls (PCBs) exert thyroid hormone-like effects in the fetal rat brain but do not bind to thyroid hormone receptors. *Environ. Health Perspect.* **112**, 516 (2004).
92. Brown, V. J. Blocking Brain Development: How PCBs Disrupt Thyroid Hormone. (2005).
93. Salama, J., Chakraborty, T. R., Ng, L. & Gore, A. C. Effects of polychlorinated biphenyls on estrogen receptor-beta expression in the anteroventral periventricular nucleus. *Environ. Health Perspect.* **111**, 1278 (2003).
94. Perkins, J. T., Petriello, M. C., Newsome, B. J. & Hennig, B. Polychlorinated biphenyls and links to cardiovascular disease. *Environ. Sci. Pollut. Res.* **23**, 2160–2172 (2016).
95. Sumner, R. N., Tomlinson, M., Craigon, J., England, G. C. W. & Lea, R. G. Independent and combined effects of diethylhexyl phthalate and polychlorinated biphenyl 153 on sperm quality in the human and dog. *Sci. Rep.* **9**, 3409 (2019).
96. Crinnion, W. J. Polychlorinated biphenyls: persistent pollutants with immunological, neurological, and endocrinological consequences. *Altern. Med. Rev.* **16**, (2011).
97. Robertson, L. W. *PCBs : Recent Advances in Environmental Toxicology and Health Effects*.

(2001).
98. Espandiari, P. *et al.* Polychlorinated biphenyls as initiators in liver carcinogenesis: resistant hepatocyte model. *Toxicol. Appl. Pharmacol.* **186**, 55–62 (2003).
99. Lehmann, L., L. Esch, H., A. Kirby, P., W. Robertson, L. & Ludewig, G. 4-monochlorobiphenyl (PCB3) induces mutations in the livers of transgenic Fisher 344 rats. *Carcinogenesis* **28**, 471–478 (2007).
100. Plíšková, M. *et al.* Impact of polychlorinated biphenyls contamination on estrogenic activity in human male serum. *Environ. Health Perspect.* **113**, 1277 (2005).
101. Sánchez-Alonso, J. A., López-Aparicio, P., Recio, M. N. & Pérez-Albarsanz, M. A. Apoptosis-mediated neurotoxic potential of a planar (PCB 77) and a nonplanar (PCB 153) polychlorinated biphenyl congeners in neuronal cell cultures. *Toxicol. Lett.* **144**, 337–349 (2003).
102. Reiner, E. J., Clement, R. E., Okey, A. B. & Marvin, C. H. Advances in analytical techniques for polychlorinated dibenzo-p-dioxins, polychlorinated dibenzofurans and dioxin-like PCBs. *Anal. Bioanal. Chem.* **386**, 791–806 (2006).
103. Yoshimura, T. Yusho in Japan. *Ind. Health* **41**, 139–148 (2003).
104. Li, M.-C. *et al.* Mortality after exposure to polychlorinated biphenyls and dibenzofurans: 30 years after the "Yucheng accident." *Environ. Res.* **120**, 71–75 (2013).
105. Hsu, C.-C., Mei-Lin, M. Y., Chen, Y.-C. J., Guo, Y.-L. L. & Rogan, W. J. The Yu-cheng rice oil poisoning incident. in *Dioxins and health* 661–684 (Springer, 1994).
106. Masuda, Y. Toxic effects of PCB/PCDF to human observed in Yusho and other poisonings. *Fukuoka igaku zasshi= Hukuoka acta medica* **100**, 141–155 (2009).
107. Guo, Y. L., Lambert, G. H., Hsu, C.-C. & Hsu, M. M. L. Yucheng: health effects of prenatal exposure to polychlorinated biphenyls and dibenzofurans. *Int. Arch. Occup. Environ. Health* **77**, 153–158 (2004).
108. Lauby-Secretan, B. *et al.* Carcinogenicity of polychlorinated biphenyls and polybrominated biphenyls. *Lancet Oncol.* **14**, 287–288 (2013).
109. Wang, Y. *et al.* Enhanced hepatotoxicity induced by repeated exposure to polychlorinated biphenyls and 2, 3, 7, 8-tetrachlorodibenzo-p-dioxin in combination in male rats. *J. Environ. Sci.* **23**, 119–124 (2011).
110. Conolly, R. B. & Jaeger, R. J. Acute hepatotoxicity of ethylene and halogenated ethylenes after PCB pretreatment. *Environ. Health Perspect.* **21**, 131 (1977).
111. Lu, C. *et al.* NMR-based metabonomic analysis of the hepatotoxicity induced by combined exposure to PCBs and TCDD in rats. *Toxicol. Appl. Pharmacol.* **248**, 178–184 (2010).
112. Carpenter, D. O. Polychlorinated biphenyls and human health. *Int. J. Occup. Med. Environ. Health* **11**, 291–303 (1998).
113. EPA. Impaired Waters and TMDLs. (2017). Available at: https://www.epa.gov/tmdl/pcb-tmdl-handbook. (Accessed: 30th April 2018)
114. Muir, D. & Sverko, E. Analytical methods for PCBs and organochlorine pesticides in environmental monitoring and surveillance: a critical appraisal. *Anal. Bioanal. Chem.* **386**, 769–789 (2006).
115. Gohlke, R. S. Time-of-flight mass spectrometry and gas-liquid partition chromatography. *Anal. Chem.* **31**, 535–541 (1959).
116. Gohlke, R. S. & McLafferty, F. W. Early gas chromatography/mass spectrometry. *J. Am. Soc. Mass Spectrom.* **4**, 367–371 (1993).
117. Hites, R. A. Development of gas chromatographic mass spectrometry. *Anal. Chem.* **88**,

6955–6961 (2016).
118. Bush, B., Baker, F., Dell'Acqua, R., Houck, C. L. & Lo, F.-C. Analytical response of polychlorinated biphenyl homologues and isomers in thin-layer and gas chromatography. *J. Chromatogr. A* **109**, 287–295 (1975).
119. Chau, A. S. Y. & Sampson, R. C. J. Electron capture gas chromatographic methodology for the quantitation of polychlorinated biphenyls: survey and compromise. *Environ. Lett.* **8**, 89–101 (1975).
120. Rote, J. W. & Murphy, P. G. A method for the quantitation of polychlorinated biphenyl (PCB) isomers. *Bull. Environ. Contam. Toxicol.* **6**, 377–384 (1971).
121. Klikauer, T. Reflections on Phishing for Phools–The Economics of Manipulation and Deception. *tripleC Commun. Capital. Crit. Open Access J. a Glob. Sustain. Inf. Soc.* **14**, 260–264 (2016).
122. Ahmad, I., Weng, J., Stromberg, A. J., Hilt, J. Z. & Dziubla, T. Fluorescence Based Detection of Poly Chlorinated Biphenyls (PCBs) in Water Using Hydrophobic Interaction. *Analyst* (2018). doi:10.1039/C8AN00867A
123. Liu, B. L. & Saltman, M. A. Immunosensor Technology: Historical Perspective and Future Outlook. *Lab. Med.* **27**, 109–115 (1996).
124. Banica, F.-G. *Chemical sensors and biosensors: fundamentals and applications*. (John Wiley & Sons, 2012).
125. Turner, A., Karube, I. & Wilson, G. S. *Biosensors: fundamentals and applications*. (Oxford university press, 1987).
126. Gui, Q., Lawson, T., Shan, S., Yan, L. & Liu, Y. The application of whole cell-based biosensors for use in environmental analysis and in medical diagnostics. *Sensors* **17**, 1623 (2017).
127. Derraik, J. G. B. The pollution of the marine environment by plastic debris: a review. *Mar. Pollut. Bull.* **44**, 842–852 (2002).
128. Gutiérrez, J. C., Amaro, F. & Martín-González, A. Heavy metal whole-cell biosensors using eukaryotic microorganisms: an updated critical review. *Front. Microbiol.* **6**, 48 (2015).
129. Belkin, S. Microbial whole-cell sensing systems of environmental pollutants. *Curr. Opin. Microbiol.* **6**, 206–212 (2003).
130. Nováková, H. *et al.* PCB metabolism by Pseudomonas sp. P2. *Int. Biodeterior. Biodegradation* **50**, 47–54 (2002).
131. Gavlasova, P., Kuncova, G., Kochankova, L. & Mackova, M. Whole cell biosensor for polychlorinated biphenyl analysis based on optical detection. *Int. Biodeterior. Biodegradation* **62**, 304–312 (2008).
132. Weiland-Bräuer, N., Fischer, M. A., Schramm, K.-W. & Schmitz, R. A. Polychlorinated Biphenyl (PCB)-Degrading Potential of Microbes Present in a Cryoconite of Jamtalferner Glacier. *Front. Microbiol.* **8**, 1105 (2017).
133. Komancová, M., Jurčová, I., Kochánková, L. & Burkhard, J. Metabolic pathways of polychlorinated biphenyls degradation by Pseudomonas sp. 2. *Chemosphere* **50**, 537–543 (2003).
134. Turner, K. *et al.* Hydroxylated polychlorinated biphenyl detection based on a genetically engineered bioluminescent whole-cell sensing system. *Anal. Chem.* **79**, 5740–5745 (2007).
135. Pilehvar, S. *et al.* Carbon nanotubes based electrochemical aptasensing platform for the detection of hydroxylated polychlorinated biphenyl in human blood serum. *Biosens. Bioelectron.* **54**, 78–84 (2014).

136. Xu, S. *et al.* Detection of polychlorinated biphenyls employing chemical dechlorination followed by biphenyl whole cell sensing system. *Toxicol. Environ. Chem.* **87**, 287–298 (2005).
137. Darwish, I. A. Immunoassay methods and their applications in pharmaceutical analysis: basic methodology and recent advances. *Int. J. Biomed. Sci. IJBS* **2**, 217 (2006).
138. Sharma, S., Byrne, H. & O'Kennedy, R. J. Antibodies and antibody-derived analytical biosensors. *Essays Biochem.* **60**, 9–18 (2016).
139. Scientific, T. F. Introduction to Immunoglobulins. *eBioscience* (2016). Available at: http://www.ebioscience.com/knowledge-center/antigen/immunoglobulin.htm. (Accessed: 10th March 2018)
140. Pei, X. *et al.* Sandwich-type immunosensors and immunoassays exploiting nanostructure labels: A review. *Anal. Chim. Acta* **758**, 1–18 (2013).
141. Wild, D. *The immunoassay handbook*. (Elsevier, 2005).
142. Urusov, A. E., Zherdev, A. V & Dzantiev, B. B. Immunochemical methods of mycotoxin analysis (review). *Prikl. Biokhim. Mikrobiol.* **46**, 276–290 (2010).
143. Přibyl, J., Hepel, M. & Skládal, P. Piezoelectric immunosensors for polychlorinated biphenyls operating in aqueous and organic phases. *Sensors Actuators B Chem.* **113**, 900–910 (2006).
144. Luppa, P. B., Sokoll, L. J. & Chan, D. W. Immunosensors—principles and applications to clinical chemistry. *Clin. Chim. acta* **314**, 1–26 (2001).
145. Zhao, C. Q. *et al.* Fiber optic immunosensor for polychlorinated biphenyls. *J. Agric. Food Chem.* **43**, 2308–2315 (1995).
146. Zhu, C., Yang, G., Li, H., Du, D. & Lin, Y. Electrochemical sensors and biosensors based on nanomaterials and nanostructures. *Anal. Chem.* **87**, 230–249 (2015).
147. ADI. ADI Micropower Toxic Gas Detector Solutions Based on Electrochemical Sensors. (2012). Available at: https://www.analog.com/media/cn/technical-documentation/apm-pdf/adi-gas-detection-and-analysis-solutions_en.pdf. (Accessed: 1st December 2019)
148. Ju, H., Zhang, X. & Wang, J. *NanoBiosensing: principles, development and application*. (Springer Science & Business Media, 2011).
149. Gao, J. *et al.* Ultrasensitive electrochemical immunoassay for CEA through host–guest interaction of β-cyclodextrin functionalized graphene and Cu@ Ag core–shell nanoparticles with adamantine-modified antibody. *Biosens. Bioelectron.* **63**, 465–471 (2015).
150. Reverté, L., Prieto-Simon, B. & Campàs, M. New advances in electrochemical biosensors for the detection of toxins: Nanomaterials, magnetic beads and microfluidics systems. A review. *Anal. Chim. Acta* **908**, 8–21 (2016).
151. Akter, R., Rhee, C. K. & Rahman, M. A. Sensitivity enhancement of an electrochemical immunosensor through the electrocatalysis of magnetic bead-supported non-enzymatic labels. *Biosens. Bioelectron.* **54**, 351–357 (2014).
152. Jia, X., Chen, X., Han, J., Ma, J. & Ma, Z. Triple signal amplification using gold nanoparticles, bienzyme and platinum nanoparticles functionalized graphene as enhancers for simultaneous multiple electrochemical immunoassay. *Biosens. Bioelectron.* **53**, 65–70 (2014).
153. Tu, M.-C. *et al.* Immunosensor based on carbon nanotube/manganese dioxide electrochemical tags. *Anal. Chim. Acta* **853**, 228–233 (2015).
154. Wang, H. *et al.* Electrochemical immunosensor for α-fetoprotein detection using ferroferric oxide and horseradish peroxidase as signal amplification labels. *Anal.*

Biochem. **465**, 121–126 (2014).
155. Omidfar, K., Zarei, H., Gholizadeh, F. & Larijani, B. A high-sensitivity electrochemical immunosensor based on mobile crystalline material-41–polyvinyl alcohol nanocomposite and colloidal gold nanoparticles. *Anal. Biochem.* **421**, 649–656 (2012).
156. Pinacho, D. G., Sánchez-Baeza, F., Pividori, M.-I. & Marco, M.-P. Electrochemical detection of fluoroquinolone antibiotics in milk using a magneto immunosensor. *Sensors* **14**, 15965–15980 (2014).
157. Wu, L. *et al.* A novel electrochemical PCB77-binding DNA aptamer biosensor for selective detection of PCB77. *J. Electroanal. Chem.* **771**, 45–49 (2016).
158. Fillmann, G. *et al.* Validation of immunoassay methods to determine hydrocarbon contamination in estuarine sediments. *J. Braz. Chem. Soc.* **18**, 774–781 (2007).
159. Tian, W., Xie, H. Q., Fu, H., Pei, X. & Zhao, B. Immunoanalysis methods for the detection of dioxins and related chemicals. *Sensors* **12**, 16710–16731 (2012).
160. Pohanka, M. & Skládal, P. Electrochemical biosensors--principles and applications. *J. Appl. Biomed. (De Gruyter Open)* **6**, (2008).
161. Moina, C. & Ybarra, G. Fundamentals and applications of immunosensors. in *Advances in immunoassay technology* (InTech, 2012).
162. Centi, S., Laschi, S., Fránek, M. & Mascini, M. A disposable immunomagnetic electrochemical sensor based on functionalised magnetic beads and carbon-based screen-printed electrodes (SPCEs) for the detection of polychlorinated biphenyls (PCBs). *Anal. Chim. Acta* **538**, 205–212 (2005).
163. Del Carlo, M. & Mascini, M. Immunoassay for polychlorinated biphenyls (PCB) using screen printed electrodes. *F. Anal. Chem. Technol.* **3**, 179–184 (1999).
164. Endo, T. *et al.* Fluorescence-based assay with enzyme amplification on a micro-flow immunosensor chip for monitoring coplanar polychlorinated biphenyls. *Anal. Chim. Acta* **531**, 7–13 (2005).
165. Bender, S. & Sadik, O. A. Direct electrochemical immunosensor for polychlorinated biphenyls. *Environ. Sci. Technol.* **32**, 788–797 (1998).
166. Devadoss, A., Sudhagar, P., Terashima, C., Nakata, K. & Fujishima, A. Photoelectrochemical biosensors: New insights into promising photoelectrodes and signal amplification strategies. *J. Photochem. Photobiol. C Photochem. Rev.* **24**, 43–63 (2015).
167. Zhang, L., Mohamed, H. H., Dillert, R. & Bahnemann, D. Kinetics and mechanisms of charge transfer processes in photocatalytic systems: a review. *J. Photochem. Photobiol. C Photochem. Rev.* **13**, 263–276 (2012).
168. Fan, G.-C., Han, L., Zhu, H., Zhang, J.-R. & Zhu, J.-J. Ultrasensitive photoelectrochemical immunoassay for matrix metalloproteinase-2 detection based on CdS: Mn/CdTe cosensitized TiO2 nanotubes and signal amplification of SiO2@ Ab2 conjugates. *Anal. Chem.* **86**, 12398–12405 (2014).
169. Zhang, X., Liu, M., Mao, Y., Xu, Y. & Niu, S. Ultrasensitive photoelectrochemical immunoassay of antibody against tumor-associated carbohydrate antigen amplified by functionalized graphene derivates and enzymatic biocatalytic precipitation. *Biosens. Bioelectron.* **59**, 21–27 (2014).
170. Li, R., Liu, Y., Cheng, L., Yang, C. & Zhang, J. Photoelectrochemical aptasensing of kanamycin using visible light-activated carbon nitride and graphene oxide nanocomposites. *Anal. Chem.* **86**, 9372–9375 (2014).
171. Shi, H., Zhao, J., Wang, Y. & Zhao, G. A highly selective and picomolar level

photoelectrochemical sensor for PCB 101 detection in environmental water samples. *Biosens. Bioelectron.* **81**, 503–509 (2016).
172. Blackie, E. J., Le Ru, E. C. & Etchegoin, P. G. Single-molecule surface-enhanced Raman spectroscopy of nonresonant molecules. *J. Am. Chem. Soc.* **131**, 14466–14472 (2009).
173. Sharma, B., Frontiera, R. R., Henry, A.-I., Ringe, E. & Van Duyne, R. P. SERS: Materials, applications, and the future. *Mater. today* **15**, 16–25 (2012).
174. Liu, H. *et al.* Single molecule detection from a large-scale SERS-active Au 79 Ag 21 substrate. *Sci. Rep.* **1**, srep00112 (2011).
175. Wang, Y. & Irudayaraj, J. Surface-enhanced Raman spectroscopy at single-molecule scale and its implications in biology. *Philos. Trans. R. Soc. B Biol. Sci.* (2013).
176. Le Ru, E. C., Meyer, M. & Etchegoin, P. G. Proof of single-molecule sensitivity in surface enhanced Raman scattering (SERS) by means of a two-analyte technique. *J. Phys. Chem. B* **110**, 1944–1948 (2006).
177. Nie, S. & Emory, S. R. Probing single molecules and single nanoparticles by surface-enhanced Raman scattering. *Science (80-.).* **275**, 1102–1106 (1997).
178. Zhou, Q., Zhang, X., Huang, Y., Li, Z. & Zhang, Z. Rapid detection of polychlorinated biphenyls at trace levels in real environmental samples by surface-enhanced Raman scattering. *Sensors* **11**, 10851–10858 (2011).
179. Fu, C. *et al.* Aptamer-based surface-enhanced Raman scattering-microfluidic sensor for sensitive and selective polychlorinated biphenyls detection. *Anal. Chem.* **87**, 9555–9558 (2015).
180. Roudaut, G. & Debeaufort, F. Moisture loss, gain and migration in foods. in *Food and beverage stability and shelf life* 63–105 (Elsevier, 2011).
181. Chasteen, T. Coupling Gas Chromatography to Mass Spectrometry. *Dep. Chem. Sam Houst. State Univ.* (2016).
182. De Koning, S., Janssen, H.-G. & Brinkman, U. A. T. Modern Methods of Sample Preparation for GC Analysis. doi:10.1365/s10337-008-0937-3
183. Borgerding, M. F., Perfetti, T. A. & Ralapati, S. Determination of nicotine in tobacco, tobacco processing environments and tobacco products. *Anal. Determ. nicotine Relat. Compd. their Metab. Amsterdam Elsevier* 285–391 (1999).
184. Chinen, A. B. *et al.* Nanoparticle probes for the detection of cancer biomarkers, cells, and tissues by fluorescence. *Chem. Rev.* **115**, 10530–10574 (2015).
185. Lakowicz, J. R. Principles of Fluorescence Spectroscopy, (1999). (2004).
186. Kattke, M. D., Gao, E. J., Sapsford, K. E., Stephenson, L. D. & Kumar, A. FRET-based quantum dot immunoassay for rapid and sensitive detection of Aspergillus amstelodami. *Sensors* **11**, 6396–6410 (2011).
187. Jindal, K. K. & Sharma, R. C. *Recent trends in horticulture in the Himalayas: Integrated Development Under the Mission Mode*. (Indus Publishing, 2004).
188. Wu, F.-Y., Sun, M.-Z., Xiang, Y.-L., Wu, Y.-M. & Tong, D.-Q. Curcumin as a colorimetric and fluorescent chemosensor for selective recognition of fluoride ion. *J. Lumin.* **130**, 304–308 (2010).
189. Bhopate, D. P., Mahajan, P. G., Garadkar, K. M., Kolekar, G. B. & Patil, S. R. A highly selective and sensitive single click novel fluorescent off–on sensor for copper and sulfide ions detection directly in aqueous solution using curcumin nanoparticles. *New J. Chem.* **39**, 7086–7096 (2015).
190. Baharuddin, N. H., Sulaiman, N. M. N. & Aroua, M. K. Removal of zinc and lead ions by polymer-enhanced ultrafiltration using unmodified starch as novel binding polymer. *Int.*

J. Environ. Sci. Technol. **12**, 1825–1834 (2015).
191. Uludag, Y., Özbelge, H. Ö. & Yilmaz, L. Removal of mercury from aqueous solutions via polymer-enhanced ultrafiltration. *J. Memb. Sci.* **129**, 93–99 (1997).
192. Pascall, M. A., Zabik, M. E., Zabik, M. J. & Hernandez, R. J. Uptake of polychlorinated biphenyls (PCBs) from an aqueous medium by polyethylene, polyvinyl chloride, and polystyrene films. *J. Agric. Food Chem.* **53**, 164–169 (2005).
193. Barcelo, D. *Sample Handling and Trace Analysis of Pollutants: techniques, applications and quality assurance*. **21**, (Elsevier, 2000).
194. Meng, Z., Chen, W. & Mulchandani, A. Removal of estrogenic pollutants from contaminated water using molecularly imprinted polymers. *Environ. Sci. Technol.* **39**, 8958–8962 (2005).
195. Zelmanov, G. & Semiat, R. Iron (3) oxide-based nanoparticles as catalysts in advanced organic aqueous oxidation. *Water Res.* **42**, 492–498 (2008).
196. Huang, D.-L. *et al.* Bioremediation of Pb-contaminated soil by incubating with Phanerochaete chrysosporium and straw. *J. Hazard. Mater.* **134**, 268–276 (2006).
197. Haupt, K. & Mosbach, K. Molecularly imprinted polymers and their use in biomimetic sensors. *Chem. Rev.* **100**, 2495–2504 (2000).
198. Hilt, J. Z. Nanotechnology and biomimetic methods in therapeutics: molecular scale control with some help from nature. *Adv. Drug Deliv. Rev.* **56**, 1533–1536 (2004).
199. Sanchez, C., Belleville, P., Popall, M. & Nicole, L. Applications of advanced hybrid organic–inorganic nanomaterials: from laboratory to market. *Chem. Soc. Rev.* **40**, 696–753 (2011).
200. Tse Sum Bui, B. & Haupt, K. Preparation and evaluation of a molecularly imprinted polymer for the selective recognition of testosterone—application to molecularly imprinted sorbent assays. *J. Mol. Recognit.* **24**, 1123–1129 (2011).
201. Awawdeh, A. M. & Harmon, H. J. Spectrophotometric detection of pentachlorophenol (PCP) in water using immobilized and water-soluble porphyrins. *Biosens. Bioelectron.* **20**, 1595–1601 (2005).
202. Johnson, B. J. *et al.* Fluorescent silicate materials for the detection of paraoxon. *Sensors* **10**, 2315–2331 (2010).
203. Pellequer, J. *et al.* Structural basis for preferential binding of non-ortho-substituted polychlorinated biphenyls by the monoclonal antibody S2B1. *J. Mol. Recognit. An Interdiscip. J.* **18**, 282–294 (2005).
204. Hrycay, E. G. & Bandiera, S. M. Spectral interactions of tetrachlorobiphenyls with hepatic microsomal cytochrome P450 enzymes. *Chem. Biol. Interact.* **146**, 285–296 (2003).
205. Yang, J.-H. & Kodavanti, P. R. S. Possible molecular targets of halogenated aromatic hydrocarbons in neuronal cells. *Biochem. Biophys. Res. Commun.* **280**, 1372–1377 (2001).
206. Lin, C., Chinnappan, R., Acharya, K., Pellequer, J.-L. & Jankowiak, R. On stabilization of a neutral aromatic ligand by π–cation interactions in monoclonal antibodies. *Biophys. Chem.* **154**, 35–40 (2011).
207. Inui, H. *et al.* Enzyme-linked immunosorbent assay with monoclonal and single-chain variable fragment antibodies selective to coplanar polychlorinated biphenyls. *J. Agric. Food Chem.* **60**, 1605–1612 (2012).
208. Sharma, B., Gardner, K. H., Melton, J., Hawkins, A. & Tracey, G. Evaluation of activated carbon as a reactive cap sorbent for sequestration of polychlorinated biphenyls in the presence of humic acid. *Environ. Eng. Sci.* **26**, 1371–1379 (2009).
209. Howell, N. L. & Shoeib, T. DFT modeling of sorbate-sorbent interactions for PCBs with natural organic matter and black carbon. (2010).

210. Koelmans, A. A., Meulman, B., Meijer, T. & Jonker, M. T. O. Attenuation of polychlorinated biphenyl sorption to charcoal by humic acids. *Environ. Sci. Technol.* **43**, 736–742 (2009).
211. Patil, V. S. *et al.* Curcumin Acrylation for Biological and Environmental Applications. *J. Nat. Prod.* **80**, 1964–1971 (2017).
212. Lakowicz, J. R. *Principles of Fluorescence Spectroscopy*. (Springer Nature, 2006).
213. Lu, G.-N., Tao, X.-Q., Dang, Z., Yi, X.-Y. & Yang, C. Estimation of n-octanol/water partition coefficients of polycyclic aromatic hydrocarbons by quantum chemical descriptors. *Open Chem.* **6**, 310–318 (2008).
214. *Anal. Chem.*20057751275-1281.
215. Sun, Y., Day, R. N. & Periasamy, A. Investigating protein-protein interactions in living cells using fluorescence lifetime imaging microscopy. *Nat. Protoc.* **6**, 1324–40 (2011).
216. Albrecht, C. Joseph R. Lakowicz: Principles of fluorescence spectroscopy. *Anal. Bioanal. Chem.* **390**, 1223–1224 (2008).
217. O'connell, M. *Optimizing Solvent Extraction of PCBs from Soil*.
218. Walsh, M. E. & Taylor, S. Analytical method for white phosphorus residues in munitions-contaminated sediments. *Anal. Chim. Acta* **282**, 55–61 (1993).
219. Wang, M. *et al.* FITC-modified PPy nanotubes embedded in nanoporous AAO membrane can detect trace PCB20 via fluorescence ratiometric measurement. *Chem. Commun.* **47**, 3808–3810 (2011).
220. Zhang, J. F., Zhou, Y., Yoon, J. & Kim, J. S. Recent progress in fluorescent and colorimetric chemosensors for detection of precious metal ions (silver, gold and platinum ions). *Chem. Soc. Rev.* **40**, 3416–3429 (2011).
221. Venkatramaiah, N., Kumar, S. & Patil, S. Fluoranthene based fluorescent chemosensors for detection of explosive nitroaromatics. *Chem. Commun.* **48**, 5007–5009 (2012).
222. Strianese, M. *et al.* Fluorescence-based biosensors. in *Spectroscopic Methods of Analysis* 193–216 (Springer, 2012).
223. US EPA. *Method 8082A polychlorinated bipenyls (PCBs) by gas chromatography*. *USEP Agency* (2007).
224. Murov, D. S. L. Properties of Organic Solvents. (1998). Available at: http://murov.info/orgsolvents.htm. (Accessed: 12th February 2017)
225. Stenutz, R. isooctane. (2010). Available at: http://www.stenutz.eu/chem/solv6.php?name=isooctane.
226. Myers, R. J. & Gwinn, W. D. The Microwave Spectra, Structure, Dipole Moment, and Chlorine Nuclear Quadrupole Coupling Constants of Methylene Chloride. *J. Chem. Phys.* **20**, 1420–1427 (1952).
227. Sigm-Aaldrich. Physical Properties of Solvents. (2004). Available at: https://www.sigmaaldrich.com/content/dam/sigma-aldrich/docs/Aldrich/General_Information/labbasics_pg144.pdf. (Accessed: 12th February 2017)
228. LeBel, R. G. & Goring, D. A. I. Density, Viscosity, Refractive Index, and Hygroscopicity of Mixtures of Water and Dimethyl Sulfoxide. *J. Chem. Eng. Data* **7**, 100–101 (1962).
229. Electro, K. Dielectric Constants of Common Materials. (2002). Available at: https://www.kabusa.com/Dilectric-Constants.pdf.
230. Sigma-Aldrich. Dimethyl Sulfoxide. (2008). Available at: https://www.sigmaaldrich.com/chemistry/solvents/dimethyl-sulfoxide-center.html. (Accessed: 12th February 2017)

231. Perov, A. N. Energy of intermolecular pair interactions as a characteristic of their nature. Theory of the solvato (fluoro) chromism of three-component solutions. *Opt. Spectrosc.* **49**, 371–374 (1980).
232. Neporent, B. S. & Bakhshiev, N. G. On the role of universal and specific intermolecular interactions in the influence of the solvent on the electronic spectra of molecules. *Opt. Spectrosc.* **8**, 408 (1960).
233. Shamia, I. S., Halabi, M. N. & El-Ashgar, N. M. Humic Acid Determination in some Compost and Fertilizer Samples. *IUG J. Nat. Stud.* (2017).
234. *POLYCHLORINATED BIPHENYLS AND POLYBROMINATED BIPHENYLS*. (IARC, 2016).
235. Chemspider. PCB-126. (2008). Available at: http://www.chemspider.com/Chemical-Structure.56775.html.
236. Series, S. I. I. POLYCHLORINATED BIPHENYLS: HUMAN HEALTH ASPECTS.
237. Atsdr. Toxicological Profile for Polychlorinated Biphenyls (PCBs). (2014). Available at: https://www.atsdr.cdc.gov/toxprofiles/tp.asp?id=142&tid=26.
238. Robertson, L. W. & Hansen, L. G. *PCBs: recent advances in environmental toxicology and health effects*. (University Press of Kentucky, 2015).
239. Yalkowsky, S. H., He, Y. & Jain, P. *Handbook of aqueous solubility data*. (CRC press, 2016).
240. Elmer, P. An introduction to fluorescence spectroscopy. *PerkinElmer Ltd Post Off. Lane Beaconsfld. Buckinghamsh. HP9 1QA Google Sch.* (2000).
241. *JIMD Reports, Volume 24*. (Springer Nature, 2015).
242. Brian Oram, P. The pH of Water. *Water Research Watershed Center* (2001). Available at: https://www.water-research.net/index.php/ph.
243. Rodrigues, A., Brito, A., Janknecht, P., Proença, M. F. & Nogueira, R. Quantification of humic acids in surface water: effects of divalent cations, pH, and filtration. *J. Environ. Monit.* **11**, 377–382 (2009).
244. Yee, M. M., Miyajima, T. & Takisawa, N. Evaluation of amphiphilic properties of fulvic acid and humic acid by alkylpyridinium binding study. *Colloids Surfaces A Physicochem. Eng. Asp.* **272**, 182–188 (2006).
245. IUPAC. *Compendium of Chemical Terminology Gold Book*. (2014).
246. Zangi, R., Hagen, M. & Berne, B. J. Effect of ions on the hydrophobic interaction between two plates. *J. Am. Chem. Soc.* **129**, 4678–4686 (2007).
247. SID PERKINS. Explainer: What are polymers? | Science News for Students. Available at: https://www.sciencenewsforstudents.org/article/explainer-what-are-polymers. (Accessed: 16th May 2019)
248. Mohiti-Asli, M. & Loboa, E. G. Nanofibrous smart bandages for wound care. *Wound Heal. Biomater.* 483–499 (2016). doi:10.1016/B978-1-78242-456-7.00023-4
249. Hutmacher, D. W. Polymers for Medical Applications. *Encycl. Mater. Sci. Technol.* 7664–7673 (2001). doi:10.1016/B0-08-043152-6/01371-1
250. Bockstaller, M. R. Progress in polymer hybrid materials. (2015). doi:10.1016/j.progpolymsci.2014.11.001
251. Shukla, S. K., Kushwaha, C. S. & Singh, N. B. Recent developments in conducting polymer based composites for sensing devices. *Mater. Today Proc.* **4**, 5672–5681 (2017).
252. Fang, X., Zong, B. & Mao, S. Metal-Organic Framework-Based Sensors for Environmental Contaminant Sensing. *Nano-Micro Lett* **10**, 64 (2018).
253. Pietsch, C., Vollrath, A., Hoogenboom, R. & Schubert, U. S. A fluorescent thermometer based on a pyrene-labeled thermoresponsive polymer. *Sensors* **10**, 7979–7990 (2010).
254. González-Benito, J. *et al.* Fluorescence-labeled pyrenesulfonamide response for

characterizing polymeric interfaces in composite materials. *J. Fluoresc.* **10**, 141 (2000).
255. Ferrari, R., Agostini, A., Brunel, L., Morosi, L. & Moscatelli, D. Self-assembling amphiphilic block copolymer from renewable δ-decalactone and δ-dodecalactone. *J. Polym. Sci. Part A Polym. Chem.* **55**, 3788–3797 (2017).
256. Mongay, C. & Cerda, V. Britton–Robinson buffer of known ionic strength. *Anal Chim* **64**, 409–412 (1974).
257. Ottonelli, M., Piccardo, M., Duce, D., Thea, S. & Dellepiane, G. Tuning the photophysical properties of pyrene-based systems: A theoretical study. *J. Phys. Chem. A* **116**, 611–630 (2011).
258. Stevenson, F. J. *Humus chemistry: genesis, composition, reactions*. (John Wiley & Sons, 1994).

VITA

Irfan Ahmad was born in Faisalabad, Punjab, Pakistan. He earned his Bachelor degree in Chemical Engineering with Honor from NFC Institute of Engineering and Fertilizer Research (NFC-IEFR) with distinction in 2007. He persuaded an industrial career as a Chemical Engineer by joining the Sitara Chemical Industries, Faisalabad. He got a master's degree from Hanyang University, South Korea in Chemical Engineering in 2010. He served in the COMSATS Institute of Information Technology, Lahore, Pakistan for around two years. He joined the Department of Chemical and Materials Engineering at the University of Kentucky in August 2012 and graduated with a Master of Science in Chemical Engineering in January 2015, and pursued Doctorate of Philosophy in Chemical Engineering.

PUBLICATIONS

Ahmad, Irfan, Jiaying Weng, A. J. Stromberg, J. Z. Hilt, and T. D. Dziubla. "Fluorescence based detection of polychlorinated biphenyls (PCBs) in water using hydrophobic interactions." Analyst 144, no. 2 (2019): 677-684.

Irfan Ahmad, Manwar Hussain, Keum-Suk Seo, Yong-Ho Choa, "Synthesis and Characterization of Polymer–Nanoclay Conductive Nanocomposites" *Journal of Applied Polymer Science (Wiley), Volume 116 Issue 1, Pages 314 – 319.*

Ghauri, Moinuddin, Suhaib Umer Ilyas, and Irfan Ahmad. "Application of Nanoparticles in the Removal of Micro-Organisms from Water." Science International 25.1 (2013).

Tahir, M. A., Irfan Ahmad, Suhaib Umer, Sharjeel Waqas, and M. Tayyeb Javed. "Selective Non-Catalytic Reduction of Nox." NFC IEFR Journal of Engineering and Scientific Research 1 (2017).

CONFERENCE PRESENTATIONS

Irfan Ahmad, J. Zach Hilt, Thomas D. Dziubla, "Detection of Polychlorinated Biphenyls in Water using Fluorescent Nanoparticles" *NIEHS SRP 2018 Annual meeting*, Nov 2018, Davis, California

I.Ahmad, J.Z.Hilt, T. Dziubla, "Fluorescence based detection of polychlorinated biphenyls in water" *AIChE Annual Meeting*, Nov 2017, Minneapolis

Irfan Ahmad,Shuo Tang, Angela M. Gutierrez, J. Zach Hilt and Thomas D. Dziubla. Polyphonic nanocomposite materials for the capture and sensing of chlorinated organic contaminants in water source, *2017 Northeast Superfund Research Program Meeting, Northeastern University*, April 2017, MA

Irfan Ahmad, Angela M. Gutierrez, J.Z.Hilt and TD Dziubla, “Polyphenolic Molecules Based Fluorescence Detection of PCBs.” *NIEHS Environmental Health Science FEST, Durham, NC*, Dec 2016, NC

Irfan Ahmad, J. Zach Hilt, Thomas D. Dziubla, "Direct UV Excitation of PCBs for Coupled Fluorescence Detection." *NIEHS SRP Annual Meeting*, Nov 2015, Puerto Rico

Irfan Ahmad, Manwar Hussain, Keum-Suk Seo, Yong-Ho Choa “Improvement of Electrical Performance of Clay Nanocomposites”, The Korean Society of Industrial and Engineering Chemistry, April 2009, Daegu, South Korea